José Antonio Santos Souza

NANOPARTÍCULAS DE PRATA OBTIDAS PELA SÍNTESE '*GREEN*' COMBINADAS OU NÃO COM GLICEROFOSFATO DE CÁLCIO E TIROSOL: EFEITO ANTIMICROBIANO, ANTI-INFLAMATÓRIO E NA RESPOSTA TRANSCRIPTÔMICA EM PATÓGENOS ORAIS

ARAÇATUBA - SP

2018

José Antonio Santos Souza

Nanopartículas de prata obtidas pela síntese '*green*' combinadas ou não com glicerofosfato de cálcio e tirosol: efeito antimicrobiano, anti-inflamatório e na resposta transcriptômica em patógenos orais

Tese apresentada à Faculdade de Odontologia da Universidade Estadual Paulista "Júlio de Mesquista Filho", Campus de Araçatuba para obtenção do título de Doutor em Ciência Odontológica, área de concentração Saúde Bucal da Criança.

Orientador: Prof. Tit. Alberto Carlos B. Delbem

ARAÇATUBA - SP

2018

Catalogação-na-Publicação

Diretoria Técnica de Biblioteca e Documentação – FOA / UNESP

S729n

Souza, José Antonio Santos.
Nanopartículas de prata obtidas pela síntese 'green' combinadas ou não com glicerofosfato de cálcio e tirosol : efeito antimicrobiano, anti-inflamatório e na resposta transcriptômica em patógenos orais / José Antonio Santos Souza. - Araçatuba, 2018
186 f. : il. ; tab.

Tese (Doutorado) – Universidade Estadual Paulista, Faculdade de Odontologia de Araçatuba
Orientador: Alberto Carlos Botazzo Delbem

1. Candidíase bucal 2. Cárie dentária 3. Nanotecnologia 4. Prata 5 Toxicidade I. T.

Black D27
CDD 617.645

Claudio Hideo Matsumoto – CRB-8/5550

ERRATA

SOUZA, J.A.S. **Nanopartículas de prata obtidas pela síntese '*green*' combinadas ou não com glicerofosfato de cálcio e tirosol: efeito antimicrobiano, anti-inflamatório e na resposta transcriptômica em patógenos orais**. 2018. 186 f. Tese (Doutorado em Ciência Odontológica, área de concentração Saúde Bucal da Criança) – Faculdade de Odontologia de Araçatuba, Universidade Estadual Paulista, 2018.

Folha	Linha	Onde se lê	Leia-se
8	1	***À Fundação de Amparo à Pesquisa do Estado de São Paulo (FAPESP)*** Pelo grande incentivo nas formas de Bolsa de Doutorado (FAPESP, Processo 2015/00825-5) e de Bolsa de Estágio de Pesquisa no Exterior (BEPE, Processo 2016/22039-4).	***À Fundação Coordenação de Aperfeiçoamento de Pessoal de Nível Superior CAPES/DS*** Pelo grande incentivo na forma de Bolsa de Doutorado, no seguinte período: 01/01/2015 a 30/06/2015. ***À Fundação de Amparo à Pesquisa do Estado de São Paulo (FAPESP)*** Pelo grande incentivo nas formas de Bolsa de Doutorado (FAPESP, Processo nº 2015/00825-5) e de Bolsa de Estágio de Pesquisa no Exterior (BEPE, Processo nº 2016/22039-4).

DADOS CURRICULARES

JOSÉ ANTONIO SANTOS SOUZA

NASCIMENTO	07/09/1990 – Clementina – SP
FILIAÇÃO	João Carlos de Souza Mariauva Ribeiro dos Santos Souza
2008/2011	Curso de Graduação em Odontologia Faculdade de Odontologia de Araçatuba – Universidade Estadual Paulista "Júlio de Mesquita Filho"
2012/2014	Curso de Pós-Graduação em Ciência Odontológica, área de concentração Saúde Bucal da Criança, nível de Mestrado, na Faculdade de Odontologia de Araçatuba – UNESP
2015/2017	Obtenção dos créditos referentes ao Curso de Pós-Graduação em Ciência Odontológica, área de concentração em Saúde Bucal da Criança, nível de Doutorado
2015/2016	Curso de Especialização em Odontopediatria, na Faculdade de Odontologia de Araçatuba – UNESP
Associações	CROSP – Conselho Regional de Odontologia de São Paulo SBPqO – Sociedade Brasileira de Pesquisa Odontológica

DEDICATÓRIA

Aos meus queridos pais: João Carlos e Mariauva

A vocês, queridos pais, que dedicaram suas vidas em favor da minha vida. Foram muitas as batalhas que travamos ao longo destes anos, mas o Senhor Deus nos concedeu a vitória em todas elas. Vocês nos ensinaram a obedecer, a respeitar, a ensinar e, principalmente, a amar os nossos semelhantes. Por esta razão, cheguei até aqui. Sem vocês, nada disso teria acontecido. Sendo assim, dedico esta vitória a vocês, que já são, aqui na terra, merecedores do Reino dos Céus. “Como é grande o meu amor por vocês”.

A minha irmã: Izabella

Você é mais que uma amiga e companheira; é um anjo que Deus colocou em minha vida para me alegrar, me fazer sorrir e chorar. Estará para sempre em meu coração. Obrigado pela força, pelos conselhos e pelas “brigas”, rs. Amo você.

Aos meus amigos

Orgulho-me de olhar para trás e ver uma longa jornada já percorrida, mas me alegro ainda mais ao ver quantos bons amigos eu conquistei em meio a essa caminhada.

AGRADECIMENTOS ESPECIAIS

A Deus

Senhor, desde o ventre de minha mãe, já me conhecias, porque Tu me criaste com carinho e amor. Diante disso, agradeço pelo dom da vida. Tu me acompanhaste na minha infância e na minha adolescência sempre me corrigindo com carinho e atenção. Agradeço pelas correções, pois, através delas, cresci em sabedoria e graça diante de Ti e diante dos homens. Passei por dificuldades e encontrei obstáculos em meu caminho, mas Tu não me abandonaste em meio às tempestades. Hoje, é um dia de muita alegria, pois conquistei mais uma vitória em minha vida. Assim, venho te louvar, agradecer e engrandecer por esse momento que proporcionaste para mim. Obrigado Senhor!!

Aos meus pais e à minha irmã

Aos meus pais, que se doaram inteiros e renunciaram aos seus sonhos, para que, muitas vezes, nós, seus filhos, pudéssemos realizar os nossos, não bastaria um muitíssimo obrigado. Faltam palavras para expressar minha gratidão por vocês. Agradeço pelas correções fraternas. Eu sei que foram feitas com amor e sabedoria visando o meu crescimento pessoal. Vocês nos mostram diariamente como uma família deve se comportar: Amando a Deus sobre todas as coisas e ao próximo como a nós mesmos, seguindo assim os belíssimos ensinamentos do Mestre Jesus Cristo. Izabella, agradeço pela sua companhia. Com certeza, Deus te colocou em meu caminho para ser meu anjo guardião. Também não há palavras que expressam meu amor incondicional por você. Assim, agradeço por estarem ao meu lado neste momento grandioso da minha vida. Sem vocês, não teria sentido receber este título.

A minha família

A família sempre está ali, pronta para o que der e vier, não espera nada em troca. Neste momento, tão especial em minha vida, é claro que não poderia deixá-los de agradecer. Obrigado pelas orações, apoio, respeito e paciência. Desculpem-me por não ter compartilhado com vocês algumas conversas, risadas, almoços, entre outras coisas. Saibam que vocês sempre ocuparão um lugar especial em meu coração e em minhas

orações. Por esta razão, agradeço a vocês que me ajudaram em minha formação. Meu muito obrigado!!

Ao meu orientador Prof. Alberto Carlos Botazzo Delbem

Ser mestre não é apenas lecionar, ensinar não é apenas transmitir o conteúdo programático. Ser mestre é ser orientador e amigo, guia e companheiro, é caminhar com o aluno passo a passo. É transmitir a este os segredos da caminhada. É por isso e muito mais que agradeço, a você meu orientador, cada dia, cada oportunidade que tive ao seu lado, o senhor será sempre um exemplo de dedicação, de doação, de dignidade pessoal e de amor. Obrigado por tudo!

À Profª. Débora Barros Barbosa

A realização deste trabalho não seria possível sem a sua colaboração. Obrigado pela oportunidade de ter trabalhado com a Sra. ao longo destes 4 anos. Seu contato com o Prof. Nuno fez com que eu pudesse fazer meu doutorado sanduíche. Muito obrigado!! A Sra. é um verdadeiro exemplo de pessoa íntegra, generosa e competente. A sua paixão pela pesquisa serve de estímulo para que eu possa seguir trilhando neste caminho. Um grande abraço de carinho e eterna gratidão.

À Profª. Sandra Helena Penha de Oliveira

Obrigado pela acolhida em seu grupo de pesquisa e por permitir a utilização do seu laboratório para o desenvolvimento deste trabalho. Foi um prazer trabalhar ao seu lado!! Espero ter outras oportunidades.

Ao meu orientador estrangeiro Prof. Nuno Gonçalo Pereira Mira

No período de 2017-2018, fiz meu doutorado sanduíche sob a orientação do Prof. Nuno Mira. Foi uma experiência ímpar em minha vida. Obrigado professor pela recepção em seu grupo de pesquisa, pelos momentos de descontração e, também, pelas correções visando nosso aprendizado. Além disso, nós agradecemos a sua importante participação na minha banca de Defesa de Tese. Obrigado por tudo!

À ***Fundação de Amparo à Pesquisa do Estado de São Paulo (FAPESP)***

Pelo grande incentivo nas formas de Bolsa de Doutorado (FAPESP, Processo 2015/00825-5) e de Bolsa de Estágio de Pesquisa no Exterior (BEPE, Processo 2016/22039-4).

AGRADECIMENTOS

À ***Faculdade de Odontologia de Araçatuba – UNESP***, na pessoa de seu diretor ***Prof. Tit. Wilson Roberto Poi***, pela oportunidade de aprendizado e crescimento pessoal e profissional.

Ao atual ***coordenador do Programa de Pós-Graduação em Ciência Odontológica***, da Faculdade de Odontologia de Araçatuba – UNESP, ***Prof. Adj. Luciano Tavares Angelo Cintra***, pela competência e acessibilidade.

Ao ***Departamento de Química*** da Universidade Federal de São Carlos – UFSCar e ao ***LIEC (Laboratório Interdisciplinar de Eletroquímica e Cerâmica)***, por permitirem a realização da síntese das nanopartículas de prata.

Ao ***Prof. Emerson Camargo***, por ter contribuído com o desenvolvimento desta pesquisa.

À ***APIS FLORA INDUSTRIAL E COMERCIAL LTDA***, onde parte fundamental deste trabalho foi realizado com a ajuda de extrema importância de alguns dos alunos e funcionários em especial Andrei, Elina e Rebeca.

Ao ***Departamento de Ciências Básicas***, pela receptividade, pelas novas amizades e pelo carinho com a minha pessoa.

À ***Pesquisadora Drª. Alessandra Marçal Agostinho***, por ter colaborado com o desenvolvimento deste Projeto. Suas correções foram fundamentais para a publicação do nosso primeiro artigo e, também para o meu aprendizado.

À ***Dra. Jackeline Gallo do Amaral, ao Dr. Renan Aparecido Fernandes, ao Dr. Luiz Fernando Gorup, ao Pós-doutorando Francisco Nunes de Souza Neto e à aluna de Doutorado Gabriela Lopes Fernandes***, pelo companheirismo e pela ajuda no desenvolvimento desta pesquisa.

À ***Dra. Aline Satie Takamiya***, pessoa gentil, educada e muito competente. Obrigado de coração, pela amizade, pelo incentivo, pela paciência e pelo carinho com que sempre me tratou. Obrigado por todo conhecimento que dividiu comigo e por toda a ajuda na execução deste trabalho. Foi um prazer ter convivido com você nestes últimos anos.

Ao ***Instituto Superior Técnico*** e ao ***Departamento de Bioengenharia e Biociências***, pela receptividade, pelas novas amizades e pelo carinho com a minha pessoa.

À ***Profª. Isabel Sá-Correia***, pela receptividade em seu Departamento.

Aos alunos de Pós-Graduação ***Sara Salazar, Nuno Pedro e Rita***, pela ajuda no desenvolvimento desta pesquisa no Departamento de Bioengenharia e Biociências do Instituto Superior Técnico durante o meu doutorado sanduíche.

À ***Pós-Doutoranda Marta***, pela ajuda na caracterização das nanopartículas no início dos nossos estudos em Lisboa, Portugal e dos biofilmes na presença dos compostos avaliados. Sua ajuda e amizade foram essenciais para o bom êxito deste trabalho.

Aos meus ***amigos brasileiros que conheci em Lisboa: Rejane, Carmem, Diego, Abdon, Mateus, Bárbara, Soraia, Eloá, Pe. Robson, Daniel, Oswaldo, Inah Mara, Marina, Thiago, Cris, Gisele; aos meus amigos colombianos e venezuelanos: Leslye, Pino e Piedy; aos grandes amigos estrangeiros: Sileshi Demesie, Aldona, Chaima, Luan, Giovani, Isabel Bento, Alexey; aos colegas de Departamento de Bioengenharia e Biociências: Tiago, Diana, João, Mafalda, Marta, Isabel Seixas, Nuno Bourbon, Rúben, Andréia, Carina Galhofa, Sara Gomes, Joana Correia, Inês Sá, Jésica Alexandra, Maria João, Ana, Pedro, ao professor Miguel Teixeira, Ricardo, Carla Coutinho, Luís, Cláudia, Joana, Mônica, Romeu, Miguel, André, Nuno Bernardes, Margarida; aos professores do Departamento de Química do Instituto Superior Técnico***, agradeço por terem me recebido com muito carinho e por terem me ajudado nos experimentos.

Aos meus ***amigos do Coro Gerações da Paróquia São João de Deus em Lisboa: Philippe Catarino (nosso maestro), Nuno Eusébio, Diogo, Nela Cabral, Tina Melo, Andréia***

Amorim, Carina Brandão, Arlete, e demais integrantes do grupo, agradeço de coração sincero pela acolhida no coral. Vocês são muito especiais! Que Deus os abençoe!

Às ***funcionárias da Residência dos Baldaques: Ana Bela, Cândida e Cecília (in memoriam).*** Obrigado por terem me tratado como um filho! Realmente, me senti em casa!

Aos colegas do ***Departamento de Ciências Básicas: Victor, Murilo, Jésica, Rodrigo, Sabrina, Mariana, Kellen, Wanessa, Maria Fernanda, José Vitor, Beatriz, Carol, Cau, Laura, Vitor Bonetti, Ayná, aos professores: Antônio, Cristina, Rita, João, Ana Claúdia, Dóris*** pelo convívio no laboratório. Muitas vezes, vocês alegraram meu dia!

Aos meus queridos amigos do ***Departamento de Odontopediatria: Liliana, Thayse, Márjully, Mariana Nagata, Karina Caiaffa, Caio Sampaio, Vanessa, Jésse, Nayara, Mayra, Jorge, Isabel, Luhana, Leonardo, Gabriel, Sara, Francyenne, Priscila, Emanuelle, Lenara, Sâmia, Valéria, Igor, Laís, Douglas, Marcelle Danelon, Thamires, Heitor, Carla Mendes, Ana Paula, Isabela, Silvio, Suéllen, Carla Favretto***. Obrigado pelo convívio, pelas parcerias. Desculpem-me por alguma coisa… Amo vocês!

Aos ***Profs. Robson Frederico Cunha***, ***Célio Percinoto***, ***Rosangela Santos Nery***, ***Sandra Maria Herondina Ávila de Aguiar***, ***Juliano Pelim Pessan*** e ***Cristiane Duque***, pela orientação não só no âmbito da pesquisa, mas, principalmente, na área clínica. Durante o curso de Especialização, aprendi muito com vocês. Além disso, nossos momentos de descontração ficarão guardados em meu coração. Amo vocês. Obrigado por tudo!

Às excelentes funcionárias da seção de Pós-Graduação da Faculdade de Odontologia de Araçatuba – UNESP, ***Valéria*** e ***Cristiane***, pelo apoio, suporte e ajuda a mim dispensados.

Aos funcionários do departamento de Odontopediatria ***Ricardo***, pelo carinho e preocupação e ***Mário***, pela amizade e ajuda; aos ***funcionários da disciplina de Ortodontia Bertolina e Luís*** pela ajuda na organização do departamento; aos funcionários da Biblioteca, em especial a ***Ana Paula e Cláudio***, por sempre me acolherem nos momentos de dúvidas e por sempre estarem dispostos a ajudar.

Aos meus pequenos pacientes e responsáveis, obrigado pela sua paciência, pelo seu respeito ao nosso aprendizado, pela sua colaboração e incentivo ao nosso aprimoramento técnico-científico. Talvez a minha ajuda ainda seja pequena diante do universo carente em que vocês corajosamente vivem, mas ajudá-los está representando para mim uma magnífica lição de amor e fraternidade.

“A santidade não está nesta ou naquela prática, ela consiste numa disposição do coração que nos torna humildes e pequenos nas mãos de Deus, conscientes de nossa fraqueza, e confiantes até a audácia na sua bondade de Pai.”

Santa Teresa de Lisieux

Souza JAS. **Nanopartículas de prata obtidas pela síntese '*green*' combinadas ou não com glicerofosfato de cálcio e tirosol: efeito antimicrobiano, anti-inflamatório e na resposta transcriptômica em patógenos orais** [tese]. Araçatuba: Faculdade de Odontologia da Universidade Estadual Paulista; 2018.

RESUMO GERAL

O objetivo deste estudo foi avaliar a atividade antimicrobiana/antibiofilme e a viabilidade celular de nanopartículas de prata (NPsAg) obtidas por uma síntese '*green*' associadas ou não ao β-glicerofosfato de cálcio (GPCa) contra *Streptococcus mutans* e espécies de *Candida* (cepas de referência e isolados clínicos orais incluindo cepas resistentes ao fluconazol). O efeito destes nanocompostos em combinação com o tirosol (TIR), fluconazol (FLC), nistatina (NIT) e anfotericina B (AnB) também foi avaliado. Além disso, nós avaliamos comparativamente as alterações do transcriptoma de células de *C. glabrata* CBS138 após exposição às NPsAg e ao Íon prata (Ag^{+}). Inicialmente, as NPsAg foram sintetizadas por meio da redução do nitrato de prata com extratos de diferentes partes (casca, folha e semente) de uma romã (*Punica granatum L.*) associadas ou não ao GPCa. A Concentração Inibitória Mínima (CIM) e as Concentrações Fungicida/Bactericida Mínima (CFM e CBM) dos nanocompostos (NPsAg e NPsAg-GPCa) associados ou não ao TIR contra *S. mutans* e *C. albicans* foram determinadas pelo método de microdiluição. E, a ação das NPsAg combinadas com FLC, NIT e AnB também foi avaliada em condição planctônica contra isolados clínicos orais de espécies de *Candida*. O efeito dos nanocompostos associados ou não ao TIR sobre a viabilidade celular de fibroblastos da linhagem L929 e a produção de citocinas foi avaliado através dos ensaios de MTT e ELISA, respectivamente. O número de hifas foi quantificado em biofilmes de *C. albicans* formados na presença das NPsAg com ou sem soro fetal bovino (SFB). O efeito das NPsAg em inibir a formação do biofilme (em *C. albicans* e *C. glabrata*) também foi investigado através do ensaio de PrestoBlue e por meio da microscopia eletrônica de varredura. Os nanocompostos (NPsAg e NPsAg-GPCa) associados ou não ao TIR foram aplicados sobre biofilmes de *S. mutans* e de espécies de *Candida* (12 e 24 h) e, após 24 h de contato, sua atividade antibiofilme foi determinada por meio da enumeração das unidades formadoras de colônias (UFCs) e ensaio de PrestoBlue. Além disso, uma análise transcriptômica foi realizada utilizando microchips de DNA ('microarrays') a fim de avaliar quais genes estão mais ou menos expressos como

resposta às NPsAg (no estado planctônico e formando biofilmes) e ao Íon Ag^+ (formando biofilmes). As soluções antimicrobianas sintetizadas neste estudo (NPsAg e NPsAg-GPCa) apresentaram atividade antimicrobiana contra os microrganismos testados. Além disso, menores valores de CIM foram obtidos quando estes nanocompostos foram associados ao TIR, FLC, NIT e AnB apresentando um efeito sinérgico. NPsAg e NPsAg-GPCa não foram tóxicas às células L929, aumentaram a produção de fator de crescimento celular e não promoveram alterações significativas na liberação de Interleucina-6. Os nacompostos associados ao TIR não apresentaram efeito citotóxico sobre culturas de L929, exceto para a maior concentração (NPsAg – 39,05 µg/mL + TIR – 1,25 mM). A presença das NPsAg reduziu drasticamente o número de hifas em biofilmes de *C. albicans* na presença ou na ausência de SFB. A quantidade de biofilme das espécies de *Candida* formado na presença das NPsAg reduziu para mais de 50%. Após 24 h de tratamento com os nanocompostos (NPsAg e NPsAg-GPCa) em biofilmes de *S. mutans*, houve uma redução significativa no número de UFCs sendo similar à clorexidina. Uma redução na viabilidade de biofilmes de *C. glabrata* também foi observada após exposição às NPsAg (24 h). Entretanto, os nanocompostos (NPsAg e NPsAg-GPCa) associados ou não ao TIR não foram efetivos contra biofilmes de *C. albicans*. Após exposição às NPsAg e ao Íon Ag^+, alterações no transcriptoma de células de *C. glabrata* CBS138 foram observadas: no estado planctônico, houve uma superexpressão dos genes responsáveis pela biossíntese de metionina e de lisina e uma subexpressão dos genes relacionados com o transporte transmembrana; e, as células expostas às NPsAg responderam de forma distinta em relação ao Íon Ag^+, indicando que as NPsAg podem apresentar um mecanismo de ação diferente. Estes achados podem auxiliar nas decisões terapêuticas com formulações contendo NPsAg ou NPsAg-GPCa associadas ou não a diferentes drogas em pacientes com cárie dentária e candidíase oral.

Palavras-chaves: Candidíase Bucal. Cárie Dentária. Prata. Nanotecnologia. Toxicidade.

Souza JAS. **Silver nanoparticles obtained by the '*green*' synthesis combined or not with calcium glycerophosphate and tyrosol: antimicrobial, anti-inflammatory effect and in the transcriptomic response in oral pathogens** [thesis]. Araçatuba: UNESP – São Paulo State University; 2018.

GENERAL ABSTRACT

The aim of this study was to evaluate the antimicrobial/antibiofilm activities and the cell viability of silver nanoparticles (AgNPs) obtained by a '*green*' synthesis associated or not to β-calcium glycerophosphate (CaGP) against *Streptococcus mutans* and *Candida* species (reference strains and oral clinical isolates including azole-resistant strains). The effect of these nanocompounds in combination with tyrosol (TYR), fluconazole (FLC), nystatin (NYT) and amphotericin B (AmB) also was evaluated. Furthermore, we evaluated, comparatively, the transcriptome alterations of cells of *C. glabrata* CBS138 after exposition to AgNPs and to silver ion (Ag^{+}). Initially, AgNPs were synthesized by reducing silver nitrate with extracts of different parts (peel, leaves and seeds) of a pomegranate (*Punica granatum L.*) associated or not to CaGP. Minimum Inhibitory Concentration (MIC) and Minimum Fungicidal/Bactericidal Concentrations (MFC and MBC) of the nanocomposites (AgNPs and AgNPs-CaGP) associated or not to TYR against *S. mutans* and *C. albicans* were determined by the microdilution method. And, the action of the AgNPs combined with FLC, NYT and AmB also was evaluated in planktonic condition against oral clinical isolates of *Candida* species. The effect of the nanocomposites associated or not to TYR on cell viability of fibroblasts (L929) and cytokines production was evaluated through MTT and ELISA assays, respectively. The number of cells undergoing filamentation was quantified in *C. albicans* biofilms formed in the presence of AgNPs with or without fetal bovine serum (FBS). The effect of AgNPs in inhibit the formation of biofilm (in *C. albicans* and *C. glabrata*) also was investigated through PrestoBlue assay and scanning electron microscope. Biofilms of *S. mutans* and *Candida* species (12 and 24 h) were treated with nanocomposites (AgNPs and AgNPs-CaGP) associated or not to TYR for 24 h and, then, the viability of these biofilms was determined through PrestoBlue assay and colony forming units (CFUs). Moreover, a transcriptome analysis was performed using microarrays to determine which genes are up- or down-regulated as response to AgNPs (in the planktonic state and forming biofilms) and to Ag^{+} ion (forming biofilms). Antimicrobial solutions synthesized in this

study (AgNPs and AgNPs-CaGP) presented antimicrobial activity against tested microorganisms. Furthermore, lower values of MIC were obtained when these nanocompounds were associated to TYR, FLC, NYT and AmB showing a synergistic effect. AgNPs and AgNPs-CaGP were not toxic to L929 cells, increased the stem cell factor production and did not promote significant alterations in the Interleukine-6 release. The nanocomposites associated to TYR did not present cytotoxic effect on L929 cultures, except for the higher concentration (AgNPs – 39.05 µg/mL + TYR – 1.25 mM). The incubation in the presence of the AgNPs drastically reduced the number of cells exhibiting hyphae, this effect being observed either in the presence or absence of FBS. The amount of biofilm formed by *Candida* species in the presence of the AgNPs was reduced by more than 50% the one formed in the absence of the nanoparticles, this reduction being further increased to more than 90% when the concentration of the AgNPs was increased. After 24 h of treatment with the nanocompounds (AgNPs and AgNPs-CaGP) in *S. mutans* biofilms, there was a significant reduction in the number of CFUs being similar to chlorhexidine. A reduction in the viability of *C. glabrata* biofilms also was observed after exposition to AgNPs (24 h). However, the nanocomposites (AgNPs and AgNPs-CaGP) associated or not to TYR were not effective against *C. albicans* biofilms. After exposition to AgNPs and to Ag^+ ion, alterations in the transcriptome of cells of *C. glabrata* CBS138 were observed: in the planktonic state, genes responsible by the methionine and lysine biosynthesis are up-regulated, and genes related with the transmembrane transport are down-regulated. And, finally, the cells exposed to AgNPs responded differently in relation to the Ag^+ ion, indicating that the AgNPs might present a different mechanism of action. All these results may help guide therapeutic decisions with formulation containing AgNPs or AgNPs-CaGP associated or not with different compounds in patients with dental caries and oral candidiasis.

Keywords: Oral Candidiasis. Dental Caries. Silver. Nanotechnology. Toxicity.

LISTA DE FIGURAS

LISTA DE TABELAS

SUMÁRIO

INTRODUÇÃO GERAL

A cavidade bucal abriga nichos que permitem o crescimento de diversas comunidades de microrganismos – vírus, bactérias, fungos e protozoários (Wade, 2013). Estas comunidades persistem em todas as superfícies (tecidos moles ou duros) como biofilmes multiespécies formando, assim, a microbiota oral residente, que geralmente existe em harmonia com o hospedeiro. Os microrganismos encontrados dentro destes biofilmes orais vivem em proximidade um com outro, que resulta em uma ampla variedade de interações, que podem ser sinérgicas ou antagônicas. A composição da microbiota é influenciada pelo ambiente oral, e mudanças nas condições locais podem afetar as interações microbianas dentro destas comunidades orais e determinar, em parte, se a relação entre a microbiota oral e o hospedeiro é simbiótica ou potencialmente prejudicial, aumentando, assim, o risco de doenças como a cárie dentária ou a candidíase oral (Roberts e Darveau, 2015).

A cárie dentária é uma doença biofilme-sacarose dependente causada por ácidos provenientes da fermentação microbiana dos carboidratos da dieta que, com o tempo, causam a desmineralização dos tecidos duros do dente (Whitford *et al*., 2002). Bactérias cariogênicas como *Streptococcus mutans*, *S. sobrinus*, e lactobacilos são importantes na patogênese da cárie dentária (Balakrishnan *et al*., 2000). Dentre essas bactérias, *S. mutans*, uma bactéria Gram-positiva anaeróbia facultativa, é um dos principais agentes etiológicos desta patologia. Os principais fatores de virulência de *S. mutans* que contribuem para a colonização da superfície do esmalte dentário e desenvolvimento de biofilmes são produção de polissacarídeos extra e intracelulares, produção de ácidos a partir de uma variedade de açúcares fermentáveis e tolerância ao baixo pH do ambiente (Krzyściak *et al*., 2014). Embora o desenvolvimento da cárie esteja inicialmente relacionado à formação de biofilme cariogênico por *S. mutans*, a progressão de lesões estabelecidas pode incluir as espécies de *Candida*, particularmente *C. albicans*. Estudos microbiológicos de biofilmes de crianças com cárie precoce da infância revelaram que, além dos altos níveis de *S. mutans*, a *C. albicans*, um patógeno fúngico oportunista, também é frequentemente detectado (Raja *et al*., 2010; Yang *et al*., 2012). Raja e colaboradores (2010) relataram que a ocorrência de cavidades dentárias em crianças está positivamente correlacionada com a frequência de candidíase oral. As leveduras podem facilitar a formação do biofilme pelos estreptococos, enquanto que estes melhoram as propriedades invasivas de *Candida* (Diaz *et al*. 2012; Xu *et al*., 2014). Além disso, quando

a sacarose está presente, a interação entre esses microrganismos em termos de adesão (e co-agregação) é melhorada (Metwalli *et al*., 2013).

A candidíase oral, por sua vez, é uma importante entidade dermatológica oral que pode estar presente na mucosa bucal, língua, gengiva e palato (Millsop *et al*., 2016; Moyes *et al*., 2015). *C. albicans* é a causa mais prevalente de candidíase oral devido a alguns fatores de virulência que este microrganismo possui, como por exemplo sua adesão às superfícies do hospedeiro, transição do estado de leveduras a hifas, e produção de enzimas extracelulares; a formação de hifas contribui na adesão à superfície da mucosa assim como auxilia a penetração no epitélio oral (Silva *et al*., 2017; Rautemaa e Ramage, 2011). Entretanto, infecções causadas por outras espécies de *Candida* estão aumentando. Na candidíase oral, um aumento na frequência de *C. glabrata* tem sido observado (Miranda-Cadena *et al*., 2018); este fato pode ser devido à maior resiliência às drogas da família dos azóis (especialmente o fluconazol) largamente utilizado no tratamento e na profilaxia de pacientes em risco (Tscherner *et al*., 2011; Benett *et al*., 2004).

O controle da formação de biofilmes orais não é uma tarefa fácil, mas, nos últimos anos, a Nanotecnologia tem sido amplamente utilizada em diversas áreas da saúde através da incorporação de nanopartículas em diversos materiais (médicos e dentários) a fim de controlar ou tratar biofilmes patogênicos, fornecendo, assim, novos tratamentos contra uma ampla gama de doenças (Noronha *et al*., 2017; Ramasamy e Lee, 2016). Neste contexto, as nanopartículas de prata (NPsAg) tem ganhado considerável atenção no campo científico. Na forma nanoparticulada, a prata possui uma maior área de superfície por volume (esta característica aumenta a área de contato com o microrganismo), o que a torna potencialmente mais reativa (Chairuangkitti *et al*., 2013). NPsAg possuem comprovada atividade antimicrobiana contra um amplo espectro de microrganismos, bactérias, fungos e vírus, como por exemplo *S. mutans* (Fernandes *et al*., 2018; Souza *et al*., 2018; Perez-Diaz *et al*., 2015), *Staphylococcus aureus* (Fernandes *et al*., 2018), *Pseudomonas aeruginosa* (Chowdhury *et al*., 2016), *C. albicans*, *C. glabrata*, *C. krusei* e *C. guilliermondii* (Souza *et al*., 2018; Soares M *et al*., 2018; Monteiro *et al*., 2015; Szweda *et al*., 2015; Monteiro *et al*., 2012; Wady *et al*., 2012), incluindo cepas resistentes às drogas que são habitualmente usadas para tratar infecções causadas por estes microrganismos (Franci *et al*., 2015; Ravishankar Rai e Jamuna Bai, 2011).

Muitos procedimentos físicos e químicos tem sido usados para sintetizar nanopartículas metálicas (Goodsell, 2014); entretanto, muitas dessas técnicas utilizam substâncias químicas tóxicas, podendo afetar o meio ambiente e o sistema biológico (Ali

et al., 2016). Além disso, são técnicas extremamente caras. Assim, estas abordagens podem resultar em efeitos colaterais indesejáveis quando estas partículas forem utilizadas. Desta forma, um método alternativo para síntese de nanopartículas metálicas para reduzir seus efeitos citotóxicos se faz necessário. A síntese fitoquímica, onde compostos de diferentes plantas são utilizados na redução de íons, tem-se mostrado bastante eficaz na produção de nanopartículas, fornecendo compostos menos tóxicos e economicamente mais viáveis (Roy *et al*., 2013). A *Punica granatum* L. (romã) é uma planta que tem sido utilizada na medicina para o tratamento de distúrbios causados por estresse oxidativo (Rao *et al*., 2013; Jurenka, 2008; Lansky e Newman, 2007). Diferentes partes da planta, incluindo as folhas, apresentam excelentes propriedades anti-oxidantes (Pande *et al*., 2009). O extrato da casca da romã tem sido bastante utilizado na síntese das NPsAg (Fernandes *et al*., 2018; Souza *et al*., 2018; Nasiriboroumand *et al*., 2018; Goudarzi *et al*., 2016; Edison e Sethuraman, 2013) uma vez que a casca da romã é uma fonte importante de substâncias fenólicas incluindo taninos, ácidos elágico e gálico, etc que são agentes antioxidantes responsáveis pela redução do sal de prata (Goudarzi *et al*., 2016; Ahmad *et al*., 2012).

Além das NPsAg, compostos à base de fosfato de cálcio estão sendo desenvolvidos com o intuito de prevenir a cárie dentária bem como preservar também a vitalidade pulpar e estimular a formação de uma barreira de dentina (Xu *et al*., 2011). Estes materiais podem liberar íons de cálcio (Ca) e fosfato inorgânico (P) a fim de remineralizar lesões dentárias (Xie *et al*., 2016). Muitos estudos tem demonstrado bons resultados na remineralização do esmalte com polifosfatos (Dalpasquale *et al*., 2017; Danelon *et al*., 2017; Amaral *et al*., 2014; Zaze *et al*., 2014). Entre estes compostos, o glicerofosfato de cálcio (GPCa), que é usado como uma fonte de Ca e P, tem demonstrado propriedades anti-cariogênicas (Nagata *et al*., 2017; Freire *et al*., 2016). Além disso, Imai e Hayashi (1993) demonstraram que o β-GPCa, um dos isômeros do GPCa (Inoue, 1980) utilizado como capeamento pulpar direto em um estudo animal foi convertido imediatamente em hidroxiapatita no assoalho da cavidade. Desta forma, devido à complexidade dos biofilmes orais e o desenvolvimento da cárie, a associação das NPsAg com GPCa pode resultar em um biomaterial promissor com forte atividade antimicrobiana e propriedades de remineralização desejáveis.

Entretanto, existe uma preocupação em relação a dose das NPsAg utilizada, uma vez que uma toxicidade dose-dependente em fibroblastos (L929) tem sido documentada (Takamiya *et al*., 2016). Uma outra questão a ser levada em consideração seria o

aparecimento de isolados clínicos resistentes a drogas convencionais. Portanto, o uso combinado destas soluções antimicrobianas (NPsAg e NPsAg-GPCa) com outros compostos em baixas concentrações poderia aumentar a eficácia antimicrobiana contra biofilmes resistentes e reduzir os efeitos colaterais destes agentes. Neste sentido, Sun e colaboradores (2016) obtiveram bons resultados com o uso combinado das NPsAg com fluconazol contra isolados clínicos resistentes aos azóis. Longhi e colaboradores (2016) também demonstraram uma diminuição na viabilidade de biofilmes maduros de cepas resistentes aos azóis com o uso de fluconazol em combinação com NPsAg produzidas por uma via fitoquímica. Moléculas de sinalização, conhecidas como *Quorum-Sensing* (QS) tem sido testadas como agentes antimicrobianos alternativos (Albuquerque e Casadevall, 2012; Monteiro *et al*., 2015). Neste sentido, o tirosol (TIR) mostrou propriedades antibiofilme contra espécies de *Candida* e *S. mutans* em biofilmes simples e mistos (Arias *et al*., 2016). Sendo assim, a associação das NPsAg (com ou sem GPCa) com antifúngicos utilizados na prática clínica (fluconazol, nistatina e anfotericina B) bem como com estas moléculas de sinalização pode ser uma estratégia viável para combater infecções resistentes às terapias convencionais e para reduzir os efeitos colaterais destes compostos.

Portanto, o objetivo deste trabalho foi avaliar a atividade antimicrobiana/antibiofilme e a viabilidade celular de nanopartículas de prata (NPsAg) obtidas por uma síntese '*green*' associadas ou não ao β-glicerofosfato de cálcio (GPCa) contra *Streptococcus mutans* e espécies de *Candida* (cepas de referência e isolados clínicos orais incluindo cepas resistentes ao fluconazol). O efeito destes nanocompostos em combinação com o tirosol, fluconazol, nistatina e anfotericina B também foi determinado. Além disso, nós avaliamos comparativamente as alterações do transcriptoma de células de *C. glabrata* CBS138 após exposição às NPsAg e ao Íon prata.

Para abordar o tema proposto, o estudo será apresentado em seis capítulos distintos, conforme descrito abaixo:

- Capítulo 1: **"Green synthesis of silver nanoparticles combined to calcium glycerophosphate: antimicrobial and antibiofilm activities"** (Artigo publicado no periódico *Future Microbiology*);
- Capítulo 2: **"Evaluation of silver nanoparticles associated or not to calcium glycerophosphate on fibroblast viability and cytokine production"** (Artigo formatado nas normas do periódico *Clinical Oral Investigations* - www.springer.com/medicine/dentistry/journal/784?detailsPage=pltci_1060698);

- Capítulo 3: **"Antimicrobial activity of compounds containing silver nanoparticles and calcium glycerophosphate in combination with tyrosol"** (Artigo formatado nas normas do periódico *Journal of Applied Microbiology* - onlinelibrary.wiley.com/page/journal/13652672/homepage/forauthors.html);
- Capítulo 4: **"Green silver nanoparticles combined with tyrosol as potential oral antimicrobial therapy"** (Artigo formatado nas normas do periódico *Journal of Applied Microbiology* – onlinelibrary.wiley.com/page/journal/13652672/homepage/forauthors.html);
- Capítulo 5: **"Green-synthesized silver nanoparticles are strong inhibitors of *Candida albicans* and *Candida glabrata*"** (Artigo formatado nas normas do periódico *Medical Micology* – academic.oup.com/mmy/pages/Manuscript_Preparation);
- Capítulo 6: **"Resposta transcriptômica de *Candida glabrata* após exposição às nanopartículas de prata sintetizadas por uma via '*green*'".**

REFERÊNCIAS BIBLIOGRÁFICAS

1. Wade WG. The oral microbiome in health and disease. *Pharmacol Res*. 2013; 69(1): 137-143.
2. Roberts FA, Darveau RP. Microbial protection and virulence in periodontal tissue as a function of polymicrobial communities: symbiosis and dysbiosis. *Periodontol 2000*. 2015; 69(1): 18-27.
3. Whitford GM, Wasdin JL, Schafer TE, Adair SM. Plaque fluoride concentrations are dependent on plaque calcium concentrations. *Caries Res*. 2002; 36(4): 256-265.
4. Balakrishnan M, Simmonds RS, Tagg JR. Dental caries is a preventable infectious disease. *Aus Dent J*. 2000; 45(4): 235-245.
5. Krzyściak W, Jurczak A, Kościelniak D, Bystrowska B, Skalniak A. The virulence of Streptococcus mutans and the ability to form biofilms. *Eur J Clin Microbiol Infect Dis*. 2014; 33(4): 499-515.
6. Raja M, Hannan A, Ali K. Association of oral candidal carriage with dental caries in children. *Caries Res*. 2010; 44(3): 272-276.

7. Yang XQ, Zhang Q, Lu LY, Yang R, Liu Y, Zou J. Genotypic distribution of Candida albicans in dental biofilm of Chinese children associated with severe early childhood caries. *Arch Oral Biol*. 2012; 57(8): 1048-1053.
8. Diaz PI, Xie Z, Sobue T, *et al*. Synergistic interaction between Candida albicans and commensal oral streptococci in a novel in vitro mucosal model. *Infect Immun*. 2012; 80(2): 620-632.
9. Xu H, Jenkinson HF, Dongari-Bagtzoglou A. Innocent until proven guilty: mechanisms and roles of Streptococcus-Candida interactions in oral health and disease. *Mol Oral Microbiol*. 2014; 29(3): 99-116.
10. Metwalli KH, Khan SA, Krom BP, Jabra-Rizk MA. Streptococcus mutans, Candida albicans, and the human mouth: a sticky situation. *PLoS Pathog*. 2013; 9(10): e1003616.
11. Millsop JW, Fazel N. Oral candidiasis. *Clin Dermatol* 2016; 34(4): 487-94.
12. Moyes DL, Richardson JP, Naglik JR. Candida albicans-epithelial interactions and pathogenicity mechanisms: scratching the surface. *Virulence* 2015; 6(4): 338-46.
13. Silva S, Rodrigues CF, Araujo D, Rodrigues ME, Henriques M. Candida Species Biofilms' Antifungal Resistance. *J Fungi (Basel)* 2017; 3(1).
14. Rautemaa R, Ramage G. Oral candidosis--clinical challenges of a biofilm disease. *Crit Rev Microbiol* 2011; 37(4): 328-36.
15. Miranda-Cadena K, Marcos-Arias C, Mateo E, *et al*. Prevalence and antifungal susceptibility profiles of Candida glabrata, Candida parapsilosis and their close-related species in oral candidiasis. *Arch Oral Biol* 2018; 95: 100-107.
16. Tscherner M, Schwarzmüller, T., Kuchler, K. Pathogenesis and antifungal drug resistance of the human fungal pathogen Candida glabrata. *Pharmaceuticals (Basel)* 2011; 4: 169-186.
17. Bennett JE, Izumikawa K, Marr KA. Mechanism of increased fluconazole resistance in Candida glabrata during prophylaxis. *Antimicrob Agents Chemother* 2004; 48(5): 1773-7.
18. Noronha VT, Paula AJ, Durán G, et al. Silver nanoparticles in dentistry. *Dent Mater*. 2017; 33(10): 1110-1126.
19. Ramasamy M, Lee J. Recent Nanotechnology Approaches for Prevention and Treatment of Biofilm-Associated Infections on Medical Devices. *Biomed Res Int* 2016; 1851242.

20. Chairuangkitti P, Lawanprasert S, Roytrakul S, *et al*. Silver nanoparticles induce toxicity in A549 cells via ROS-dependent and ROS-independent pathways. *Toxicol In Vitro* 2013; 27(1): 330-338.
21. Fernandes GL, Delbem ACB, do Amaral JG, *et al.* Nanosynthesis of Silver-Calcium Glycerophosphate: Promising Association against Oral Pathogens. *Antibiotics (Basel)* 2018; 7(3).
22. Souza JA, Barbosa DB, Berretta AA, *et al.* Green synthesis of silver nanoparticles combined to calcium glycerophosphate: antimicrobial and antibiofilm activities. *Future Microbiol* 2018; 13: 345-357.
23. Perez-Diaz MA, Boegli L, James G, *et al.* Silver nanoparticles with antimicrobial activities against Streptococcus mutans and their cytotoxic effect. *Mater Sci Eng C Mater Biol Appl* 2015; 55: 360-6.
24. Fernandes RA, Berretta AA, Torres EC, *et al.* Antimicrobial Potential and Cytotoxicity of Silver Nanoparticles Phytosynthesized by Pomegranate Peel Extract. *Antibiotics (Basel)* 2018; 7(3).
25. Chowdhury NR, MacGregor-Ramiasa M, Zilm P, Majewski P, Vasilev K. 'Chocolate' silver nanoparticles: Synthesis, antibacterial activity and cytotoxicity. *J Colloid Interface Sci* 2016; 482: 151-158.
26. Soares M, Correa RO, Stroppa PHF, *et al.* Biosynthesis of silver nanoparticles using Caesalpinia ferrea (Tul.) Martius extract: physicochemical characterization, antifungal activity and cytotoxicity. *PeerJ* 2018; 6: e4361.
27. Monteiro DR, Takamiya AS, Feresin LP, *et al.* Susceptibility of Candida albicans and Candida glabrata biofilms to silver nanoparticles in intermediate and mature development phases. *J Prosthodont Res* 2015; 59(1): 42-8.
28. Szweda P, Gucwa K, Kurzyk E, *et al.* Essential Oils, Silver Nanoparticles and Propolis as Alternative Agents Against Fluconazole Resistant Candida albicans, Candida glabrata and Candida krusei Clinical Isolates. *Indian J Microbiol* 2015; 55(2): 175-83.
29. Monteiro DR, Silva S, Negri M, *et al.* Silver nanoparticles: influence of stabilizing agent and diameter on antifungal activity against Candida albicans and Candida glabrata biofilms. *Lett Appl Microbiol* 2012; 54(5): 383-91.
30. Wady AF, Machado AL, Zucolotto V, *et al.* Evaluation of Candida albicans adhesion and biofilm formation on a denture base acrylic resin containing silver nanoparticles. *J Appl Microbiol* 2012; 112(6): 1163-72.

31. Franci G, Falanga A, Galdiero S, *et al*. Silver nanoparticles as potential antibacterial agentes. *Molecules* 2015; 20: 8856-8874.
32. Ravishankar Rai V, Jamuna Bai A. Nanoparticles and their potential application as antimicrobials. In *Science against Microbial Pathogen: Communicating Current Research and Technological Advances*; Méndez-Vilas A., Ed.; Formatex Research Center: Badajoz, Spain, 2011; Volume 2, pp. 197-202.
33. Goodsell DS. *Bionanotechnology: Lessons from Nature*. John Wiley & Sons Publication, 2014.
34. Ali M, Kim B, Belfield KD, *et al*. Green synthesis and characterization of silver nanoparticles using Artemisia absinthium aqueous extract – A comprehensive study. *Mater Sci Eng C Mater Biol Appl*. 2016; 58: 359-365.
35. Roy N, Gaur A, Jain A, Bhattacharya S, Rani V. Green synthesis of silver nanoparticles: an approach to overcome toxicity. *Environ Toxicol Pharmacol*. 2013; 36(3): 807-812.
36. Rao A, Mahajan K, Bankar A, *et al*. Facile synthesis of size-tunable gold nanoparticles by pomegranate (*Punica granatum*) leaf extract: Applications in arsenate sensing. *Mater Res Bull*. 2013; 48(3): 1166-1173.
37. Jurenka JS. Therapeutic applications of pomegranate (Punica granatum L.): a review. *Altern Med Rev*. 2008; 13(2): 128-144.
38. Lansky EP, Newman RA. Punica granatum (pomegranate) and its potential for prevention and treatment of inflammation and cancer. *J Ethnopharmacol*. 2007; 109(2): 177-206.
39. Pande G, Akoh CC. Antioxidant capacity and lipid characterization of six Georgia-grown pomegranate cultivars. *J Agric Food Chem*. 2009; 57(20): 9427-9436.
40. Nasiriboroumand M, Montazer M, Barani H. Preparation and characterization of biocompatible silver nanoparticles using pomegranate peel extract. *J Photochem Photobiol B*. 2018; 179: 98-104.
41. Goudarzi M, Mir N, Mousavi-Kamazani M, Bagheri S, Salavati-Niasari M. Biosynthesis and characterization of silver nanoparticles prepared from two novel natural precursors by facile thermal decomposition methods. *Sci Rep*. 2016; 6: 32539.
42. Edison TJ, Sethuraman MG. Biogenic robust synthesis of silver nanoparticles using Punica granatum peel and its application as a green catalyst for the reduction

of an anthropogenic pollutant 4-nitrophenol. *Spectrochim Acta A Mol Biomol Spectrosc*. 2013; 104: 262-264.

43. Ahmad N, Sharma S, Rai R. Rapid green synthesis of silver and gold nanoparticles using peels of *Punica granatum*. *Adv Mat Lett*. 2012; 3(5): 376-380.
44. Xu HH, Moreau JL, Sun L, Chow LC. Nanocomposite containing amorphous calcium phosphate nanoparticles for caries inhibition. *Dent Mater*. 2011; 27(8): 762-769.
45. Xie X, Wang L, Xing D, *et al*. Protein-repellent and antibacterial functions of a calcium phosphate rechargeable nanocomposite. *J Dent*. 2016; 52: 15-22.
46. Dalpasquale G, Delbem ACB, Pessan JP, *et al*. Effect of the addition of nano-sized sodium hexametaphosphate to fluoride toothpastes on tooth demineralization: an in vitro study. *Clin Oral Investig*. 2017; 21(5): 1821-1827.
47. Danelon M, Pessan JP, Souza-Neto FN, de Camargo ER, Delbem AC. Effect of fluoride toothpaste with nano-sized trimetaphosphate on enamel demineralization: An in vitro study. *Arch Oral Biol*. 2017; 78: 82-87.
48. Amaral JG, Freire IR, Valle-Neto EF, Cunha RF, Martinhon CC, Delbem AC. Longitudinal evaluation of fluoride levels in nails of 18-30-month-old children that were using toothpastes with 500 and 1,100 µg F/g. *Community Dent Oral Epidemiol*. 2014; 42(5): 412-419.
49. Zaze AC, Dias AP, Amaral JG, Miyasaki ML, Sassaki KT, Delbem AC. In situ evaluation of low-fluoride toothpastes associated to calcium glycerophosphate on enamel remineralization. *J Dent*. 2014; 42(12): 1621-1625.
50. Nagata ME, Delbem AC, Hall KB, Buzalaf MA, Pessan JP. Fluoride and calcium concentrations in the biofilm fluid after use of fluoridated dentifrices supplemented with polyphosphate salts. *Clin Oral Investig*. 2017; 21(3): 831-837.
51. Freire IR, Pessan JP, Amaral JG, Martinhon CC, Cunha RF, Delbem AC. Anticaries effect of low-fluoride dentifrices with phosphates in children: A randomized, controlled trial. *J Dent*. 2016; 50: 37-42.
52. Imai M, Hayashi Y. Ultrastructure of wound healing following direct pulp capping with calcium-beta-glycerophosphate (Ca-BGP). *J Oral Pathol Med*. 1993; 22(9): 411-417.
53. Inoue M. Physicochemical studies on calcium glycerophosphate. I. X-Ray diffraction study of calcium glycerophosphate crystals and their water of crystallization.*Chem Pharm Bull (Tokyo)*. 1980; 28(5): 5.

54. Takamiya AS, Monteiro DR, Bernabé DG, *et al*. *In Vitro* and *In Vivo* Toxicity Evaluation of Colloidal Silver Nanoparticles Used in Endodontic Treatments. *J Endod*. 2016; 42: 953-960.
55. Sun L, Liao K, Li Y, *et al*. Synergy between polyvinylpyrrolidone-coated silver nanoparticles and azole antifungal against drug-resistant Candida albicans. *J Nanosci Nanotechnol*. 2016; 16(3): 2325-2335.
56. Longhi C, Santos JP, Morey AT, *et al*. Combination of fluconazole with silver nanoparticles produced by Fusarium oxysporum improves antifungal effect against planktonic cells and biofilm of drug-resistant Candida albicans. *Med Mycol*. 2016; 54(4): 428-432.
57. Albuquerque P, Casadevall A. Quorum sensing in fungi – a review. *Med Mycol*. 2012; 50: 337-345.
58. Monteiro DR, Feresin LP, Arias LS, Barão VA, Barbosa DB, Delbem AC. Effect of tyrosol on adhesion of *Candida albicans* and *Candida glabrata* to acrylic surfaces. *Med Mycol*. 2015; 53: 656-665.
59. Arias LS, Delbem AC, Fernandes RA, Barbosa DB, Monteiro DR (2016) Activity of tyrosol against single and mixed-species oral biofilms. *J Appl Microbiol*. 2016; 120: 1240-1249.

CAPÍTULO 1

'*Green*' synthesis of silver nanoparticles combined to calcium glycerophosphate: antimicrobial and antibiofilm activities *

***** *Artigo publicado no periódico Future Microbiology*

'*Green*' synthesis of silver nanoparticles combined to calcium glycerophosphate: antimicrobial and antibiofilm activities

Running Head: Silver nanoparticles combined to calcium phosphate

José Antonio Santos Souza[1], Debora Barros Barbosa[1], Andresa Aparecida Berretta e Silva[2], Jackeline Gallo do Amaral[1], Luiz Fernando Gorup[3], Francisco Nunes de Souza Neto[4], Renan Aparecido Fernandes[5], Gabriela Lopes Fernandes[1], Emerson Rodrigues Camargo[4], Alessandra Marçal Agostinho[6], Alberto Carlos B. Delbem[1]

[1]São Paulo State University (UNESP), School of Dentistry, Araçatuba, São Paulo, Brazil.
[2]Laboratory of Research, Development and Innovation, APIS FLORA INDL. COML. LTDA., Ribeirão Preto, São Paulo, Brazil.
[3]Federal University of Grande Dourados, Dourados, Mato Grosso do Sul, Brazil.
[4]Federal University of São Carlos, São Carlos, São Paulo, Brazil.
[5]University Center of Adamantina (UNIFAI), Adamantina, São Paulo, Brazil.
[6]Michigan State University, East Lansing, Michigan, USA.

[*]Corresponding author:
Alberto Carlos Botazzo Delbem
São Paulo State University (UNESP), School of Dentistry
Department of Pediatric Dentistry and Public Health
Rua José Bonifácio, 1193.
16015-050 Araçatuba – SP
Brazil
Tel. +55 18 3636 3314
Fax +55 18 3636 3332
Email: alberto.delbem@unesp.br

'*Green*' synthesis of silver nanoparticles combined to calcium glycerophosphate: antimicrobial and antibiofilm activities

Abstract

Aim: To synthesize, characterize and evaluate the antimicrobial and antibiofilm activities of novel nanocomposites containing silver nanoparticles (AgNPs) associated or not to β-calcium glycerophosphate (CaGP). **Materials and Methods:** These nanocomposites were produced through a '*green*' route using extracts of different parts of pomegranate. Antimicrobial and antibiofilm properties against *Candida albicans* and *Streptococcus mutans* were determined by the minimum bactericidal/fungicidal concentration and biofilm density after treatments. **Results:** All extracts used were successful in producing AgNPs. Composites made with peel extracts showed the highest antimicrobial and antibiofilm activity against both microorganisms tested and performed similarly or even better than chlorhexidine. **Conclusion:** AgNPs associated or not to CaGP produced by a '*green*' process may be a promising novel antimicrobial agent against oral microorganisms.

Keywords: '*Green*' synthesis; Silver nanoparticles; Biofilm.

1. Introduction

Biofilms are defined as microbial communities that can harbor multiple bacterial and fungal species [1] embedded in extracellular polymeric substances, and are associated to virtually any surface on the planet including hard and soft tissues of humans [2]. In the oral cavity, in particular, the accumulation of acidogenic biofilms on tooth surfaces causes the dissolution of the enamel, a process known as demineralization [3] which, if maintained for prolonged periods, may lead to development of dental caries.

One of the main etiological agents in caries is *Streptococcus mutans* [4], a Gram-positive, facultative anaerobic, coccus-shaped bacterium, which is able to ferment several sugars, including sucrose, glucose, dextrose and lactose, producing lactic acid [5]. Recently, however, studies have demonstrated a significant association between *S. mutans* and *Candida albicans* and early childhood caries [6,7]. *C. albicans* is a commensal fungal species commonly colonizing human mucosal surfaces and, as *S. mutans*, presents high acidogenic and cariogenic potentials [8]. In 97% of children with caries, *C. albicans* can be isolated from dental lesions [9]. In fact, many *in vitro* studies have shown that *C. albicans* can enhance the adherence of *S. mutans* indicating a possible mechanism of interaction between them [10].

Controlling oral biofilm formation is not an easy task, but in recent years nanotherapeutics have been used with success by incorporating nanoparticles into several dental materials [11,12]. Silver nanoparticles (AgNPs) have gained importance in medicine, biology, physics and chemistry fields [13-15] due to antimicrobial effects against bacteria, fungi and viruses, and anti-inflammatory properties [16-19]. Sondi et al. (2004) demonstrated that AgNPs have excellent antibacterial activity against *Escherichia coli* [19]. In the presence of 10^5 CFU of *E. coli*, 10 µg cm^{-3} of AgNPs inhibited bacterial growth by 70%. In addition to this, SEM microscopy showed that the treated bacterial cells were significantly changed and presented major damage, which was characterized by the formation of "pits" in their cell walls. Moreover, Monteiro at al. (2011) showed that AgNPs ranging from 0.4 to 3.3 µg ml^{-1} exhibited fungicidal activity against *C. albicans* and *C. glabrata* [12].

Despite the promising antimicrobial effects, most techniques used to synthetize these nanoparticles are expensive and may affect the environment, biological systems and human health, because they involve the use of toxic and hazardous chemicals [20]. As a solution, '*green*' processes to synthetize AgNPs have been developed. This alternative utilizes biological systems, such as yeast, fungi, bacteria and plant extracts offering, thus,

a comparatively safer and eco-friendly approach in relation to the chemical methods, because no-toxic substances are used. The use of plant extracts is considered a popular technique due to many reasons that include vast and accessible reserves, large distribution, safe handling, availability of wide range of metabolites with strong reducing potentials and minimal waste and energy costs [20,21]. Extracts from plants, in particular, *Punica granatum L.* (pomegranate) have been widely used as reducing agents for Ag^+ ions [22-24]. Pomegranate is characterized by high phenolic contents – punicalagin, punicalin, ellagitannins, gallic acid, ellagic acid and anthocyanins – that exhibit favorable properties against various inflammatory disorders [25]. It is believed that the polyphenols, including ellagic acid and gallic acid, are the elements responsible for the reduction of Ag^+ ions and the stabilization of AgNP [26,27].

In addition to AgNPs, some calcium phosphate composites are being developed to prevent dental caries. These materials, which are similar to the mineral phase of hard tissues, can release calcium (Ca) and phosphate (P) ions to remineralize tooth lesions [28]. Several studies have demonstrated great results on enamel remineralization with polyphosphates [29-32]. Among these compounds, calcium glycerophosphate (CaGP), which is used medically as a source of Ca and P, has demonstrated anti-cariogenic properties [33,34].

Because of the complexity of oral biofilms, and considering the caries development process we predicted that the association of AgNPs with CaGP may result in a promising novel biomaterial with strong antimicrobial activity and desirable remineralization properties. Thus, the aim of this study was to synthesize and characterize nanocomposites produced through a '*green*' process using extracts of different parts of a *Punica granatum* associated to calcium glycerophosphate and evaluate their antimicrobial activity against planktonic cells and biofilms of *S. mutans* and *C. albicans*.

2. Materials and methods

2.1. Preparation of the extracts

Pomegranate samples were collected from a crop cultivated in Eixo (21º08'05.2'' S, 51º06'06.5'' W), Mirandópolis, São Paulo, Brazil, during May 2015. A specimen of the plant was kept in the Herbarium of the University of São Paulo, Ribeirão Preto, SP, Brazil. Extracts of the peels, leaves and seeds of pomegranate (*Punica granatum L.*) were produced.

Pomegranate fruits and leaves of the plants were washed with deionized water several times to remove impurities. The fruits were manually peeled and the seeds separated. Peels, leaves and seeds were dried in an incubator at 50°C, and ground into powder form using a blender [35]. The powder was then filtered through a 42-mesh sieve to obtain a standardized particle size [36].

A maceration and percolation process was employed to prepare the extracts of the different pomegranate parts [37]. For this, 30 g of each powder were macerated in 70% ethanol solution at room temperature for approximately 1 hour, followed by percolation. The extracts obtained were concentrated in a rotary evaporator under reduced pressure and controlled temperature (40-60°C) [36]. After solvent evaporation, the soft extract was resolubilized to be used as the reducing agent to synthesize the nanocomposites. In order to evaluate the efficiency of the extraction process, chemical analyzes of the extracts were performed.

2.2. Chemical analyzes of the extracts

Total phenolic concentration (TPC) in the extracts was measured using the Folin-Denis method as described by Singleton et al. (1965) [38]. Briefly, the extracts (70-95 mg) were diluted in deionized water (50 mL), homogenized and kept for 30 minutes in UV-bath. A volume of 0.5 mL of the samples was mixed with 2.5 mL of reagent of Folin-Denis followed by addition of 5.0 mL of 29% sodium carbonate. The samples were kept at room temperature (25°C) for 30 minutes. The mixture was vortexed and absorbance read at 760 nm using a UV-Visible spectrophotometer (Thermo Scientific Technologies, Madison, Wisconsin). TPC was calculated using a gallic acid (Sigma-Aldrich, Germany) standard curve and expressed as milligram gallic acid equivalent per gram.

For ellagic acid content (EAC) quantification, the extracts were weighed, dissolved in methanol and properly homogenized using a vortex. The samples remained for 30 minutes in a UV bath and, after this, they were filtered. Quantification of EAC was conducted on a HPLC (Shimadzu apparatus equipped with a CBM controller, LC-20AT quaternary pump, a SPD-M 20A diode-array detector and auto sampler, Shimadzu LC solution software, version 1.21 SP1) using a 100 mm x 2.6 mm Shim pack ODS C18 column [39,40]. The wavelength was set at 254 nm and separations were carried out at a column oven temperature of 25°C. The mobile phase used for ellagic acid consisted of methanol (A) and 2% acetic acid aqueous solution, at a flow rate adjusted to 1.0 mL min^{-1}. A gradient program was applied as follows: (0-7 min, 20-72.5% A; 7-7.5 min, 72.5-

95% A; 7.5-8.5 min, 95% A; 8.5-9 min, 95-20% A; 9-10 min, 20% A). The concentrations of ellagic acid were obtained using calibration curves. All assays were carried out in triplicates.

2.3. Synthesis and characterization of nanocomposites

Nanoparticles of β-calcium glycerophosphate (CaGP) were prepared at the Interdisciplinary Laboratory of Electrochemistry and Ceramics (Department of Chemistry, Federal University of São Carlos, São Carlos, SP, Brazil). Seventy grams of micrometric CaGP (80% β-isomer and 20% rac-α-isomer, CAS 58409-70-4, Sigma-Aldrich Chemical Co, St Louis, Missouri, USA) were ball milled using 500 g of zirconia spheres (diameter of 2 mm) in 1 L of isopropanol (Merck KGaA, Darmstadt, Deutschland, Germany). After 24 h, the resulting powder was separated from the alcoholic media and ground in a mortar. Scanning electron microscopy (SEM) was used to image the resulting nanoparticles of CaGP.

The '*green*' synthesis of silver nanoparticles and association with CaGP was conducted according to Gorup et al. (2011) [41] with some modifications. Initially, 0.042 g of silver nitrate ($AgNO_3$, Merck KGaA, Germany) were dissolved in 10 mL of deionized water heated to 90°C. Then, 0.25 g of CaGP and 0.5 mL of ammonium salt of polymethacrylic acid (NH-PM, Polysciences Inc., Warrington, Pensyvania, USA) were added followed, by 0.07 g of aqueous extracts of *Punica granatum* (peels, seeds or leaves). The reaction happened under constant agitation at 95°C for 10 minutes. The same process was repeated without the addition of CaGP to produce a control consisting of nanocomposites without CaGP. In total, six antimicrobial solutions were obtained: from peels extract: AgNP+CaGP (P1) and AgNP (P2), from leaves extract: AgNP+CaGP (L1) and AgNP (L2) and from seeds extract: AgNP+CaGP (S1) and AgNP (S2). During the study, all antimicrobial solutions were stored in dark bottles at 4°C.

The formation of the nanoparticles was confirmed by UV-Visible spectroscopy (spectrophotometer Shimadzu MultiSpec-1501, Shimadzu Corporation, Tokyo, Japan) and, later, by X-ray diffraction (XRD) (Difractometer Rigaku DMax-2000PC, Rigaku Corportation Tokyo, Japan). Scanning electron microscopy (SEM) on a Zeiss Supra 35VP microscope (S-360 microscope, Leo, Cambridge, Massachusetts, USA) was used in order to characterize the particles morphology. In addition, analyzes by Energy Dispersive X-Ray Detector (EDX) with mapping in 2D were also performed. The images were reconstructed by evaluating the energy release from the emission of some chemicals: Si

Kα, O Kα, P Kα, Ag Lα1 and Ca Kα and assigning random colors to highlight silver (Ag), oxygen (O), silicon (Si), phosphate (P) and calcium (Ca).

In addition, the Ag^+ content of the nanocompounds was determined using a specific electrode 9616 BNWP (Thermo Scientific, Beverly, MA, USA) connected to an ion analyzer (Orion 720 A^+; Orion Research Inc.). The combined electrode was previously calibrated with standards containing 6.25 to 100 µg Ag^+/mL and silver ionic strength adjuster solution (ISA, Cat. No. 940011) was used (1 mL of each sample/standard: 0.02 mL ISA). The results were expressed as µg Ag^+/mL.

2.4. Antimicrobial Activity

2.4.1. Minimum Fungicidal Concentration (MFC) and Minimum Bactericidal Concentration (MBC)

Initially, the minimum fungicidal/bactericidal concentrations (MFC and MBC) were determined using the microdilution method according to the Clinical Laboratory Standards Institute (documents M27-A2 and M07-A9) [42,43] with modifications. Two reference strains from the American Type Culture Collection (ATCC, University Boulevard, Manassas, USA) were used: *C. albicans* (ATCC 10231) and *S. mutans* (ATCC 25175). These microorganisms were subcultured on Sabouraud Dextrose Agar (SDA, Difco) aerobically and Mueller-Hinton (MH, Difco, Le Pont de Claix, France) at 5% of CO_2, respectively, both for 24 h at 35°C. The concentrations of the suspensions were adjusted in 0.85% saline solution to a turbidity equivalent to 0.5 McFarland Standard (1 x 10^6 for *C. albicans* UFC/mL and 1 x 10^8 for *S. mutans* UFC/mL). *S. mutans* was then diluted 20 times (5 x 10^6 UFC/mL) in MH supplemented with 5% of glucose while *C. albicans* was diluted 100 times (1 x 10^4 UFC/mL) in Roswell Park Memorial Institute medium (RPMI-1640, Sigma-Aldrich) to obtain the final inocula concentrations.

Plates were set up by adding a volume of 100 µL of each compound to the first column of 96 well microtiter plates (Costar, Tewksbury, MA, USA) containing 100 µL of RPMI for testing of *C. albicans* and 100 µL of MH with 5% glucose for testing of *S. mutans*. Sequentially, the compounds were serially diluted to a final concentration ranging from 1:2 to 1:512. Finally, 5 µL of *C. albicans* and 10 µL of *S. mutans* suspension were added to each well. The plates were incubated aerobically for 48 h for *C. albicans* and for 24 h in 5% CO_2 for *S. mutans* both at 35°C. After the incubation period, the contents of the wells were plated on SDA (for *C. albicans*) and BHI agar (for *S. mutans*) to determine the minimum fungicidal and bactericidal concentrations (MFC and MBC).

Ellagic acid (≥96.0%, CAS 476-66-4, Sigma-Aldrich Chemical Co, St Louis, Missouri, USA) and Punicalagin (≥98.0%, CAS 65995-63-3, Sigma-Aldrich Chemical Co, St Louis, Missouri, USA) also were tested, since the pomegranate peel extract presents these compounds in its composition. Three independent MFC/MBC assays were conducted for each compound/microorganism combination.

2.4.2. Biofilm killing

Twenty-four hour-old biofilms of *C. albicans* and *S. mutans* formed in 96-well polystyrene plates (Costar, Tewksbury, MA, USA) were challenged with the nanocomposites.

For the obtainment of the biofilms, *S. mutans* ATCC 25175 was subcultured on Brain Heart Infusion Agar (BHI; Difco, Le Point de Claix, France) at 5% CO_2, and *C. albicans* ATCC 10231 was subcultured on Sabouraud Dextrose Agar (SDA; Difco) both at 37°C for 24 h. Colonies were picked to inoculate 10 mL of BHI broth (Difco) for *S. mutans* and 10 mL of Sabouraud Dextrose Broth (SDB, Difco) medium for *C. albicans*. After incubation at 37°C for 18 h in the presence of 5% CO_2 for *S. mutans*, cells were harvested by centrifugation (8,000 rpm, 5 min), washed twice in phosphate buffered saline (PBS; pH 7 0.1 M) and concentrations adjusted in artificial saliva medium (AS) [12]. For *C. albicans*, we used 1 x 10^7 cells/mL and for *S. mutans* 1 x 10^8 cells/mL.

For biofilm formation, a volume of 200 µL of cell suspensions was placed into each well and incubated at 37°C in a 5% CO_2 atmosphere. After 24 h, the medium was aspirated and the wells washed with 200 µL of PBS to remove non-adherent cells before treatments.

To test killing, two antimicrobial solutions were chosen: P1 and P2. *S. mutans* biofilms were treated with 1,562.0, 781.0 and 312.4 mg Ag/L of the drug P1 which represents 10-fold, 5-fold and 2-fold the MBC's value respectively. For drug P2, biofilms were treated with 781.0, 390.5, 156.2, 78.1, 39.0 and 19.5 mg Ag/L, corresponding to 10 MBC, 5 MBC, 2 MBC, MBC, ½ MBC and ¼ MBC. *Candida* biofilms were treated with 1,562.0 (P1) and 3,125.0 (P2) mg Ag/L which translates to ten-fold the MFC's value. The antimicrobial solutions (P1 and P2) were diluted in AS medium to obtain the concentrations mentioned above. Positive and negative controls used were: chlorhexidine gluconate (CHG; Periogard, Colgate Palmolive Industrial Ltda, São Paulo, Brazil) at a concentration of 180 mg/L and AS medium, respectively.

After treatment for 24 h at 37°C in 5% CO_2, the solutions were aspirated and biofilms washed once with PBS to remove planktonic cells. Afterwards, the wells containing biofilms and PBS were scraped using cell scraper. Resulting suspensions were, then, transferred to an eppendorf tubes (1.0 mL), vigorously vortexed for 1 min to disaggregate biofilm cells, serially diluted in PBS and plated on SDA and BHI agar. The plates were incubated at 37°C and after 24-48 h the total number of colony-forming units (CFUs) per unit area (log_{10} cm^{-2}) of each well was quantified.

All assays were performed independently and in triplicate.

2.4.3. Statistical analysis

For statistical analysis, SigmaPlot 12.0 (Systat Software Inc., San Jose, CA, USA) was used, and the significance level was set at 5%. The content of ellagic acid and phenolic compounds at the pomegranate extracts and CFU data for *C. albicans* showed normal (Shapiro-Wilk test) and homogeneous (Cochran test) distributions, and, one-way ANOVA was performed, followed by the Student-Newman-Keuls test. CFU data for *S. mutans* did not pass the normality test, therefore the Kruskal-Wallis test was performed followed by the Student-Newman-Keuls test.

3. Results

3.1. Chemical characterization of the extracts

The concentrations of ellagic acid and phenolic compounds in the peels, leaves and seeds of pomegranate are presented in Table 1. The ellagic acid content in the peel extract was statistically higher than the values for the other extracts ($p<0.001$). However, the leaves extract presented the highest concentrations for phenolic compounds, when compared to the other extracts ($p<0.001$). The seeds extract presented the lowest values for both ellagic acid and phenolic compounds ($p<0.001$).

3.2. Structural characterization of nanocomposites

Figures 1a and 1b show the diffractograms of the nanocomposites obtained by the '*green*' via. The typical powder XRD pattern of the prepared CaGP showed diffraction peaks at 2θ = 6.38°, 12.5°, 26.4°, 41.1° and 44.3° (Figure 1a) and the corresponding crystallographic form (PDF № 1-17) [44]. The typical powder XRD pattern of the silver nanoparticles showed (Figure 1b) diffraction peaks at 2θ = 38.3°, 44.5°, 64.7°, 77.6° and 81.7°, which can be indexed to (111), (200), (220), (311) and (222) planes of pure silver

with face-centered cubic system (PDF № 04-0783). No alteration of the crystalline structure was observed in the nanocompounds when compared with the XRD patterns of CaGP and silver nanoparticles (PDF № 04-0783).

The nanocomposites produced in this study presented chocolate brown color indicating, thus, the formation of AgNPs. The reduction of silver ions by pomegranate extracts and formation of AgNPs was also confirmed by the presence of a plasmon band between 420 and 450 nm (UV-Vis) for all the nanocomposites (Figures 1c and 1d).

Figure 2A (a-f) shows SEM micrographs of the AgNPs produced with the different extracts. The NPs exhibited spherical shape and regular distribution with size of approximately 50 nm. In the nanocompounds P1, L1 e S1 the silver nanoparticles were decorating surface of the CaGP without a definite shape. Figure 2B shows the EDX images mapped in 2D of the compound P1 and set up by the analyzing the energy released from the issuance Si Kα, O Kα, P Kα, Ca Kα and Ag Kα, indicating the distribution of these elements on the demarcated area in the micrograph.

3.3. Ag^+ ions concentration

The results of the Ag^+ ions concentration and are shown in Table 2. The nanocomposites P1, P2, S1 and S2 presented the smallest values of Ag^+ ions when compared to the compounds L1 and L2.

3.4. Antimicrobial Activity

3.4.1. MFC and MBC

Table 3 presents the minimum fungicidal/bactericidal concentrations (MFC and MBC) of compounds against the microorganisms tested. *C. albicans* ATCC 10231 was more susceptible to the nanocomposites L1 and L2 while *S mutans* ATCC 25175 was more susceptible to the nanocomposites P1 and P2. In general, the CaGP-AgNPs presented lower MFC/MBC values than the solutions without the polyphosphate, with the exception of P1 for *S. mutans* and L1 for *C. albicans*. Ellagic acid and Punicalagin were not effective against *C. albicans* ATCC 10231 and *S. mutans* ATCC 25175.

3.4.2. Biofilm killing

Figure 3 shows the results of the quantification of cultivable biofilm cells. Treatment of *C. albicans* ATCC 10231 biofilms with the nanocomposites associated or not to CaGP (P1 and P2) did not result in statistically significant reduction of CFUs

compared to the negative control (Figure 3B). However, for *S. mutans* ATCC 25175, treatments significantly killed biofilms in a concentration-depend manner (Figure 3A). There was no statistical difference between P1 at a concentration of 312.4 mg Ag/L in comparison to the positive control (CHG). Concentrations above 312.4 mg Ag/L were more effective than the CHG resulting in significant reduction of CFUs when compared to the NC (negative control) ($p < 0.001$). For the P2 concentrations below 156.2 mg Ag/L were similar to CHG while, concentrations equal or higher than 156.2 mg Ag/L significantly reduced the numbers of CFUs ($p < 0.001$) even more effectively than the PC.

4. Discussion

In this study, we synthesized novel nanocomposites through a '*green*' route with extracts of pomegranate (*Punica granatum L*). Pomegranate extracts have been used to obtain a series of metallic nanoparticles, such as silver and gold [22,23,26]. The synthesis of nanoparticles using a '*green*' process is an alternative to traditional methods, with many advantages because it is an eco-friendly, clean, nontoxic and inexpensive method [14].

Plants have been used in the biosynthesis of nanoparticles as they have the capacity of producing a large variety of secondary metabolites with strong reducing potentials [20,45]. We utilized extracts of different parts of the pomegranate (peels, leaves and seeds) in order to obtain AgNPs since these extracts presented high concentrations of phenolic compounds, including ellagic acid and gallic acid, known for their antimicrobial properties [46]. These compounds are probably the elements responsible for the reduction of Ag^+ ions and the stabilization of AgNP [26,27]. The addition of CaGP to produce AgNP-CaGPs did not interfere with the reduction process of the Ag^+ ions. Sodagar et al. (2016) also synthesized a novel compound containing AgNPs and hydroxyapatite (HA) and similarly did not observe interference of the calcium compound in the production of the nanoparticles [47].

The first qualitative indication of nanoparticle synthesis is the color change of the reaction solution from yellow to brown due to surface plasmon vibration [48]. In our study, all nanocompounds had an immediate change in color, becoming chocolate brown. In addition, the quantification of Ag^+ ions in the compounds solutions showed a reduced presence of Ag^+ ions compared to the pre-synthesis mixture measurements indicating the conversion of Ag^+ ions into nanoparticles. The reduction of Ag^+ ions by pomegranate

extracts was also confirmed by the presence of a plasmon band (UV-Vis) between 420 and 450 nm for all composites, evidencing the formation of AgNPs [48]. The antioxidant activity of pomegranate extracts might be responsible for the reduction of the Ag^+ ions, since plant extracts contain phytochemicals (ellagic acid, gallic acid and punicalagin) and secondary metabolites [48] that lead to formation of H^+ radicals, which reduce the size of silver to nanosize [22].

Calcium phosphate composites have been developed to release calcium and phosphate ions to remineralize tooth lesions because of their demonstrated anti-cariogenic properties [49-52,30,34]. In fact, Hannig *et al*. (2010) reported the successful remineralization of incipient enamel lesions with AgNPs combined with hydroxyapatite [53]. Therefore, one of the goals of this study was to combine the potential remineralization benefits of CaGP to the microbial killing effects of nanoparticles. The novel composites obtained through the '*green*' route here presented possess antimicrobial activity against *S. mutans* and *C. albicans*. Some solutions, namely L1 and L2 were more effective against *C. albicans*, which can be explained by the higher concentration of Ag^+ ions present in these compounds in comparison to the others where a greater conversion of Ag^+ ions to nanoparticles was achieved. Literature reports that ionic silver presents notable antimicrobial activity [54,55] despite the associated cytotoxicity [56,57].

Although the antimicrobial mode of action of nanoparticles is not completely understood it has been suggested that the interaction of silver with thiol groups of proteins on the cell wall increases the membrane permeability leading to pore formation and thereby causing bacterial death [58-61]. On the other hand, activity against *S. mutans* required a higher concentration of AgNPs in these compounds (L1 and L2). Probably, this fact is related with particle size. The compounds L1 and L2 presented larger particles in relation to the other compounds. The literature reveals that smaller particles penetrate more easily through cell membrane, interacting with intracellular materials and finally resulting in cell destruction in the process of multiplication [48]. Some authors also have reported that Gram-negative bacteria are more susceptible to AgNPs compared with Gram-positive bacteria [48], because Gram-positive bacteria possess a three-dimensional peptidoglycan layer of ~ 80 nm (10 times thicker than Gram-negative bacteria) [62-65].

Microorganisms can form structured, coordinated and functional communities consisted of adherent cells (sessile cells) called biofilms that pose a major clinical concern due to antimicrobial tolerance. Many antimicrobial agents, who are effective against free living planktonic bacterial cells, are ineffective against the same species growing in a

biofilm state. This has motivated the scientific community to search for agents capable of eradicating these resistant bacterial phenotypes. The challenge is extended to developing formulations suitable for oral use and efficient not only against microorganisms causing dental caries and denture stomatitis [65] but also capable of preventing and reverting enamel demineralization. In this study, a model of biofilm formation on the wells of microtiter plates was used in order to evaluate the antimicrobial effects of selected AgNPs associated or not to CaGP against *S. mutans* and *C. albicans* preformed biofilms. The pomegranate was just utilized to produce AgNPs and the phenolic compounds present in the pomegranate (ellagic acid and punicalagin) were previously tested and did not present antimicrobial effect. The nanocomposites P1 and P2 were chosen to be tested against biofilms because presented low MFC (for *C. albicans*) and MCB (for *S. mutans*) values. These nanocomposites were effective against *S. mutans* 24-hour biofilms with results similar or even better than chlorhexidine, which is the gold standard in terms of oral antiseptics. Furthermore, our results indicated that there was a dose-dependent inhibitory effect both for P1 and P2. It can be also observed that the presence of calcium glycerophosphate reduced the effect of the nanoparticles. It might have occurred because AgNPs were decorating the surface of the glycerophosphate and, therefore, were are not completely available. However, a pilot study conducted by our research group showed that the concentration of 312.4 mg Ag/L (that reduced the CFU similarly to chlorhexidine) of the antimicrobial solution P1 was not toxic to odontoblastic cells [Botazzo Delbem AC, Barbosa DB Unpublished data]. One hypothesis to explain the effect of AgNPs against *S. mutans* is their interaction with the bacterial cell membrane. It induces formation of pores in the membrane, with consequent internalization of NPs, and then causes further damage to the cells due to their interaction with both intracellular proteins and DNA affecting the cell's ability to replicate [67,68]. Another hypothesis of how the nanoparticles affects the cells is that they the release active silver ions that interact with proteins and receptors in the cell membranes [68].

AgNPs have shown efficacy against *C. albicans* [69,70], by disturbing the membrane and creating pores; provoking, thus, cellular apoptosis [71]. Interestingly, in our study, composites P1 and P2 were not effective against *C. albicans* preformed biofilms (Fig. 2). Biofilms are enclosed in a self-produced protective extracellular matrix which can hamper the penetration of the AgNPs. Lara *et al*. (2015) demonstrated that this matrix may contribute to the reduced susceptibility of preformed biofilms to AgNPs [71]. Another factor that can explain its resistance to NPs is the presence of persister cells. This

mechanism is observed in chronic infections [72] and, recently, has gathered special attention in fungal biofilms [73]. Persister cells are “dormant variants” of regular cells that form in microbial populations and are able to survive even in the presence of antibiotics well above the MIC [74,75]. Moreover, *C. albicans* presents a cell wall besides a cellular membrane. The cell wall is essential to nearly every aspect of the biology and pathogenicity of fungi, with pivotal functions in adhesion properties and morphogenetic conversions and it is composed mostly of glucans, chitin and mannoproteins [76]. These characteristics may hinder the effect of AgNPs.

5. Conclusion

Here we described the successful synthesis of novel AgNPs associate to CaGP using a ‘*green*’ process with pomegranate extracts. In conclusion, the compounds possess antimicrobial and antibiofilm activity against important microorganisms causing caries and candidiasis, and may be a promising novel biomaterial in dental applications. Additional studies are necessary to evaluate their effect against mixed biofilms, ability to remineralize enamel and cytotoxicity.

6. Future perspective

This study shows that it is possible to obtain a promising novel biomaterial with strong antimicrobial activity (silver nanoparticles) and desirable remineralization properties (calcium phosphate – β-calcium glycerophosphate). Moreover, we utilized a ‘*green*’ synthesis (different extracts of pomegranate were utilized) that is a comparatively safer and eco-friendly approach in relation to other techniques that involve the use of toxic and hazardous chemicals. Oral Bacteria and Candida species have been reported in many studies that are resistant to antimicrobial agents. Thus, studies with AgNPs synthesized through a ‘*green*’ via and oral clinical isolates are being planned by our research group.

7. Financial & competing interests disclosure

This work was supported by CAPES Foundation, Ministry of Education of Brazil (Processes 88881.030445/2013-01 and 88887.068358/2014-00) and the São Paulo Research Foundation (FAPESP, process 2015/00825-5). The authors have no other relevant affiliations or financial involvement with an organization or entity with a

financial interest in or financial conflict with the subject matter or materials discussed in the manuscript.

8. Executive Summary

- One of the main etiological agents in caries is *Streptococcus mutans*, a Gram-positive, facultative anaerobic, coccus-shaped bacterium which is able to ferment several sugars, including sucrose, glucose, dextrose and lactose, producing lactic acid.
- Recently, studies have demonstrated a significant association between *S. mutans* and *Candida albicans* and early childhood caries.
- Controlling oral biofilm formation is not an easy task but in recent years, nanotherapeutics have been used with success by incorporating nanoparticles into several dental materials.
- Because of the complexity of oral biofilms and the caries development process we believe that the association of silver nanoparticles (AgNPs) with β-calcium glycerophosphate (CaGP) can result in a promising novel biomaterial with strong antimicrobial activity and desirable remineralization properties.
- Nanocomposites (AgNP-CaGP) were synthesized through a '*green*' route with different extracts of pomegranate.
- Compounds possess antimicrobial/antibiofilm activity against *S. mutans* and *C. albicans*.
- Composites made with peel extracts showed similarly or even better than chlorhexidine.
- The association AgNP-CaGP may be a promising biomaterial in dental applications. However, additional studies are necessary to evaluate their effect against mixed biofilms, ability to remineralize enamel and cytotoxicity.

9. References

Papers of special note have been highlighted as: * of interest; ** of considerable interest

1. Kuboniwa M, Tribble GD, Hendrickson EL, Amano A, Lamont RJ, Hackett M. Insights into the virulence of oral biofilms: discoveries from proteomics. *Expert Rev. Proteomics.* 9(3), 311-323 (2012).
2. Jakubovics NS, Kolenbrander PE. The road to ruin: the formation of disease-associated oral biofilms. *Oral Dis.* 16(8), 729-739 (2010).
3. Senneby A, Davies JR, Svensäter G, Neilands J. Acid tolerance properties of dental biofilms in vivo. *BMC Microbiol.* 17(1):165 (2017).
4. Krzyściak W, Jurczak A, Kościelniak D, Bystrowska B, Skalniak A. The virulence of *Streptococcus mutans* and the ability to form biofilms. *Eur. J. Clin. Microbiol. Infect. Dis.* 33(4), 499-515 (2014).
5. Shimada A, Noda M, Matoba Y, Kumagai T, Kozai K, Sugiyama M. Oral lactic acid bacteria related to the occurrence and/or progression of dental caries in Japanese preschool children. *Biosci. Microbiota Food Health.* 34(2), 29-36 (2015).
6. Willems HM, Kos K, Jabra-Risk MA, Krom BP. Candida albicans in oral biofilms could prevent caries. *Pathog. Dis.* 74(5), pii: ftw039 (2016).
7. Fragkou S, Balasouli O, Tsuzukibashi A *et al*. *Streptococcus mutans, Streptococcus sobrinus* and *Candida albicans* in oral samples from caries-free and caries-active children. *Eur. Arch. Paediatric. Dent.* 17(5), 367-375 (2016).
   ** Describes the occurrence of *S. mutans, S. sobrinus* and *C. albicans* in dental plaque of caries-active children.
8. Metwalli KH, Khan SA, Kromp BP, Jabra-Rizk MA. *Streptococcus mutans*, *Candida albicans*, and the human mouth: a sticky situation. *PLoS Pathog.* 9(10), e1003616 (2013).
9. Klinke T, Guggenheim B, Klimm W, Thurnheer T. Dental caries in rats associated with *Candida albicans*. *Caries Res.* 45(2), 100-106 (2011).
10. Gregoire S, Xiao J, Silva BB *et al*. Role of glucosyltransferase B in interactions of Candida albicans with Streptococcus mutans and with an experimental pellicle on hydroxyapatite surfaces. *Appl. Environ. Microbiol.* 77(18), 6357-6367 (2011).
11. Noronha VT, Paula AJ, Durán G *et al*. Silver nanoparticles in dentistry. *Dent. Mater.* S0109-5641(17), 30376-30377 (2017) [Epud ahead of print].
12. Monteiro DR, Gorup LF, Silva S *et al*. Silver coloidal nanoparticles: antifungal effect against adhered cells and biofilms of *Candida albicans* and *Candida glabrata*. *Biofouling.* 27(7), 711-719 (2011).

* Describes the effect of silver nanoparticles against *Candida albicans* adhered cells and biofilms.

13. Jahromi MAM, Zangabad PS, Basri SMM *et al*. Nanomedicine and advanced technologies for burns: Preventing infection and facilitating wound healing. *Adv. Drug Deliv. Rev.* S0169-409X(17), 30129-30131 (2017) [Epud ahead of print].
14. Krishna IM, Reddy GB, Veerabhadram G, Madhusudhan A. Eco-friendly green synthesis of silver nanoparticles using salmalia malabarica: synthesis, characterization, antimicrobial and catalytic activity studies. *Appl. Nanosci.* 6(5), 681-689 (2016).
15. Kushwaha A, Singh VK, Bhartariya J, Singh P, Yasmeen K. Isolation and identification of *E. coli* bacteria for the synthesis of silver nanoparticles: Characterization of the particles and study of antibacterial activity. *Eur. J. Exp. Biol.* 5(1), 65-70 (2015).
16. Beyth N, Haddad YH, Domb A, Khan W, Hazan R. Alternative antimicrobial approach: nano-antimicrobial materials. *Evid. Based Complement. Alternat. Med.* 2015:246012 (2015).
17. Nam G, Rangasamy S, Purushothaman B, Song JM. The application of bactericidal silver nanoparticles in wound treatment. *Nanomater. Nanotechno.* 1, 5-23 (2015).
18. Tran, HV, Tran, LD, Ba CT. *et al*. Synthesis, characterization, antibacterial and antiproliferative activities of monodisperse chitosan- based silver nanoparticles. *Colloids and Surfaces A: Physicochem. Eng. Aspects.* 360, 32-40 (2010).
19. Sondi I, Salopek-Sondi B. Silver nanoparticles as antimicrobial agent: a case study on *E. coli* as a model for Gram-negative bacteria. *J. Colloid. Interface Sci.* 275(1), 177-182 (2004).
20. Ali M, Kim B, Belfield KD, Norman D, Brennan M, Ali GS. Green synthesis and characterization of silver nanoparticles using *Artemisia absinthium* aqueous extract – A comprehensive study. *Mater. Sci. Eng. C Mater. Biol. Appl.* 58, 359-365 (2016).
21. Roy N, Gaur A, Jain A, Bhattacharya S, Rani V. Green synthesis of silver nanoparticles: an approach to overcome toxicity. *Environ. Toxicol. Pharmacol.* 36(3), 807-812 (2013).
22. Ahmad N, Sharma S, Rai R. Rapid green synthesis of silver and gold nanoparticles using peels of *Punica granatum*. *Adv. Mat. Lett.* 3, 376-380 (2012).

** Describes a simple and eco-friendly biosynthesis of silver nanoparticles using Pomegranate peel extracts as the reducing agent.

23. Gnanajobitha G, Rajeshkumar S, Annadurai G, Kannan C. Preparation and characterization of fruit-mediated silver nanoparticles using pomegranate extract and assessment of its antimicrobial activities. *J. Environ. Nanotechnol.* 2(1), 04-10 (2013).
24. Nadagouda MN, Iyanna N, Lalley J *et al*. Synthesis of silver and gold nanoparticles using antioxidants from blackberry, blueberry, pomegranate and turmeric extracts. *ACS Sustainable Chem. Eng.* 2(7), 1717-1723 (2014).
25. Shaygannia E, Bahmani M, Zamanzad B, Rafieian-Kopaei M. A review study on Punica granatum L. *J. Evid. Based Complementary Altern. Med.* 21(3): 221-227 (2016).
26. Edison TJI, Sethuraman MG. Biogenic robust synthesis of silver nanoparticles using Punica granatum peel and its application as a green catalyst for the reduction of an anthropogenic pollutant 4-nitrophenol. *Spectrochim. Acta A Mol. Biomol. Spectrosc.* 104, 262-264 (2013).
27. Kumari A, Guliani A, Singla R, Yadav R, Yadav SK. Silver nanoparticles synthesized using plant extracts show strong antibacterial activity. *IET Nanobiotechnol.* 9(3), 142-152 (2015).
28. Xie X, Wang L, Xing D *et al*. Protein-repellent and antibacterial functions of a calcium phosphate rechargeable nanocomposite. *J. Dent.* 52, 15-22 (2016).
29. Amaral JG, Freire IR, Valle-Neto EF, Cunha RF, Martinhon CC, Delbem AC. Longitudinal evaluation of fluoride levels in nails of 18-30-month-old children that were using toothpastes with 500 and 1,100 µg F/g. *Community Dent. Oral Epidemiol.* 42(5): 412-419 (2014).
30. Zaze AC, Dias AP, Amaral JG, Miyasaki ML, Sassaki KT, Delbem AC. In situ evaluation of low-fluoride toothpastes associated to calcium glycerophosphate on enamel remineralization. *J. Dent.* 42(12), 1621-1625 (2014).
31. Dalpasquale G, Delbem ACB, Pessan JP *et al*. Effect of the addition of nano-sized sodium hexametaphosphate to fluoride toothpastes on tooth demineralization: an in vitro study. *Clin. Oral Investig.* 21(5), 1821-1827 (2017).
32. Danelon M, Pessan JP, Souza-Neto FN, de Camargo ER, Delbem AC. Effect of fluoride toothpaste with nano-sized trimetaphosphate on enamel demineralization: An in vitro study. *Arch. Oral Biol.* 78, 82-87 (2017).

33. Nagata ME, Delbem AC, Hall KB, Buzalaf MA, Pessan JP. Fluoride and calcium concentrations in the biofilm fluid after use of fluoridated dentifrices supplemented with polyphosphate salts. *Clin. Oral Investig.* 21(3), 831-837 (2017).
34. Freire IR, Pessan JP, Amaral JG, Martinhon CC, Cunha RF, Delbem AC. Anticaries effect of low-fluoride dentifrices with phosphates in children: A randomized, controlled trial. *J. Dent.* 50, 37-42 (2016).

    * This paper reports that calcium glycerophosphate has anti-cariogenic properties.
35. Fawole OA, Makunga NP, Opara UL. Antibacterial, antioxidant and tyrosinase-inhibition activities of pomegranate fruit peel methanolic extract. *BMC Complement. Altern. Med.* 30, 12:200 (2012).
36. Rocha BA, Bueno PC, Vaz MM *et al*. Evaluation of a Propolis Water Extract Using a Reliable RP-HPLC Methodology and In Vitro and In Vivo Efficacy and Safety Characterization. *Evid. Based Complement. Alternat. Med.* 2013:670451 (2013).
37. Abreu Miranda M, Lemos M, Alves Cowart K *et al*. Gastroprotective activity of the hydroethanolic extract and isolated compounds from the leaves of Solanum cernuum Vell. *J. Ethnopharmacol.* 172, 421-429 (2015).
38. Singleton VL, Rossi JA. Colorimetry of total phenolics with phosphomolybdic-phosphotungstic acid reagents. *Am. J. Enol. Vitic.* 16, 144-158 (1965).
39. Masci A, Coccia A, Lendaro E, Mosca L, Paolicelli P, Cesa S. Evaluation of different extraction methods from pomegranate whole fruit or peels and the antioxidante and antiproliferative activity of the polyphenolic fraction. *Food Chem.* 202, 59-69 (2016).
40. Ferreira MR, Fernandes MT *et al*. Chromatographic and Spectrophotometric Analysis of Phenolic Compounds from Fruits of Libidibia ferrea Martius. *Pharmacoqn. Mag.* 12(2), 285-291 (2016).
41. Gorup LF, Longo E, Leite ER, Camargo ER. Moderating effect of ammonia on particle growth and stability of quasi-monodisperse silver nanoparticles synthesized by the Turkevich method. *J. Colloid. Interface Sci.* 360(2), 355-258 (2011).
42. National Committee for Clinical Laboratory Standards. Reference Method for Broth Dilution Antifungal Susceptibility Testing of Yeasts – Second Edition: Approved Standard M27-A2. *NCCLS*, Wayne, PA, USA (2002).
43. National Committee for Clinical Laboratory Standards. Methods for Dilution Antimicrobial Susceptibility Tests for Bacteria That Grow Aerobically – Ninth Edition: Approved Standard M07-A9. *NCCLS*, Wayne, PA, USA (2012).

44. Inoue M, In Y, Ishida T. Calcium binding to phospholipid: structural study of calcium glycerophosphate. *J. Lipid. Res.* 33(7), 985-994 (1992).
45. Mittal AK, Bhaumik J, Kumar S, Banerjee UC. Biosynthesis of silver nanoparticles: Elucidation of prospective mechanism and therapeutic potential. *J. Colloid. Interface Sci.* 415, 39-47 (2014).
46. Rosas-Burgos EC, Burgos-Hernández A, Noguera-Artiaga L *et al*. Antimicrobial activity of pomegranate peel extracts as affected by cultivar. *J. Sci. Food Agric.* 97(3), 802-810 (2017).
47. Sodagar A, Akhavan A, Hashemi E *et al*. Evaluation of the antibacterial activity of a conventional orthodontic composite containing silver/hydroxyapatite nanoparticles. *Prog. Orthod.* 17(1), 40 (2016).

    * Describes the antimicrobial properties of a new composite containing silver/hydroxyapatite nanoparticles.
48. Patil MP, Kim GD. Eco-friendly approach for nanoparticles synthesis and mechanism behind antibacterial activity of silver and anticancer activity of gold nanoparticles. *Appl. Microbiol. Biotechnol.* 101(1), 79-92 (2017).

    ** This review covers general information about the eco-friendly process for the synthesis of silver nanoparticles (AgNP) and focuses on mechanism of the antibacterial activity of AgNPs.
49. Weir MD, Ruan J, Zhang N *et al*. Effect of calcium phosphate nanocomposite on in vitro remineralization of human dentin lesion. *Dent. Mater.* S0109-5641(17), 30007-30016 (2017).

    * This study investigated the remineralization of human dentin lesions in vitro via restorations using nanocomposites containing calcium phosphate.
50. Weir MD, Chow LC, Xu HH. Remineralization of demineralizaed enamel via calcium phosphate nanocomposite. *J. Dent. Res.* 91(10), 979-984 (2012).
51. Melo MA, Weir MD, Rodrigues LK, Xu HH. Novel calcium phosphate nanocomposite with caries inhibition in a human in situ model. *Dent. Mater.* 29(2), 231-240 (2013).
52. do Amaral JG, Sassaki KT, Martinhon CC, Delbem AC. Effect of low-fluoride dentifrices supplemented with calcium glycerophosphate on enamel demineralization in situ. *Am. J. Dent.* 26(2), 75-80 (2013).

53. Hannig C, Hannig M. Natural enamel wear – a physiological source of hydroxyapatite nanoparticles for biofilm management and tooth repair? *Med. Hypotheses.* 74: 670-672 (2010).
54. Morrill K, May K, Leek D *et al*. Spectrum of antimicrobial activity associated with ionic colloidal silver. *J. Alter. Complement. Med.* 19(3), 224-231 (2013).
55. Belluco S, Losasso C, Patuzzi I *et al*. Silver as antimicrobial toward Listeria monocytogenes. *Front. Microbiol.* 7, 307 (2016).
56. Vrček IV, Žuntar I, Petlevski R *et al*. Comparison of in vitro toxicity of silver ions and silver nanoparticles on human hepatoma cells. *Environ. Toxicol.* 31(6), 679-692 (2016).
57. Galandáková A, Franková J, Ambrožová N *et al*. Effects of silver nanoparticles on human dermal fibroblasts and epidermal keratinocytes. *Hum. Exp. Toxicol.* 35(9), 946-957 (2016).
58. Durán N, Durán M, de Jesus MB, Seabra AB, Fávaro WJ, Nakazato G. Silver nanoparticles: A new view on mechanistic aspects on antimicrobial activity. *Nanomedicine.* 12(3), 789-799 (2016).
59. Pietrzak K, Glińska S, Gapińska M *et al*. Silver nanoparticles: a mechanism of action on moulds. *Metallomics.* 8(12), 1294-1302 (2016).
60. Durán N, Marcato PD, de Conti R, Alves OL, Costa FTM, Brocchi M. Potential use of silver nanoparticles on pathogenic bacteria, their toxicity and possible mechanisms of action. *J. Braz. Chem. Soc.* 21, 949-959 (2010).
61. Kaviya S, Santhanalakshmi J, Viswanathan B. Green synthesis of silver nanoparticles using *Polyalthia longifolia* leaf extract along with D-sorbitol: study of antibacterial activity. *J. Nanotechnol.* Article ID 152970 (2011).
62. Chaloupka K, Malam Y, Seifalian AM. Nanosilver as a new generation of nanoproduct in biomedical applications. *Trends Biotechnol.* 28(11), 580-588 (2010).
63. Gurunathan S, Hanm JW, Kwon DN, Kim JH. Enhanced antibacterial and antibiofilm activities of silver nanoparticles against Gram-negative and Gram-positive bacteria. *Nanoscale Res. Lett.* 9(1), 373 (2014).
64. Hungund BS, Dhulappanavar GR, Ayachit NH. Comparative evaluation of antibacterial activity of silver nanoparticles biosynthesized using fruit juices. *J. Nanomed. Nanotechnol.* 6, 271 (2015).

65. Choudhary MK, Kataria J, Cameotra SS, Singh J. A facile biomimetic preparation of highly stabilized silver nanoparticles derived from seed extract of Vigna radiata and evaluation of their antibacterial activity. *Appl. Nanosci.* 6, 105–111 (2016).
66. Arias LS, Delbem AC, Fernandes RA, Barbosa DB, Monteiro DR. Activity of tyrosol against single and mixed-species oral biofilms. *J. Appl. Microbiol.* 120(5), 1240-1249 (2016).
67. Rizzello L, Pompa PP. Nanosilver-based antibacterial drugs and devices: mechanisms, methodological drawbacks, and guidelines. *Chem. Soc. Rev.* 43(5), 1501-1518 (2014).
    * Describes the bactericidal effects of AgNPs.
68. Magalhães AP, Moreira FC, Alves DR *et al*. Silver nanoparticles in resin luting cements: Antibacterial and physiochemical properties. *J. Clin. Exp. Dent.* 8(4), e415-e422 (2016).
69. Monteiro DR, Takamiya AS, Feresin LP *et al*. Susceptibility of *Candida albicans* and *Candida glabrata* biofilms to silver nanoparticles in intermediate and mature development phases. *J. Prosthodont. Res.* 59(1), 42-48 (2015).
70. Selvaraj M, Pandurangan P, Ramasami N, Rajendran SB, Sangilimuthu SN, Perumal P *et al*. Highly potential antifungal activity of quantum-sized silver nanoparticles against *Candida albicans*. *Appl. Biochem. Biotechnol.* 173(1), 55-66 (2014).
71. Lara HH, Romero-Urbina DG, Pierce C, Lopez-Ribot JL, Arellano-Jiménez MJ, Jose-Yacaman M. Effect of silver nanoparticles on Candida albicans biofilms: an ultrastructural study. *J. Nanobiotechnology* 15, 13:91 (2015).
72. Fauvart M, De Groote VN, Michels J. Role of persister cells in chronic infections: clinical relevance and perspectives on anti-persister therapies. *J. Med. Microbiol.* 60(Pt 6), 699-709 (2011).
73. De Brucker K, De Cremer K, Cammue BP, Thevissen K. Protocol for determination of the persister subpopulation in Candida albicans biofilms. *Methods Mol. Biol.* 1333, 67-72 (2016).
74. Lewis K. Persister cells: molecular mechanisms related to antibiotic tolerance. *Handb. Exp. Pharmacol.* 211, 121-133 (2012).
75. Fisher RA, Gollan B, Helaine S. Persistent bacterial infections and persister cells. *Nat. Rev. Microbiol.* 15(8), 453-464 (2017).
76. Free SJ. Fungal cell wall organization and biosynthesis. *Adv. Genet.* 81, 33-82 (2013).

Tables

Table 1. Concentration of ellagic acid (mg/g) and phenolic compounds (mg GA/g) at the pomegranate extracts.

Extracts	Ellagic Acid	Polyphenols
Peels	4.2 ± 0.1^{a}	158.6 ± 4.5^{b}
Leaves	2.4 ± 0.1^{b}	286.5 ± 7.1^{a}
Seeds	1.3 ± 0.1^{c}	6.2 ± 0.1^{c}

Distinct superscript lowercase letters indicate statistical significance in each column (Student-Newman-Keuls test, $p < 0.001$). GA: gallic acid.

Table 2. Quantification of Ag^+ ions in the nanocomposites synthesized by the "*green*" route.

Extracts	GROUP	Composition	µg Ag^+/mL
Peels	P1	AgNP+CaGP	0.05
	P2	AgNP	0.11
Seeds	S1	AgNP+CaGP	0.08
	S2	AgNP	0.14
Leaves	L1	AgNP+CaGP	384.7
	L2	AgNP	286.8

Table 3. Minimum fungicidal concentration (MFC) and minimum bactericidal concentration (MBC) of the compounds against microorganisms tested.

Extracts	GROUP	Composition	MFC/MBC (mg/L)	
			C. albicans	***S. mutans***
Peels	P1	AgNP+CaGP	156.2	156.2
	P2	AgNP	312.5	78.1
Seeds	S1	AgNP+CaGP	312.5	156.2
	S2	AgNP	>1,250.0	625.0
Leaves	L1	AgNP+CaGP	9.8	625.0
	L2	AgNP	4.9	1,250.0
Ellagic Acid			>14.5	>14.5
Punicalagin			>555.1	>555.1

Figures

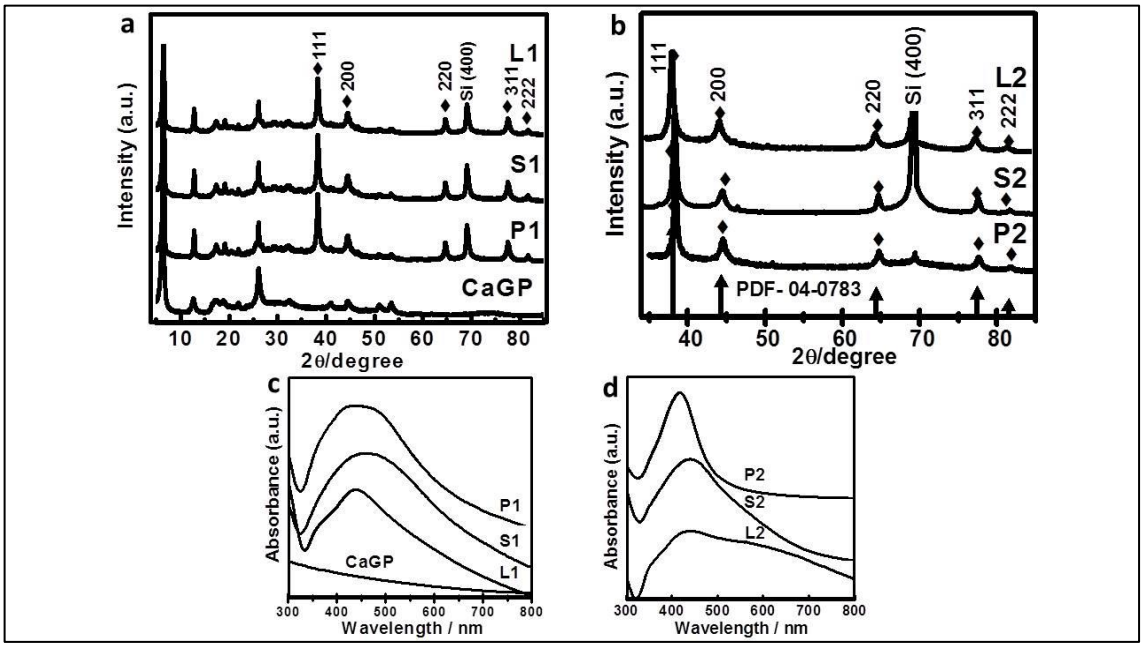

Figure 1: a) XRD pattern of the nanocomposites P1, S1 and L1 and CaGP; b) XRD pattern of the nanocomposites P2, S2 and L2; c) UV-Visible spectrum of the nanocomposites P1, S1, L1 and CaGP; d) UV-Visible spectrum of the nanocomposites P2, S2 and L2.

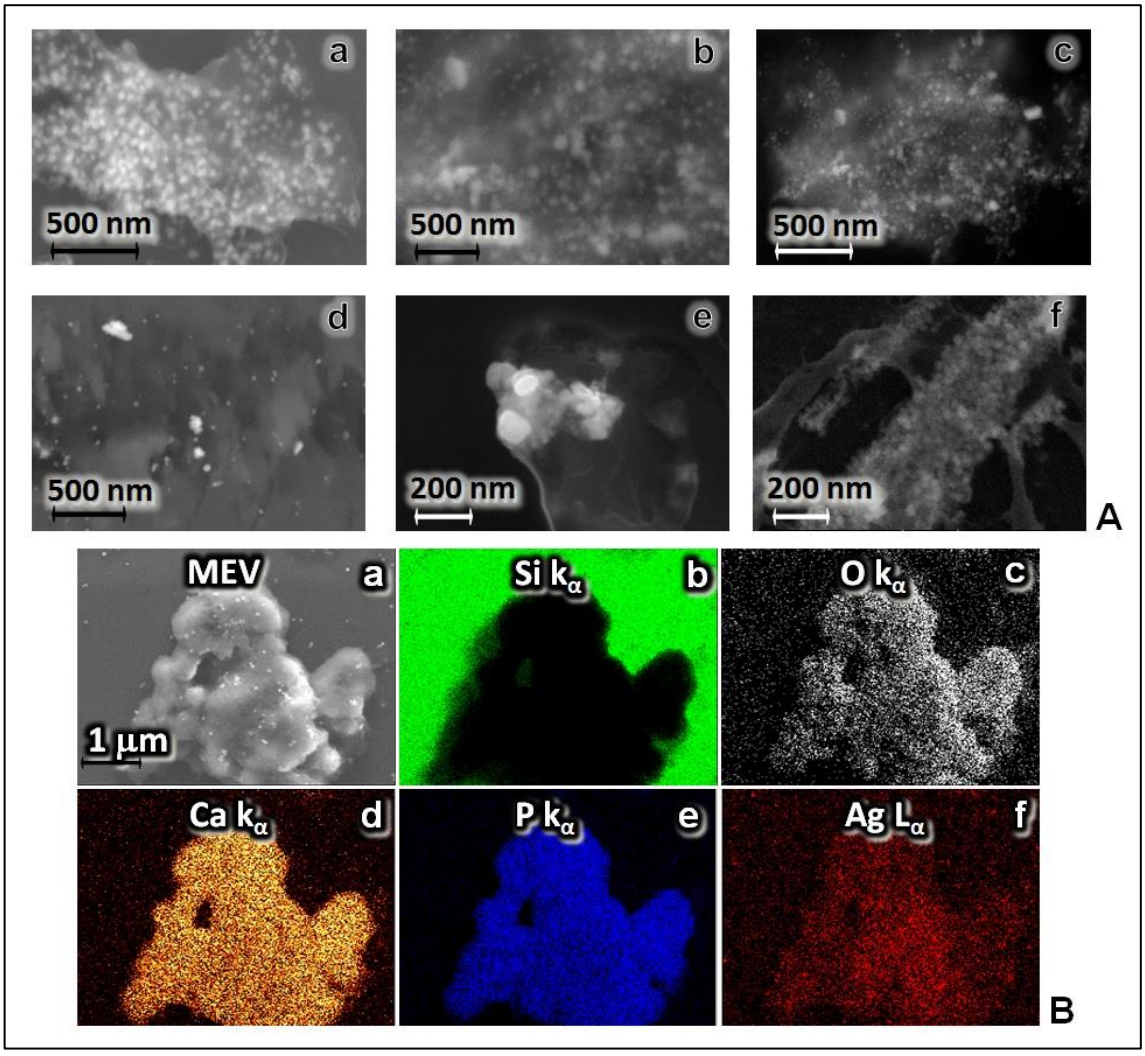

Figure 2: A) SEM micrographs of nanocompounds: a) P1; b) L1; c) S1; d) P2; e) L2 and f) S2. **B)** SEM and EDS mapping of the 2D elements issuance Si Kα, O Kα, Ca Kα, P Kα and Ag Kα false color. Analysis of the distribution of silver nanoparticles on the CaGP (P1 nanocompound); a) SEM image; b) chemical mapping of silicon element present in the substrate, where the electron beam was focused directly on the substrate and is showed in green color, and the dark regions the beam was focused in P1 nanocomposite; c-f) oxygen, calcium, phosphorus and silver, respectively, demonstrating they are constituents of the P1.

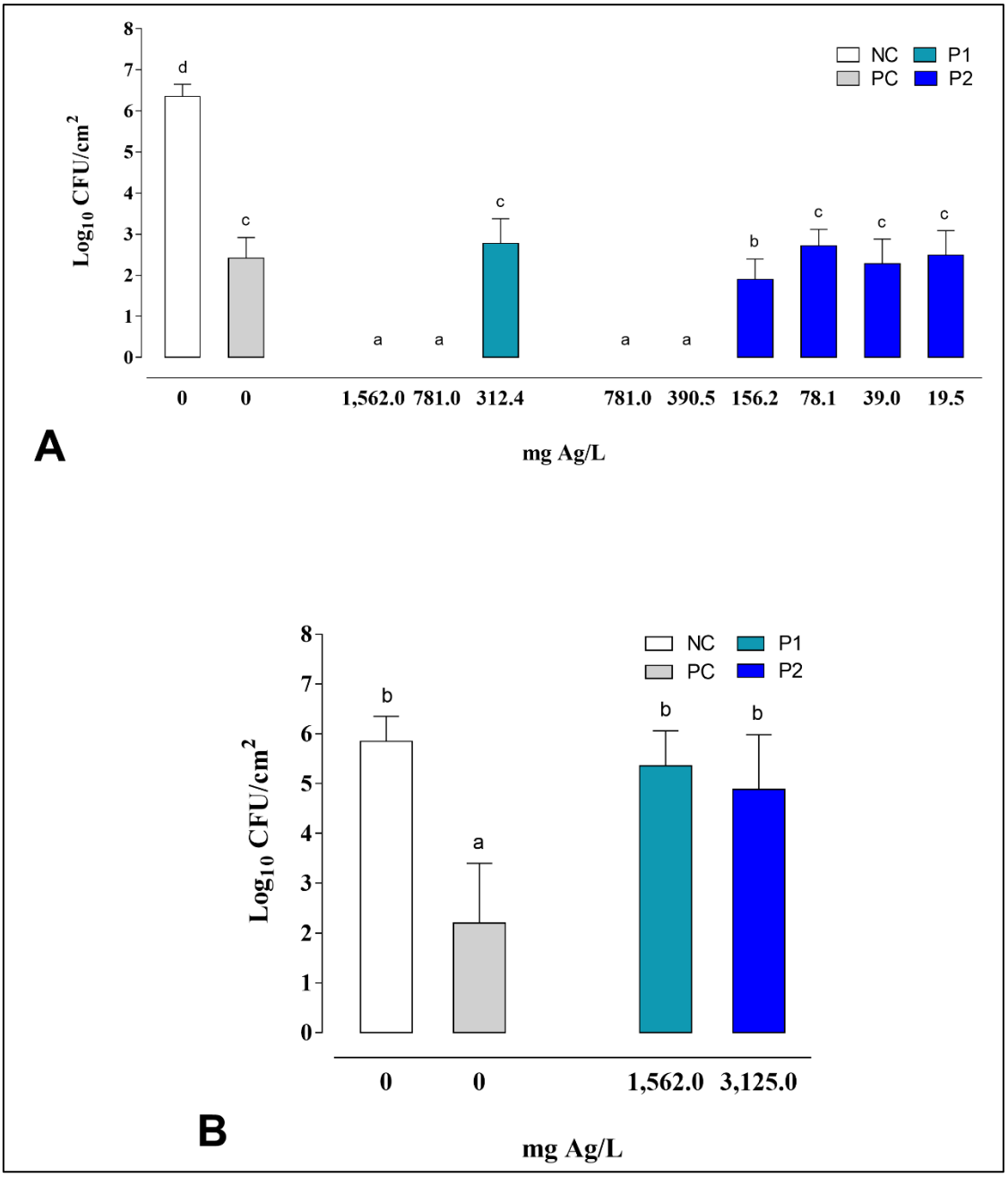

Figure 3. Mean values (±SD) of biofilm cells after treatment expressed as $\log_{10}$ CFU/cm^2 for *S. mutans* (A) and *C. albicans* (B) single biofilms. NC = negative control (saliva); PC = Chlorhexidine gluconate (180 mg/L); P1 = AgNP+CaGP; P2 = AgNP. Different lowercase letters indicate significant difference among the treatments for *S. mutans* ($p<0.05$; Kruskall-Wallis test) and *C. albicans* biofilms ($p<0.05$; Student-Newman-Keuls test).

CAPÍTULO 2

Evaluation of silver nanoparticles associated or not to calcium glycerophosphate on fibroblast viability and cytokine production *

*** *Artigo nas normas do periódico Clinical Oral Investigations***

Evaluation of silver nanoparticles associated or not to calcium glycerophosphate on fibroblast viability and inflammatory response

José Antonio Santos Souza[1], Aline Satie Takamiya[1], Luiz Fernando Gorup[2], Francisco Nunes de Souza Neto[3], Emerson Rodrigues Camargo[3], Debora Barros Barbosa[1], Sandra Helena Penha Oliveira[1], Alberto Carlos Botazzo Delbem[1]

[1]São Paulo State University (UNESP), School of Dentistry, Araçatuba, São Paulo, Brazil.
[2]Federal University of Grande Dourados, Dourados, Mato Grosso do Sul, Brazil.
[3]Federal University of São Carlos, São Carlos, São Paulo, Brazil.

[*]Corresponding author:
Alberto Carlos Botazzo Delbem
São Paulo State University (UNESP), School of Dentistry
Department of Pediatric Dentistry and Public Health
Rua José Bonifácio, 1193.
16015-050 Araçatuba – SP
Brazil
Tel. +55 18 3636 3314
Fax +55 18 3636 3332
Email: alberto.delbem@unesp.br

Evaluation of silver nanoparticles associated or not to calcium glycerophosphate on fibroblast viability and cytokine production

Objectives: The aim of this study was to evaluate the effect of silver nanoparticles (AgNPs) associated or not to β-calcium glycerophosphate (CaGP) obtained through a phytochemical method on cell viability and production of Interleukine-6 (IL-6) and stem cell factor (SCF) by mouse fibroblast cell line (L929).

Materials and methods: AgNPs associated or not to CaGP were synthesized using peel extract of a pomegranate (*Punica granatum L.*) with an average size of 35 nm. L929 was exposed to AgNPs-CaGP (C1) and AgNPs (C2), and 3-(4,5-dimethylthiazol-2-yl)-2,5-diphenyltetrazolium bromide and enzyme-linked immunosorbent assays were performed after 24, 48 and 72 hours. Culture medium was used as the control. The results were statistically analyzed by ANOVA and Bonferroni correction ($p < 0.05$).

Results: Antimicrobial solutions (C1 and C2) were not cytotoxic to L929 for all periods analyzed even in higher concentrations (C1 nanocomposite). There was an increase in the cell proliferation when the cells were exposed to C1 and C2 nanocomposites after 24 h in relation to control ($p < 0.001$). C1 was able to stimulate the release of IL-6 after 24 and 48 hours of treatment ($p < 0.001$). And, the nanocompounds (C1 and C2) significantly increased SCF levels after 72 h ($p < 0.001$).

Conclusions: In conclusion, our results showed that AgNPs associated or not to CaGP were not toxic to fibroblast cells (L929) at the evaluated concentrations. Furthermore, C1 and C2 nanocomposites increased the SCF production and did not promote significant alterations in the release of IL-6 after 72 h of treatment.

Clinical Relevance: AgNPs associated or not to CaGP might favor an appropriate inflammatory response as well as tissue repair.

Keywords: Silver nanoparticles; *Punica granatum*; Toxicity; Inflammation.

Introduction

Nanotechnology in Dentistry has gained significant attention in recent years. Nanoparticles are a class of materials with size range between 1 and 100 nm possessing different physicochemical properties since they exhibit a higher surface area to volume ratio, which makes them potentially more reactive [1,2]. Within this context, the incorporation of silver nanoparticles (AgNPs) in different dental materials such as dental adhesives [3,4], dental implants [5,6], aesthetic restorative materials [7] and denture bases [8] has improved their antimicrobial characteristics. AgNPs have demonstrated a very high antimicrobial effect against various microorganisms, such as *Streptococcus mutans*, *Lactobacillus acidophilus*, *Fusobacterium nucleatum*, *P gingivalis*, *Candida albicans*, *Candida glabrata*, etc [9-12]. Moreover, they can act synergistically with several types of antibiotics and antifungals [13].

Various methods have been devised for the synthesis of AgNPs. Among all the examined approaches, phytochemical synthesis received much attention, in particular, the use of plant extracts, because provides single step technique, economical protocol, non-pathogenic, and eco-friendly for NPs synthesis [14-15]. Plant extracts contain a variety of natural products (ellagic acid, punicalagin) known as polyphenols that possess strongly reducing properties [16-18]. For instance, extracts of different fruits rich in polyphenols as pomegranate (*Punica granatum L.*) have been successfully tested for the preparation of the AgNPs with proven antimicrobial activity [19-23]. Devanesan *et al.* [19] produced AgNPs using pomegranate peel extract with a size range of 20-40 nm; the authors observed an antibacterial activity against both Gram-positive and Gram-negative bacteria, even at low concentrations of AgNPs.

Recently, Souza *et al*. [24] developed a novel formulation containing in its composition AgNPs associated or not to β-calcium glycerophosphate (CaGP) obtained through a phytochemical method using peel extract of pomegranate as reducing agent. These novel formulations presented an antimicrobial effect against *Streptococcus mutans* and *Candida albicans*, important oral pathogens related to the dental caries and oral candidiasis. The authors believe that these nanomaterials can be used to combat dental caries due to proven antimicrobial activity of the AgNPs and release calcium and phosphate ions to the oral environment supported by the CaGP. Furthermore, these AgNPs also can be used in oral candidiasis that is frequently observed in immune suppressed patients and denture wearers [25].

'*Green*' AgNPs are usually less cytotoxic when compared to those reduced by conventional chemical agents [26]. Studies have shown that AgNPs produced with *Protium serratum* and *Nyctanthes arbortristis* extracts were biocompatible when tested in L929 fibroblasts [27,28]. Despite the good results obtained by Souza *et al*. [24] against important oral pathogens, there are few studies in the literature evaluating the cytotoxic effect of these formulations (AgNPs-CaGP and AgNPs) on mammalian cells [20].

Therefore, the aim of the present study was to investigate the effect of the silver nanoparticles (AgNPs) synthesized with peel extract of a pomegranate associated or not to β-calcium glycerophosphate (CaGP) on a mouse fibroblast cell line (L929) by evaluating the cytotoxicity and the production of interleukin-6 (IL-6) and stem cell factor (SCF).

Materials and Methods

Synthesis and Characterization of Antimicrobial solutions

The protocol described by Souza et al. [24] was used to produce silver nanoparticles (AgNPs) associated or not to β-calcium glycerophosphate (CaGP, 80% β-isomer and 20% rac-α-isomer, CAS 58409-70-4, Sigma-Aldrich Chemical Co, St Louis, Missouri, USA). Briefly, CaGP was nanoparticulated using a ball mill for 24 hours at 120 rpm, as described by Danelon *et al*. [29]. For the synthesis of the antimicrobial solutions, 0.42 g of silver nitrate ($AgNO_3$, Merck KGaA) was dissolved in 100 mL of deionized water and heated to 90° C. Next, 2.5 g of CaGP, 0.5 mL of NH-PM and 0.7 g of aqueous extracts of peels of *Punica granatum L.* were added to the flask. The reaction occurred under constant agitation at 95° C, for 10 minutes. The same process was performed in order to obtain AgNPs without CaGP. During the study, all drugs were stored at dark bottles to 4°C. Thus, two antimicrobial solutions were obtained: AgNPs-CaGP (C1) and AgNPs (C2).

The size and morphology of the nanocompounds were investigated by transmission electron microscopy (TEM) using HRTEM TECNAI F 20 Microscope operating at 200 κV. The samples were dispersed in isopropanol and deposited onto a carbon coated grid. The 2-D images were constructed by analyzing the Si Kα, P Kα, Ag Lα1 and Ca Kα energy emissions through Energy Dispersive Spectroscopy (EDS).

Cell Culture

Mouse fibroblast cell line (passage 3) L929 was cultured in Dulbecco modified Eagle medium (DMEM) supplemented with 10% fetal bovine serum, streptomycin (50 g/mL), and 1% antibiotic/antimycotic cocktail (i.e., 300 U/mL penicillin, 5 µg/mL amphotericin B, and L-glutamine 0.3 g/L). All of them were purchased from GIBCO BRL (Gaithersburg, MD). Cells were maintained under standard cell culture conditions at 37º C in a humidified atmosphere of 95% air and 5% CO_2.

In Vitro Cytotoxicity Protocol

Cytotoxicity assessment was performed using 3-(4,5-dimethylthiazol-2-yl)-2,5-diphenyltetrazolium bromide (MTT) assay; briefly, fibroblasts from cell line L929 were seeded into 24-well plates (10^5 cells/mL of medium per well). Afterward, the cells were incubated at 37º C in a humidified air atmosphere of 5% CO_2 for 24 hours. The exposure of the cells to antimicrobial solutions (C1 or C2) was initiated at ~100% of cell confluence, and the assay was done in DMEM. Concentrations of each compound used in this study were: C1 – 312.50; 156.25 and 78.12 µg/mL; C2 – 39.06; 19.53 and 9.76 µg/mL. Tween 20 (Sigma-Aldrich, St Louis, MO) and culture medium were used as controls. The exposure of cell cultures to both C1 and C2 was stopped after 24, 48 and 72 hours. Viable cells were stained with formazan dye (3-[4,5-dimethylthiazol-2-yl]-2,5-diphenyltetrazolium bromide [MTT]) (Sigma-Aldrich). Previously, MTT was dissolved in phosphate buffered saline at 5 mg/mL and, after the times of cell exposure to antimicrobial solutions, stock MTT solution (200 µL) was added directly to the cell culture in 24-well plates and incubated at 37º C for 4 hours. The MTT solution was then discarded, and 200 µL isopropyl alcohol was added to each well of the 24-well plates and mixed for 30 minutes to dissolve the dark blue crystals. The blue solution was then transferred to a 96-well plate only to measure the optical density (OD) with a microplate reader (Spectra Max 190; Molecular Devices, Sunnyvale, CA) at 570 nm wavelength. All laboratory assays were performed in triplicate. The relative cell viability (%) related to control (cell culture medium devoid of C1 and C2) was calculated by OD test/OD control x 100, where OD test is the optical density of the test samples and OD control is the optical density of the control samples.

Determination of IL-6 and SCF by Enzyme-linked Immunosorbent Assay

The production of IL-6 and SCF from cell line L929 was analyzed in the cell-free supernatants of cell culture exposure to C1 and C2 in the evaluated concentrations after

24, 48 and 72 hours using the enzyme-linked immunosorbent assay (ELISA). Culture medium was used as the control. Previously, fibroblasts from cell line L929 were seeded into 24-well plates at 10^5 cells/mL of medium per well. After that, the cells were incubated at 37º C in a humidified air atmosphere of 5% CO_2 for 24 hours until ~100% of cell confluence. The exposure of cells to antimicrobial solutions was achieved in DMEM, and the laboratory assays were performed in triplicate. Cytokines (IL-6 and SCF) were quantified according to the manufacturer's ELISA protocol. The optical density (OD) was measured with a microplate reader (Spectra Max 190; Molecular Devices, Sunnyvale, CA) at 450 nm wavelength.

Statistical Analysis

For statistical analysis, the GraphPad Prism 7.0 (GraphPad Software, CA, USA) program was used, and the significance level was set at 5%. Data were analyzed statistically by analysis of variance (ANOVA) followed by the Bonferroni correction.

Results

Synthesis and Characterization of the nanocompounds

Figures 1 shows the diffractograms of the nanocomposites C1 and C2 obtained by the '*green*' via. No alteration of the crystalline structure was observed in the nanocompounds when compared with the XRD patterns of CaGP (PDF № 1-17) [30] and AgNPs (PDF № 04-0783).

TEM shows images of the C1 and C2 nanocompounds (Figure 2A). In relation to C1 nanocomposite, AgNPs (gray shades) are dispersed and decorating the surface of the CaGP at micrometric size (white shades) (Figure 2A(a)). The 2D images were constructed by analyzing the energy released from the Ag Lα1, Ca Kα and P Kα emissions, indicating the uniform distribution of these elements in the demarcated area in the micrograph (Figure 2B). Figure 2A(b) shows different forms and sizes of AgNPs without CaGP (C2 nanocomposite).

In Vitro Cytotoxicity

The MTT assay was used to measure the cytotoxicity of both C1 and C2 nanocompounds to cell line L929 after exposure for 24, 48 and 72 h. As observed in the Figure 3A, antimicrobial solutions were not toxic to L929 for all periods analyzed even in higher concentrations (C1 nanocomposite).

Interestingly, it was observed that the cell exposure to C1 and C2 in all tested concentrations for 24 h significantly increased the cell proliferation compared with the control ($p < 0.001$) (Fig. 3A). However, after 48 and 72 h, there was a reduction in the cell proliferation, but the viability was similar to control (Fig. 3A).

Determination of IL-6 and SCF by ELISA

Cell line L929 was exposed to different concentrations of the nanocomposites (C1 and C2) for 24, 48 and 72 h. IL-6 and SCF production was constitutively detected in the cell supernatants as shown in Figure 3 (B and C). For C1 (AgNPs-CaGP), ELISA analysis of cell-free supernatants showed significant increase in levels of IL-6 after 24 h in the concentrations of 312.50 and 156.25 µg/mL, and after 48 h in the concentration of 156.25 µg/mL compared with the control ($p < 0.001$). After 72 h, IL-6 levels were similar to control group (Fig. 3B). For C2 (AgNPs) nanocomposite in the concentrations tested, significant alterations in the IL-6 levels at different times evaluated were not observed when compared to control group.

The SCF levels were significantly increased in the concentration of 78.12 µg/mL for C1 and in all concentrations for C2 after 72 hours compared with the control group ($p < 0.001$) (Fig. 3C).

Discussion

The purpose of the present study was to evaluate the potential toxicity and the effect of AgNPs associated or not to CaGP (C1 and C2) obtained by a phytochemical synthesis (using aqueous peel extract of a pomegranate) in an *in vitro* mouse fibroblast cell line (L929). The research hypothesis that C1 (AgNPs-CaGP) and C2 (AgNPs) nanocomposites do not cause toxic effects on fibroblasts cells was accepted because these compounds at the tested concentrations did not decrease mitochondrial function in fibroblasts. Interestingly, high concentrations of C1 (312.50 and 156.25 µg/mL) were not harmful to fibroblasts cells; it might have occurred because CaGP, a polyphosphate with proven anticariogenic activity [31-34], may have favored the interaction of the AgNPs with the cells. These results are very important because Souza *et al*. [24] showed that this nanocompound (AgNPs-CaGP) was effective against *S. mutans* in planktonic and biofilm states in these same concentrations. Thus, our results of viability suggest that it is possible incorporate this biocompatible novel combination (AgNPs-CaGP) in materials of medical and dental use. In relation to C2 (AgNPs) antimicrobial solution, the concentrations

evaluated were different of the analysed to the C1 nanocomposite, becuase, in previous studies carried out by our group, higher concentrations were cytotoxic (data not published). Fernandes *et al*. [20] also showed that a dosage of 100 µg/mL of AgNPs obtained by the same synthesis process with minor changes reduced approximately 40% the viability of fibroblastic cells (L929).

Several works have demonstrated that AgNPs produced by a '*green*' via are considered less toxic in comparison with other synthesis methods. For instance, Mohanta *et al*. [27] and Gogoi *et al*. [28] showed that AgNPs synthesized with extracts of *Protium serratum* and *Nyctanthes arbortristis*, respectively, were not toxic to L929 cell line. Some compounds present in the composition of the extracts may react with AgNPs [35], making them less toxic to human cells. In addition to this, other authors also observed that AgNPs obtained by a chemical via at a concentration of 6.25 µg/mL reduced drastically the percentage of viable cells [20]. This fact reinforces the idea '*green*' AgNPs are less cytotoxic when compared to those reduced by conventional chemical agents.

In the present study, increased cell proliferation was observed after treatments with C1 and C2 in all tested concentrations at 24 h. This effect was also observed by Takamiya *et al*. [36] after treatment with AgNPs synthesized with ammonia or polyvinylpyrrolidone in lower concentrations at 6 hours. One possible reason that may explain this result is the reduced uptake of particles in this period [37]. After 24 h, there was a reduction in the cell proliferation; however, the viability did not differ from the control group at the evaluated different times.

The release of proinflammatory cytokines, such as IL-6 by fibroblasts mediating inflammatory and immunologic responses after exposure to AgNPs has been reported [36,38]. We have analyzed the release of this cytokine by L929 after exposure to both C1 and C2 nanocomposites. The results showed that cell exposure to different concentrations of C2 (AgNPs) did not cause a significant release of IL-6 for all periods analyzed. On the other hand, high concentrations (312.50 and 156.25 µg/mL) of C1 (AgNPs-CaGP) led an increase in the release of this cytokine at the initial periods. Previous report also indicated alterations in the levels of IL-6 when other cell lines were treated with AgNPs [38,39]. This increase in the release of IL-6 might be related with the concentrations of the nanocomposites evaluated. Asharani *et al*. [40] reported a significant increase in IL-6 levels at 400 µg/mLof silver nanoparticles. However, it is important emphasize that in the present study the IL-6 levels were restored to normal after 72 hours. Taken together these findings are interesting since that the increase in IL-6 levels only at initial periods might

favor an inflammatory response and subsequently allowing repair with reduction in this cytokine.

Concerning the SCF, it was observed that C1 (78.12 µg/mL) and C2 (all concentrations) after 72 hours of treatment were able to induce significant SCF release. SCF has been reported to contribute to the inflammatory response by inducing dental pulp and gingival fibroblast proliferation [41]. It is possible that the increase of SCF production observed in our study at 72 h assists in the attenuation of the initial inflammatory response, contributing to tissue repair [36].

In conclusion, our results showed that AgNPs obtained by a phytochemical process, associated or not to CaGP, were not toxic to fibroblast cells (L929) at the evaluated concentrations. Furthermore, C1 and C2 nanocomposites increased the SCF production and did not promote significant alterations in the release of IL-6 after 72 h of treatment. Thus, these particles are a potent therapeutic agent against oral diseases (dental caries and oral candidiasis) since present antimicrobial activity and might favor an appropriate inflammatory response as well as tissue repair. Nevertheless, new *in vitro* studies with other cell lines and *in vivo* studies must be performed in order to ensure their safe use in the clinic.

Acknowledgments

The authors acknowledge the financial support provided by the CAPES Foundation, Ministry of Education of Brazil (Processes 88881.030445/2013-01 and 88887.068358/2014-00) and São Paulo Research Foundation (FAPESP, process 2015/00825-5).

References

1. Yadi M, Mostafavi E, Saleh B, Davaran S, Aliyeva I, Khalilov R, Nikzamir M, Nikzamir N, Akbarzadeh A, Panahi Y, Milani M (2018) Current developments in green synthesis of metallic nanoparticles using plant extracts: a review. Artif Cells Nanomed Biotechnol 25:1-8.
2. Prabhu S, Poulose EK (2012) Silver nanoparticles: mechanism of antimicrobial action, synthesis, medical applications, and toxicity effects. Int Nano Lett 2:32. https://doi.org/10.1186/2228-5326-2-32

3. Melo MA, Cheng L, Zhang K, Weir MD, Rodrigues LK, Xu HH (2013) Novel dental adhesives containing nanoparticles of silver and amorphous calcium phosphate. Dent Mater 29:199-210.
4. Zhang K, Melo MA, Cheng L, Weir MD, Bai Y, Xu HH (2012) Effect of quaternary ammonium and silver nanoparticle-containing adhesives on dentine bond strength and dental plaque microcosm biofilms. Dent Mater 28(8):842-52.
5. Godoy-Gallardo M, Rodríguez-Hernández AG, Delgado LM, Manero JM, Javier Gil F, Rodríguez D (2015) Silver deposition on titanium surface by electrochemical anodizing process reduces bacterial adhesion of Streptococcus sanguinis and Lactobacillus salivarius. Clin Oral Implants Res 26(10):1170-1179.
6. Liu Y, Zheng Z, Zara JN, Hsu C, Soofer DE, Lee KS, Siu RK, Miller LS, Zhang X, Carpenter D, Wang C, Ting K, Soo C (2012) The antimicrobial and osteoinductive properties of silver nanoparticle/poly (DL-lactic-co-glycolic acid)-coated stainless steel. Biomaterials 33(34):8745-8756.
7. Cheng L, Weir MD, Xu HH, Antonucci JM, Lin NJ, Lin-Gibson S, Xu SM, Zhou X (2012) Effect of amorphous calcium phosphate and silver nanocomposites on dental plaque microscosm biofilms. J Biomed Mater Res B Appl Biomater 100(5):1378-1386.
8. Nuñez-Anita RE, Acosta-Torres LS, Vilar-Pineda J, Martínez-Espinosa JC, de la Fuente-Hernández J, Castaño VM (2014) Toxicology of antimicrobial nanoparticles for prosthetic devices. Int J Nanomed 9:3999-4006.
9. Soares MRPS, Corrêa RO, Stroppa PHF, Marques FC, Andrade GFS, Corrêa CC, Brandão MAF, Raposo NRB (2018) Biosynthesis of silver nanoparticles using *Caesalpinia ferrea* (Tul.) Martius extract: physicochemical characterization, antifungal activity and cytotoxicity. PeerJ 6:e4361. https://doi.org/10.7717/peerj.4361.
10. Emmanuel R, Palanisamy S, Chen SM, Chelladurai K, Padmavathy S, Saravanan M, Prakash P, Ajmal Ali M, Al-Hemaid FM (2015) Antimicrobial efficacy of green synthesized drug blended silver nanoparticles against dental caries and periodontal disease causing microorganisms. Mater Sci Eng C Mater Biol Appl 56:374-379.
11. Lu Z, Rong K, Li J, Yang H, Chen R (2013) Size-dependent antibacterial activities of silver nanoparticles against oral anaerobic pathogenic bacteria. J Mater Sci Mater Med 24(6):1465-1471.

12. Acosta-Torres LS, Mendieta I, Nuñez-Anita RE, Cajero-Juárez M, Castaño VM (2012) Cytocompatible antifungal acrylic resin containing silver nanoparticles for dentures. Int J Nanomedicine 7:4777-4786.
13. Fayaz AM, Balaji K, Girilal M, Yadav R, Kalaichelvan PT, Venketesan R (2010) Biogenic synthesis of silver nanoparticles and their synergistic effect with antibiotics: a study against gram-positive and gram-negative bacteria. Nanomedicine 6(1):103-109.
14. Khan M, Shaik MR, Adil SF, Khan ST, Al-Warthan A, Siddiqui MRH, Tahir MN, Tremel W (2018) Plant extracts as green reductants for the synthesis of silver nanoparticles: lessons from chemical synthesis. Dalton Trans 47(35):1988-12010.
15. Adil SF, Assal ME, Khan M, Al-Warthan A, Siddiqui MR, Liz-Marzán LM (2015) Biogenic synthesis of metallic nanoparticles and prospects toward green chemistry. Dalton Trans. 44(21):9709-9717.
16. Della Pelle F, Scroccarello A, Sergi M, Mascini M, Del Carlo M, Compagnone D (2018) Simple and rapid silver nanoparticles based antioxidante capacity assays: Reactivity study for phenolic compounds. Food Chem 256:342-349.
17. Malik P, Shankar R, Malik V, Sharma N, Mukherjee TK (2014) Green chemistry based benign routes for nanoparticle synthesis. J Nanopart Res Article ID 302429. https://doi.org/10.1155/2014/302429.
18. El Gharras H (2009) Polyphenols: food sources, properties and applications – a review. Int J F Sci Tech 44(12):2512-2518.
19. Devanesan S, AlSalhi MS, Balaji RV, Ranjitsingh AJA, Ahamed A, Alfuraydi AA, AlQahtani FY, Aleanizy FS, Othman AH (2018) Antimicrobial and cytotoxicity effects of synthesized silver nanoparticles from Punica granatum peel extract. Nanoscale Res Lett 13(1):315. https://doi.org/10.1186/s11671-018-2731-y.
20. Fernandes RA, Berretta AA, Torres EC, Buszinski AFM, Fernandes GL, Mendes-Gouvêa CC, de Souza-Neto FN, Gorup LF, de Camargo ER, Barbosa DB (2018) Antimicrobial potential and cytotoxicity of silver nanoparticles phytosynthesized by pomegranate peel extract. Antibiotics (Basel) 7(3). pii:E51. http://doi.org/10.3390/antibiotics7030051.
21. Nasiriboroumand M, Montazer M, Barani H (2018) Preparation and characterization of biocompatible silver nanoparticles using pomegranate peel extract. J Photochem Photobiol B 179:98-104.

22. Goudarzi M, Mir N, Mousavi-Kamazani M, Bagheri S, Salavati-Niasari M (2016) Biosynthesis and characterization of silver nanoparticles prepared from two novel natural precursors by facile thermal decomposition methods. Sci Rep 6:32539. http://doi:.org/10.1038/srep32539.
23. Meena Kumari M, Jacob J, Philip D (2015) Green synthesis and applications of Au-Ag bimetallic nanoparticles. Spectrochim Acta A Mol Biomol Spectrosc 137:185-192.
24. Souza JA, Barbosa DB, Berretta AA, do Amaral JG, Gorup LF, de Souza Neto FN, Fernandes RA, Fernandes GL, Camargo ER, Agostinho AM, Delbem AC (2018) Green synthesis of silver nanoparticles combined to calcium glycerophosphate: antimicrobial and antibiofilm activities. Future Microbiol 13:345-357.
25. Pereira-Cenci T, Del Bel Cury AA, Crielaard W, Ten Cate JM (2008) Development of Candida-associated denture stomatitis: new insights. J Appl Oral Sci 16(2):86-94.
26. Das RK, Brar SK (2013) Plant mediated green synthesis: modified approaches. Nanoscale 5(21):10155-10162.
27. Mohanta YK, Panda SK, Bastia AK, Mohanta TK (2017) Biosynthesis of silver nanoparticles from *Protium serratum* and investigation of their potential impacts on food safety and control. Front Microbiol 8:626. http://doi.org/10.3389/fmicb.2017.00626.
28. Gogoi N, Babu PJ, Mahanta C, Bora U (2015) Green synthesis and characterization of silver nanoparticles using alcoholic flower extract of Nyctanthes arbortristis and in vitro investigation of their antibacterial and cytotoxic activities. Mater Sci Eng C Mater Biol Appl 46:463-469.
29. Danelon M, Pessan JP, Souza-Neto FN, de Camargo ER, Delbem AC (2017) Effect of fluoride toothpaste with nano-sized trimetaphosphate on enamel demineralization: An in vitro study. Arch Oral Biol. 78:82-87.
30. Inoue M, In Y, Ishida T (1992) Calcium binding to phospholipid: structural study of calcium glycerophosphate. J Lipid Res. 33(7):985-994.
31. Nagata ME, Delbem AC, Hall KB, Buzalaf MA, Pessan JP (2017) Fluoride and calcium concentrations in the biofilm fluid after use of fluoridated dentifrices supplemented with polyphosphate salts. Clin Oral Investig 21(3):831-837.

32. Freire IR, Pessan JP, Amaral JG, Martinhon CC, Cunha RF, Delbem AC (2016) Anticaries effect of low-fluoride dentifrices with phosphates in children: A randomized, controlled trial. J Dent 50:37-42.
33. Zaze AC, Dias AP, Amaral JG, Myasaki ML, Sassaki KT, Delbem AC (2014) In situ evaluation of low-fluoride toothpastes associated to calcium glycerophosphate on enamel demineralization. J Dent 42(12):1621-1625.
34. Amaral JG, Freire IR, Valle-Neto EF, Cunha RF, Martinhon CC, Delbem AC (2014) Longitudinal evaluation of fluoride levels in nails of 18-30-month-old children that were using toothpastes with 500 and 1100 µg F/g. Community Dent Oral Epidemiol 42(5):412-419.
35. Gengan RM, Anand K, Phulukdaree A, Chuturgoon A [2013] A549 lung cell line activity of biosynthesized silver nanoparticles using Albizia adianthifolia leaf. Colloids Surf B Biointerfaces. 105:87-91.
36. Takamiya AS, Monteiro DR, Bernabé DG, Gorup LF, Camargo ER, Gomes-Filho JE, Oliveira SH, Barbosa DB (2016) In vitro and In vivo toxicity evaluation of colloidal silver nanoparticles used in endodontic treatments. J Endod 42(6):953-960.
37. Sur I, Cam D, Kahraman M, Baysal A, Culha M (2010) Interaction of multi-functional silver nanoparticles with living cells. Nanotechnology 21(17):175104. http://doi.org/10.1088/0957-4484/21/17/175104.
38. Nakkala JR, Mata R, Raja K, Khub Chandra V, Sadras SR (2018) Green synthesized silver nanoparticles: Catalytic dye degradation, in vitro anticancer activity and in vivo toxicity in rats. Mater Sci Eng C Mater Biol Appl. 91:372-381.
39. Galandákova A, Franková J, Ambrožová N, Habartová K, Pivodová V, Zálešák B, Smékalová M, Ulrichová J (2016) Effects of silver nanoparticles on human dermal fibroblasts and epidermal keratinocytes. Hum Exp Toxicol 35(9):946-957.
40. Asharani PV, Hande MP, Valiyaveettil S (2009) Anti-proliferative activity of silver nanoparticles. BMC Cell Biol 10:65. http://doi.org/10.1186/1471-2121-10-65.
41. Oliveira SH, Santos VA (2012) Lipopolysaccharide-induced stem cell factor messenger RNA expression and production in odontoblast-like cells. J Endod 38(5):623-627.

Figures

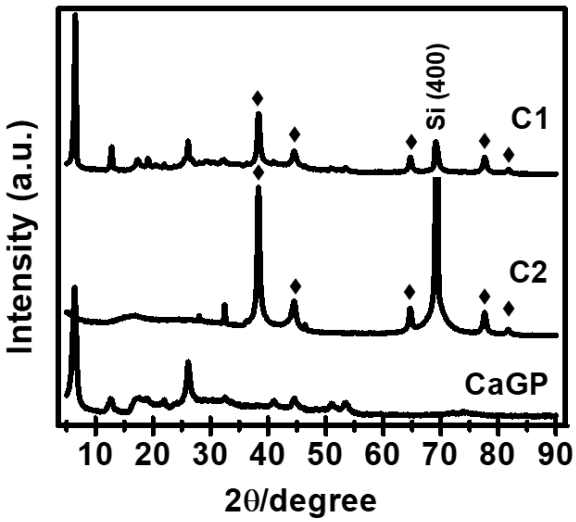

Figure 1. X-ray diffraction (XRD) of the nanocomposites: C1 (AgNPs-CaGP) and C2 (AgNPs).

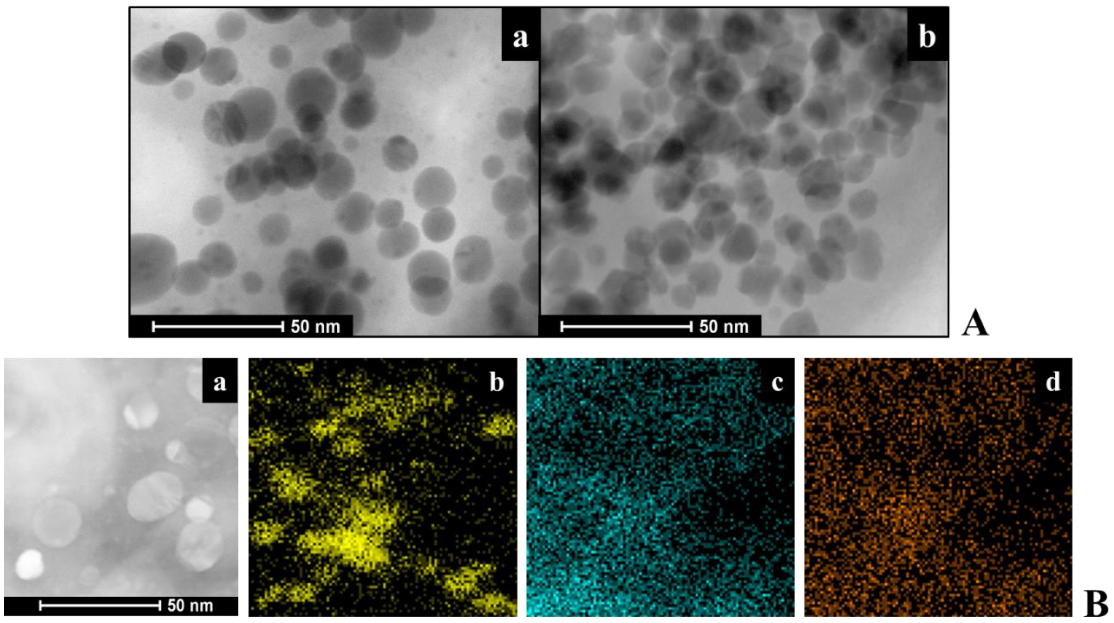

Figure 2. A) Images of transmission electron microscopy (TEM) of the nanocompounds: a) C1 (AgNPs-CaGP) and b) C2 (AgNPs). **B)** TEM and EDS mapping of the 2D elements issuance Ca Kα, P Kα and Ag Kα false color. Analysis of the distribution of silver nanoparticles on the CaGP (C1 nanocompound); a) TEM image; b-d) silver, calcium and phosphorus, respectively, demonstrating they are constituents of the C1.

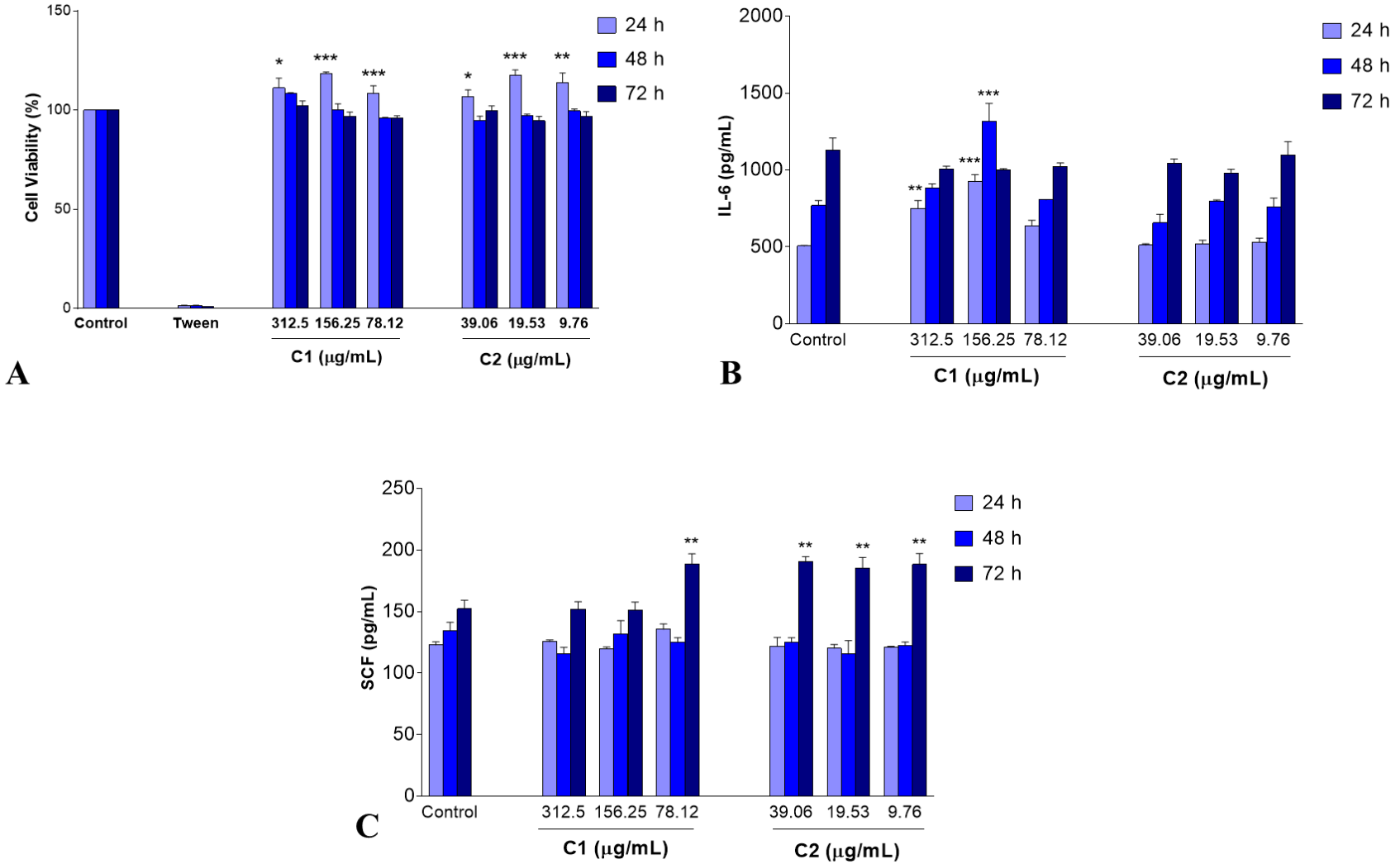

Figure 3. (A) Cytotoxicity of C1 (AgNPs-CaGP) and C2 (AgNPs) to fibroblasts (L929) after 24, 48, and 72 hours of treatment expressed as a percentage. The mean levels of proinflammatory cytokine **(B)** IL-6 and **(C)** SCF production by fibroblasts (L929) in the presence of different concentrations of C1 and C2 after 24, 48, and 72 hours expressed as pg/mL. Error bars indicate the standard deviations of the means. *, ** and ***Significant increase ($p < 0.001$) compared with the control group using ANOVA with the Bonferroni correction.

CAPÍTULO 3

Antimicrobial activity of compounds containing silver nanoparticles and calcium glycerophosphate in combination with tyrosol *

***** *Artigo nas normas do periódico Journal of Applied Microbiology*

Antimicrobial activity of compounds containing silver nanoparticles and calcium glycerophosphate in combination with tyrosol

Running Head: Silver nanoparticles/calcium phosphate and tyrosol

José Antonio Santos Souza[1], Debora Barros Barbosa[1], Jackeline Gallo do Amaral[1], Douglas Roberto Monteiro[2], Luiz Fernando Gorup[4], Francisco Nunes de Souza Neto[3], Renan Aparecido Fernandes[5], Gabriela Lopes Fernandes[1], Emerson Rodrigues Camargo[3], Alessandra Marçal Agostinho[6], Alberto Carlos B. Delbem[1]

[1]São Paulo State University (UNESP), School of Dentistry, Araçatuba, São Paulo, Brazil.
[2]Graduate Program in Dentistry (GPD – Master's Degree), University of Western São Paulo (UNOESTE), Presidente Prudente, São Paulo, Brazil.
[3]Federal University of São Carlos, São Carlos, São Paulo, Brazil.
[4]Federal University of Grande Dourados, Dourados, Mato Grosso do Sul, Brazil.
[5]University Center of Adamantina (UNIFAI), Adamantina, São Paulo, Brazil.
[6]Michigan State University, East Lansing, Michigan, USA.

[*]Corresponding author:
Alberto Carlos Botazzo Delbem
São Paulo State University (UNESP), School of Dentistry
Department of Pediatric Dentistry and Public Health
Rua José Bonifácio, 1193.
16015-050 Araçatuba – SP
Brazil
Tel. +55 18 3636 3314
Fax +55 18 3636 3332
Email: alberto.delbem@unesp.br

Antimicrobial activity of compounds containing silver nanoparticles and calcium glycerophosphate in combination with tyrosol

Running Head: Silver nanoparticles/calcium phosphate and tyrosol

Abstract

Aim: This study assessed the effect of two compounds containing silver nanoparticles (AgNPs) and β-calcium glycerophosphate (CaGP), associated or not to tyrosol (TYR), against planktonic cells and biofilms of *Candida albicans* and *Streptococcus mutans*.

Methods and Results: The nanocompounds were synthesized by chemical and '*green*' processes and characterized by scanining electron microscopy (SEM). The minimum and fractional inhibitory concentrations of each compound were determined for planktonic cells. Next, 24-h single biofilms of *C. albicans* and *S. mutans* were treated during 24 h with the nanocompounds alone or in combination with TYR, and the antibiofilm effect was assessed by enumeration of colony forming units. Biofilm data were statistically examined by one-way ANOVA and Kruskall-Wallis test (α=0.05). The nanocompound chemically synthesized in combination with TYR showed synergistic effect against planktonic cells of *C. albicans* and *S. mutans*. For the nanocompound obtained by '*green*' route associated with TYR, a synergistic effect was observed only against *C. albicans*. For biofilms, only the combination obtained by '*green*' route + TYR showed synergistic effect against *C. albicans*.

Conclusion: The combination of AgNPs/CaGP nanocompounds + TYR showed synergistic inhibitory effect against the microrganisms tested.

Significance and Impact of the Study: These findings may represent new antimicrobial strategies against bacterial and fungal oral infections, such as, denture stomatitis and dental caries.

Keywords: Antimicrobials; Quorum sensing; Biofilms; Fungi; Streptococci.

Introduction

Streptococcus mutans is highly prevalent in dental biofilms and is considered the main etiologic agent in the development of dental caries in children and adults (Krzyściak *et al*. 2014; Shimada *et al*. 2015). The acidogenic properties, resistance to acidic environments and the capacity to synthesize extracellular polysaccharides are the major virulence factors of *S. mutans* that contribute to enamel surface colonization and the development of pathogenic biofilms (Gregoire *et al*. 2011; Koo *et al*. 2013; Struzycka 2014). The progression of established dental caries lesions can also include other microorganisms such as *Candida* species, particularly *Candida albicans* (Takahashi and Nyvad 2011; Falsetta *et al*. 2014). A preponderance of *C. albicans* in dentine caries lesions of children has been found, with frequencies ranging from 66 to 97% (Ghasempour *et al*. 2011; Fragkou *et al*. 2016).

In order to control infectious oral diseases, new strategies have focused on the prevention of biofilm formation (Miranda *et al*. 2012; Bruniera *et al*. 2014; Arias *et al*. 2016; Fernandes *et al*. 2016). Among the therapeutic approaches that have been studied, the use of silver can be highlighted (Rizzello and Pompa 2014), mainly in the form of nanoparticles, which have higher ratio of surface area per volume and reactivity than microparticles. In this sense, silver nanoparticles (AgNPs) have been incorporated to different dental materials, including adhesives (Melo *et al*. 2013), implants (Godoy-Gallardo *et al*. 2015) and polymers (Nuñez-Anita *et al*. 2014), to promote caries arrestment (Santos *et al*. 2014), to prevent biofilm formation (Jia *et al*. 2016) and for osteogenic induction (Tian *et al*. 2016). Different approaches using chemical or '*green*' processes have been employed to obtain AgNPs. The '*green*' synthesis of metal nanoparticles has been proposed as a cost-effective and environmental friendly alternative and to reduce the chemical toxicity provided by agents used in the reaction (Tippayawat *et al*. 2016). *Punica granatum L.*, or pomegranate, has been used for AgNPs synthesis because it is a relatively non-toxic plant known for its antioxidant properties due to the presence of polyphenols (ellagic acid, gallic acid and punicalagin), which are present in the fruit peels (Manasathien *et al*. 2012).

Over recent years, organic or inorganic polyphosphates have been incorporated into dentifrices (Dalpasquale *et al*. 2017; Danelon *et al*. 2017), fluoridated gels (Conceição *et al*. 2015) and vernishes (Manarelli *et al*. 2017), and composite resins (Tiveron *et al*. 2015) in order to improve their anticaries and anti-erosive properties. Calcium glycerophosphate (CaGP) is an organic polyphosphate capable of adsorbing to

enamel surfaces (McGaughey and Stowell 1977; Anbar *et al*. 1979), leading to release of calcium (Ca) ions, which act on the remineralization process. Nanocomposites containing AgNPs and CaGP have been developed and shown antimicrobial and remineralizing effects, attributed to AgNP and CaGP, respectively (Fernandes *et al*. 2018; Souza *et al*. 2018). However, there is a concern regarding the use of AgNP, since a concentration-dependent toxicity has been documented (Takamiya *et al*. 2016). Thus, the combined use of these nanocomposites (AgNP-CaGP) with other compounds at low concentrations could increase the antimicrobial efficacy and reduce the side effects of these agents (Monteiro *et al*. 2013; Shanmughapriya *et al*. 2014).

Due to the increased resistance of fungal biofilms to conventional drugs, Quorum-Sensing (QS) molecules have been tested as alternative antifungals (Albuquerque and Casadevall 2012; Monteiro *et al*. 2015). In this regard, the QS molecule Tyrosol (2- [4-hydroxyphenyl] ethanol) (TYR) showed antibiofilm properties against *Candida* species and *S. mutans* in single and mixed cultures (Arias *et al*. 2016). Moreover, when TYR at 80 µM was associated with 4 mg/L amphotericin B, a synergistic effect on *Candida* biofilm formation was observed (Shanmughapriya *et al*. 2014).

Considering all above-mentioned aspects, the aim of this study was to evaluate the antimicrobial effect of AgNP/CaGP-containing solutions combined with TYR against planktonic cells and biofilms of *C. albicans* and *S. mutans.*

Materials and methods

Synthesis of test solutions

Two AgNPs/CaGP-containing solutions were synthesized using chemical and '*green'* processes. For both syntheses, β-calcium glycerophosphate (CaGP, 80% β-isomer and 20% rac-α-isomer, CAS 58409-70-4, Sigma-Aldrich Chemical Co, St Louis, Missouri, USA) was nanoparticulated using a ball mill for 24 hours at 120 rpm, as described by Danelon *et al*. (2017).

For the chemical process (compound C), sodium citrate ($Na_3C_6H_5O_7$, Merck KGaA, Germany) was used as reducing agent of silver nitrate ($AgNO_3$, Merck KGaA), and the stoichiometric ratio between these compounds was 3:1, respectively. This chemical route was based on the protocols proposed by Turkevich *et al*. (1951) and Gorup *et al*. (2011), with some modifications. Briefly, in a flask containing 100 mL of deionized water, 5 g of CaGP were added, followed by 0.5 mL of ammonium salt of polymethacrylic acid (NH-PM, Polysciences Inc., Warrington, Pensyvania, USA) and 1.4 g of $Na_3C_6H_5O_7$.

This mixture was heated and kept under magnetic stirring. After reaching 95° C, 0.85 g of $AgNO_3$ was added, and the suspension was stirred for an additional 30 minutes until the color of the solution changed for brown, which qualitatively indicated the formation of AgNPs (Patil and Kim 2017). The solution was then dried overnight at 70° C.

For the '*green*' via (compound G), 0.42 g of $AgNO_3$ was dissolved in 100 mL of deionized water and heated to 90° C. Next, 2.5 g of CaGP, 0.5 mL of NH-PM and 0.7 g of aqueous extracts of peels of *Punica granatum L.* were added to the flask. The reaction occurred under constant agitation at 95° C, during 10 minutes. For both routes, the amount of silver was equivalent to 10% of the CaGP weight (Fernandes *et al*. 2018; Souza *et al*. 2018).

Following, TYR (Sigma-Aldrich, CAS 501-94-0) was directly diluted with the nanocompounds (C and G) in deionized water, for the minimum inhibitory concentration test, and in artificial saliva (AS) (Lamfon *et al*. 2003), for the biofilm experiments.

In order to observe the particles morphology of the nanocompounds, a drop of each sample was placed on a silicon substrate, dried at 40° C for 12 hours, and characterized by scanning electron microscopy (SEM) using a Zeiss Supra 35VP microscope with field emission gun electron effect (FEG-SEM) operating at 10 eV, with magnification from 20000x to 60000x. These nanocompounds were previously characterized using UV-visible spectrum, x-ray diffraction and scanning electron microscopy followed by energy-dispersive x-ray spectroscopy with mapping in 2D as described by Fernandes *et al*. (2018) and Souza *et al*. (2018).

Antimicrobial activity

Minimum inhibitory concentration (MIC)

TYR and both nanocompounds (C and G) were tested alone or in combination (C+TYR and G+TYR). The minimum inhibitory concentration (MIC) assay against *S. mutans* ATCC 25175 and *C. albicans* ATCC 10231 was performed using the broth microdilution method, as previously reported (Arias *et al*. 2016). First, C, G, TYR, C+TYR and G+TYR were serially diluted (2 to 1024 times) in deionized water. Each concentration obtained previously was diluted (1:5) in RPMI 1640 medium (Sigma-Aldrich) or BHI broth (Difco, Le Pont de Claix, France), respectively for *C. albicans* and *S. mutans*. Inocula of both strains were adjusted to a turbidity equivalent to 0.5 McFarland standard in 0.85% saline solution. These microbial suspensions were diluted in saline solution and, posteriorly, in RPMI 1640 or BHI broth. Next, a volume of 100 µl of each

microbial suspension was added to the wells of 96-well plates (Costar, Tewksbury, USA) containing 100 µl of each specific concentration of compounds. The final drug concentrations were in the range of 1.56-1600 µg/mL for nanocompound C, 1.2-624.8 µg/mL for nanocompound G, and 5.35-2,763.2 µg/mL for TYR. The microtiter plates were aerobically incubated at 37° C during 48 h for *C. albicans*, while for *S. mutans* the plates were incubated in 5 % CO_2 for 24 h. MICs were determined by measuring the optical density at 570 nm. The background optical density was subtracted from that of each well.

MIC values were used to calculate the fractional inhibitory concentration index (FICI), which is defined as the sum of the ratio of the MIC of a compound used in combination by the MIC of the compound tested alone. FICI values ≤0.5 indicate synergism; between 0.5–4.0, no interaction; >4.0, antagonism (Wei and Bobek 2004; Monteiro *et al*. 2017). MIC and FICI were conducted in triplicate on three different occasions.

Biofilm killing

C. albicans ATCC 10231 and *S. mutans* ATCC 25175 were cultivated at 37° C on SDA (in aerobiose) and BHI agar (in 5% CO_2), respectively. After, *Candida* cells were grown in Sabouraud Dextrose Broth (SDB; Difco) medium during 20 h at 37° C (120 rpm), while S. *mutans* was inoculated in BHI broth (Difco) and statically incubated at 37° C for 18 h in 5% CO_2. Following, the fungal and bacterial cells were harvested by centrifugation (8,000 rpm, 5 min) and washed twice in phosphate-buffered saline (PBS, pH 7, 0.1 M). *S. mutans* cells were spectrophotometrically adjusted to 1×10^8 cells/mL in AS, while the number of *C. albicans* cells was adjusted to 1×10^7 cells/mL using a Neubauer chamber.

Based on the MIC results obtained, only the associations that presented synergism were tested against biofilms. Mono-species biolfims of *C. albicans* and *S. mutans* were developed during 24 h (37° C) in 96-well microtiter plates containing 0.2 mL of *C. albicans* cell suspension (1×10^7 cells/mL) or 0.2 mL of *S. mutans* (1×10^8 cells/mL), both prepared in AS. Afterwards, the biofilm-containing wells were washed with 0.2 mL of PBS to remove the nonadherent cells, and 0.2 mL of the drug association C+TYR (20×MIC for *C. albicans* and 10×MIC for *S. mutans*) and G+TYR (20×MIC for *C. albicans*) was added to the wells. All plates were re-incubated at 37° C for 24 h.

Compounds alone (C, G and TYR) were also evaluated, and AS was added to the wells designated as negative controls.

After the treatment period, the resulting biofilms were scraped from the wells with 1 mL of PBS and placed into microcentrifuge tubes. The suspensions obtained were vortexed, serially diluted in PBS and plated on SDA (for *C. albicans*) or BHI agar (for *S. mutans*). After incubation at 37° C (24-48 h), the total number of colony forming units (CFUs) was counted and the Log_{10} per unit area was calculated (Log_{10} CFU/cm^2).

The effect of drug association on biofilms was interpreted according to Miceli *et al*. (2009). When the drug combinations showed a significant CFU reduction compared to each compound alone ($p<0.05$), the association was considered synergistic. When the combinations reduced the number of CFU compared to each drug alone, but without significant difference among them ($p>0.05$), the effect was additive. An antagonistic effect was observed when the drugs alone were significantly more effective in reducing CFU than drug combinations ($p<0.05$).

Statistical Analysis

SigmaPlot 12.0 software (Systat Software Inc., San Jose, CA, USA) was used for statistical analysis, and the significance level was set at 5%. The CFU results did not pass the normalilty test for both microorganisms. Therefore, Kruskal-Wallis test was applied followed by Student-Newman-Keuls (for the combination G+TYR) and Tukey (for the combination C+TYR) tests.

Results

The formation of AgNP-CaGP occured through the reduction of Ag^+ from $AgNO_3$ in a CaGP-containing solution. Figure 1 shows phosphate surfaces decorated with AgNPs, evidencing that both methods of synthesis (chemical and '*green*') were effective in producing nanobiomaterials associating a nanoparticulated metal and an organic calcium phosphate. When the chemical process was employed, AgNPs showed diameters ranging from 35 to 50 nm. However, when the '*green*' process was employed, AgNPs exhibited relatively uniform dispersion, spherical shape and diameter around 50 nm.

Table 1 shows the MIC and FICI values for the compounds evaluated. *C. albicans* and *S. mutans* were more susceptible to the nanocompound C, with MIC values of 800 µg/mL. For both microorganisms, the combinations tested (C+TYR and G+TYR) showed MICs substantially lower than those found for each compound alone, except for the

combination G+TYR, which was not able to kill planktonic cells of *S. mutans*, even at the highest concentration tested. The combination of the nanocompound C with TYR exhibited a synergistic effect against *C. albicans* and *S. mutans*, with FICI values of 0.30 and 0.14, respectively. A synergistic killing effect on planktonic cells of *C. albicans* (FICI = 0.27) was also found when the nanocompound G (at 1/4 MIC) was associated with TYR (at 1/40 MIC). *S. mutans* was not susceptible to this association for all concentrations tested.

Regarding the effect on biofilms, when the combination C+TYR was tested against *S. mutans*, no significant reduction in the number of CFUs was observed ($p>0.05$; Figure 2). For *C. albicans*, however, this drug combination significantly reduced the number of biofilm cells when compared to the negative control ($p<0.001$), showing an additive effect (Figure 2). In turn, the combination G+TYR was tested only against *C. albicans* biofilms as no MIC was found when this association was tested against *S. mutans* planktonic cells. G+TYR showed a significant reduction in the number of CFUs in comparison to the negative control, and this drug combination was classified as synergistic (Figure 3).

Discussion

Biofilm-associated diseases and their resistance to conventional antimicrobial agents employed are still a clinical challenge. Thus, there is a growing interest in the development of new therapies to improve the antimicrobial properties of biomaterials and, at the same time, provide lower side effects. In this context, new promising agents containing AgNPs have been developed, showing encouraging results (Acosta-Torres *et al*. 2012; Emmanuel *et al*. 2015; Freire *et al*. 2015; Matsubara *et al*. 2015). Furthermore, TYR was shown to significantly reduce the adhesion and biofilm formation of *C. albicans* and *S. mutans* in single and mixed biofilms (Monteiro *et* al. 2015; Arias *et al*. 2016). Therefore, the current study was designed to evaluate the antimicrobial effect of two nanocompounds containing AgNP-CaGP (C and G), combined or not with TYR, against *S. mutans* and *C. albicans*, which could allow their use at lower concentrations.

These nanocompounds were obtained by physico-chemical and '*green*' routes. '*Green*' synthesis of AgNPs has emerged as a more viable alternative, because it is a simple, environmentally friendly and cost-effective method (Muthusamy *et al*. 2017). The use of plant extracts is the more advantageous biological material since it is free from toxic chemicals, presents lower biohazard and provides natural capping agents for AgNPs

stabilization (Aravinthan *et al*. 2015; Sengottaiyan *et al*. 2016; Balakrishnan *et al*. 2017). The synthesis of compound G was performed with polyphenols-rich pomegranate peel extract (Fernandes *et al*. 2018; Souza *et al*. 2018), which is responsible for Ag^{+} ions reduction and AgNPs stabilization, and has excellent anti-oxidant properties (Ahmad *et al*. 2012; Solgi *et al*. 2012; da Silva *et al*. 2013; Kumari *et al*. 2015).

Both nanocompounds tested in this study (C and G) were effective against *C. albicans* and *S. mutans* in planktonic state, but these microorganisms were more susceptible to the nanocompound C (Table 1). This result can be related to nanoparticles size, since the compound C presented smaller AgNPs compared to those obtained in the compound G. It is known that smaller AgNPs are more effective and have superior antimicrobial properties (Zhang *et al*. 2016). Lu *et al*. (2013) showed that AgNPs of 5 and 15 nm presented lower MIC (50 µg/mL) than 55 nm-AgNPs (200 µg/mL). Microscopic analysis also revealed that smaller AgNPs (9.3 and 21.3 nm) were more efficient in reducing *S. mutans* adherence on enamel blocks *in vitro* than larger AgNPs (93 nm) (Espinosa-Cristóbal *et al*. 2013). In addition to this, pomegranate peel is an important source of polyphenolic substances including ellagic and gallic acids. Thus, after reaction to obtain the compound G, the functional groups of polyphenols may be connected to the Ag^{+} ions (Goudarzi *et al*. 2016), hindering the antimicrobial effect of the nanoparticles.

Regarding the effect of drug associations on planktonic cells, both nanocompounds (C and G) combined with TYR were effective against *C. albicans*, but only the combination C+TYR was effective on *S. mutans* (Table 1). MIC values for TYR alone against the studied microorganisms were similar to those found by Monteiro *et al*. (2015) and Arias *et al*. (2016). However, when the nanocompounds C and G were combined with TYR, the TYR concentrations capable of inhibiting the microorganisms' growth were much lower, especially for the association with the compound C. The synergistic effect observed on planktonic cells by combining AgNP-CaGP and TYR may be due to the disruption of the cell membrane by TYR, since this molecule interferes with ergosterol biosynthesis (Cordeiro *et al*. 2015), facilitating the entry of AgNPs into the cytoplasm. Thereby, AgNPs interact with both intracellular proteins (especially sulfur rich-proteins) and DNA, causing further damage to cells (Rizzello and Pompa 2014).

For biofilms, a synergistic effect was found only for the combination G+TYR against *C. albicans*. This result could be related to the silver concentration present in the tested combinations (in the combination G+TYR, Ag concentration was of 781.0 µg/mL

and, in the combination C+TYR, Ag concentration was of 400.0 µg/mL; these values correspond to 10% of tested concentration in the biofilms), considering the AgNP action mechanisms discussed above. TYR concentrations that presented some antibiofilm effect in previous reports (Monteiro *et al*. 2015; Arias *et al*. 2016) were higher than those used in the current study for the treatment of biofilms with both associations (between 25 and 50 mM approximately). Cordeiro *et al*. (2015) also verified that exogenous TYR was able to significantly reduce biofilm formation of *C. albicans* only when tested at approximately 250 mM. In this study, an antimicrobial effect was obtained using a lower concentration of TYR, reinforcing the importance of drug combination therapy to reduce drug concentration, possibly the synergism occurred by the different action mechanisms of the TYR and AgNPs. Another point to be considered is the stage of biofilm formation, which affects the drug effectiveness. Within this context, Monteiro *et al*. (2017) demonstrated that the treatment with TYR led to no significant reductions in the number of CFUs of mature biofilms (96 h) of *C. albicans*, *C. glabrata* and *S. mutans.* In our study, however, biofilms were formed for 24 h and maintened for additional 24 h in the presence of nanocompounds; thus, the stage of biofilm formation tested in the present study may have contributed to the significant reductions observed for nanocomposites alone or in combination with TYR. Arias *et al*. (2016) also stated that although a concentration of 200 mM was necessary to reduce the number of CFUs, a lower concentration (50 mM) of TYR was able to promote significant reductions in the metabolic activity of biofilms, which could compromise their virulence. In this research, this colorimetric method was not realiable considering the color of antimicrobials solutions.

In conclusion, the AgNPs/CaGP-containing nanocompounds alone or in combination with TYR act synergistically inhibiting planktonic cells of *C. albicans* and *S. mutans* with lower concentrations of both drugs. For biofilms, synergistic effect was observed only when the compound obtained by '*green*' route was associated with TYR. Finally, these findings might be of interest for the development of new antimicrobial strategies against bacterial and fungal oral infections.

Acknowledgments

This work was supported by CAPES Foundation, Ministry of Education of Brazil (Processes 88881.030445/2013-01 and 88887.068358/2014-00) and São Paulo Research Foundation (FAPESP, process 2015/00825-5).

Conflict of Interest

Authors have declared that no competing interests exist.

References

Acosta-Torres, L.S., Mendieta, I., Nuñez-Anita, R.E., Cajero-Juárez, M. and Castaño, V.M. (2012) Cytocompatible antifungal acrylic resin containing silver nanoparticles for dentures. *Int J Nanomedicine* **7**, 4777-4786.

Ahmad, N., Sharma, S. and Rai, R. (2012) Rapid green synthesis of silver and gold nanoparticles using peels of Punica granatum. *Adv Mat Lett* **3**, 376-380.

Albuquerque, P. and Casadevall, A. (2012) Quorum sensing in fungi – a review. *Med Mycol* **50**, 337-345.

Anbar, M., Farley, E.P., Denson, D.D. and Maloney, K.R. (1979) Localized fluoride release from fluorine-carrying polyphosphonates. *J Dent Res* **58**, 1134-1145.

Aravinthan, A., Govarthanan, M., Selvam, K. Praburaman, L., Selvankumar, T., Balamurugan, R., Kamala-Kannan, S. and Kim J.H. (2015) Sunroot mediated synthesis and characterization of silver nanoparticles and evaluation of its antibacterial and rat splenocyte cytotoxic effects. *Int J Nanomedicine* **10**, 1977-1983.

Arias, L.S., Delbem, A.C., Fernandes, R.A., Barbosa, D.B. and Monteiro, D.R. (2016) Activity of tyrosol against single and mixed-species oral biofilms. *J Appl Microbiol* **120**, 1240-1249.

Balakrishnan, S., Sivaji, I., Kandasamy, S., Duraisamy, S., Kumar, N.S. and Gurusubramanian, G. (2017) Biosynthesis of silver nanoparticles using Myristica fragrans seed (nutmeg) extract and its antibacterial activity against multidrug-resistant (MDR) Salmonella enterica serovar Typhi isolates. *Environ Sci Pollut Res Int* **24**, 14758-14769.

Bruniera, J.F., Silva-Sousa, Y.T., Lara, M.G., Pitondo-Silva, A., Marcaccini, A.M. and Miranda, C.E. (2014) Development of intracanal formulation containing silver nanoparticles. *Braz Dent J* **25**, 302-306.

Conceição, J.M., Delbem, A.C., Danelon, M., da Camara, D.M., Wiegand, A. and Pessan, J.P. (2015) Fluoride gel supplemented with sodium hexametaphosphate reduces enamel erosive wear *in situ*. *J Dent* **43**, 1255-1260.

Cordeiro, R.A., Teixeira, C.E., Brilhante, R.S. Castelo-Branco, D.S., Alencar, L.P., de Oliveira, J.S., Monteiro, A.J., Bandeira, T.J., Sidrim, J.J., Moreira, J.L. and Rocha, M.F. (2015) Exogenous tyrosol inhibits planktonic cells and biofilms of *Candida*

species and enhances their susceptibility to antifungals. *FEMS Yeast Res* **15**, fov012. doi: 10.1093/femsyr/fov012.

Dalpasquale, G., Delbem, A.C.B., Pessan, J.P. and Nunes, G.P., Gorup, L.F., Neto, F.N.S., de Camargo, E.R. and Danelon, M. (2017) Effect of the addition of nano-sized sodium hexametaphosphate to fluoride toothpastes on tooth demineralization: an *in vitro* study. *Clin Oral Investig* **21**, 1821-1827.

Danelon, M., Pessan, J.P., Souza-Neto, F.N., de Camargo, E.R. and Delbem, A.C. (2017) Effect to fluoride toothpaste with nano-sized trimetaphosphate on enamel demineralization: An *in vitro* study. *Arch Oral Biol* **78**, 82-87.

da Silva, J.A.T., Rana, T.S., Narzary, D., Verma, N., Meshram, D.T. and Ranade, S.A. (2013) Pomegranate biology and biotechnology: a review. *Sci Hortic* **160**, 85-107.

Emmanuel, R., Palanisamy, S., Chen, S.M., Chelladurai, K., Padmavathy, S., Saravanan, M., Prakash, P., Ajmal Ali, M. and Al-Hemaid, F.M. (2015) Antimicrobial efficacy of green synthesized drug blended silver nanoparticles against dental caries and periodontal disease causing microorganisms. *Mater Sci Eng C Mater Biol Appl* **56**, 374-379.

Espinosa-Cristóbal, L.F., Martínez-Castañón, G.A., Téllez-Déctor, E.J., Niño-Martínez, N., Zavala-Alonso, N.V. and Loyola-Rodríguez, J.P. (2013) Adherence inhibition of *Streptococcus mutans* on dental enamel surface using silver nanoparticles. *Mater Sci Eng C Mater Biol Appl* **33**, 2197-2202.

Falsetta, M.L., Klein, M.I., Colonne, P.M., Scott-Anne, K., Gregoire, S., Pai, C.H., Gonzalez-Begne, M., Watson, G., Krysan, D.J., Bowen, W.H. and Koo, H. (2014) Symbiotic relationship between *Streptococcus mutans* and *Candida albicans* synergizes virulence of plaque biofilms in vivo. *Infect Immun* **82**, 1968-1981.

Fragkou, S., Balasouli, C., Tsuzukibashi, O., Argyropoulou, A., Menexes, G., Kotsanos, N. and Kalfas, S. (2016) *Streptococcus mutans*, *Streptococcus sobrinus* and *Candida albicans* in oral samples from caries-free and caries-active children. *Eur Arch Paediatr Dent* **17**, 367-375.

Fernandes, G.L., Delbem, A.C.B., do Amaral, J.G., Gorup, L.F., Fernandes, R.A., de Souza-Neto, F.N., Souza, J.A.S., Monteiro, D.R., Hunt, A.M.A., Camargo, E.R. and Barbosa, D.B. (2018) Nanosynthesis of Silver-Calcium Glycerophosphate: Promising Association against Oral Pathogens. *Antibiotics (Basel)* **7**, pii: E52. doi: 10.3390/antibiotics7030052.

Fernandes, R.A., Monteiro, D.R., Arias, L.S., Fernandes, G.L., Delbem, A.C. and Barbosa, D.B. (2016) Biofilm formation by *Candida albicans* and *Streptococcus mutans* in the presence of farnesol: a quantitative evaluation. *Biofouling* **32**, 329-338.

Fernandes, R.A., Berretta, A.A., Torres, E.C., Buszinski, A.F.M., Fernandes, G.L., Mendes-Gouvêa, C.C., de Souza-Neto, F.N., Gorup, L.F., de Camargo, E.R. and Barbosa, D.B. (2018) Antimicrobial potential and cytotoxicity of silver nanoparticles phytosynthesized by pomegranate peel extract. *Antibiotics (Basel)* **7**, pii: E51. doi: 10.3390/antibiotics7030051 (2018).

Freire, P.L., Stamford, T.C., Albuquerque, A.J., Sampaio, F.C., Cavalcante, H.M., Macedo, R.O., Galembeck, A., Flores M.A. and Rosenblatt, A. (2015) Action of silver nanoparticles towards biological systems: cytotoxicity evaluation using hen's egg test and inhibition of *Streptococcus mutans* biofilm formation. *Int J Antimicrob Agents* **45**, 183-187.

Ghasempour, M., Sefidgar, A.S., Eyzadian, H. and Gharakhani, S. (2011) Prevalence of *Candida albicans* in dental plaque and caries lesion of early childhood caries (ECC) according to sampling site. *Caspian J Intern Med* **2**, 304-308.

Godoy-Gallardo, M., Rodríguez-Hernández, A.G., Delgado, L.M., Manero, J.M., Javier Gil, F. and Rodríguez, D. (2015) Silver deposition on titanium surface by electrochemical anodizing process reduces bacterial adhesion of *Streptococcus sanguinis* and *Lactobacillus salivarius*. *Clin Oral Implants Res* **26**, 1170-1179.

Gorup, L.F., Longo, E., Leite, E.R. and Camargo, E.R. (2011) Moderating effect of ammonia on particle growth and stability of quasi-monodisperse silver nanoparticles sunthesized by the Turkevich method. *J Colloid Interface Sci* **360**, 355-358.

Goudarzi, M., Mir, N., Mousavi-Kamazani, M., Bagheri, S. and Salavati-Niasari, M. Biosynthesis and characterization of silver nanoparticles prepared from two novel natural precursors by facile thermal decomposition methods. *Sci Rep* **6**, 32539.

Gregoire, S., Xiao, J., Silva, B.B., Gonzalez, I., Agidi, P.S., Klein, M.I., Ambatipudi, K.S., Rosalen, P.L., Bauserman, R., Waugh, R.E. and Koo, H. (2011) Role of glucosyltransferase B in interactions of *Candida albicans* with *Streptococcus mutans* and with an experimental pellicle on hydroxyapatite surfaces. *Appl Environ Microbiol* **77**, 6357-6367.

Jia, Z., Xiu, P., Li, M., Xu, X., Shi, Y., Cheng, Y., Wei, S., Zheng, Y., Xi, T., Cai, H. and Liu, Z. (2016) Bioinspired anchoring AgNPs onto micro-nanoporous TiO_2

orthopedic coatings: Trap-killing of bacteria, surface-regulated osteoblast functions and host responses. *Biomaterials.* **75**, 203-222.

Koo, H., Falsetta, M.L. and Klein, M.I. (2013) The exopolysaccharide matrix: a virulence determinant of cariogenic biofilm. *J Dent Res* **92**, 1065-1073.

Krzyściak, W., Jurczak, A., Kościelniak, D., Bystrowska, B. and Skalniak, A. (2014) The virulence of *Streptococcus mutans* and the ability to form biofilms. *Eur J Clin Microbiol Infect Dis* **33**, 499-515.

Kumari, A., Guliani, A., Singla, R., Yadav, R. and Yadav, S.K. (2015) Silver nanoparticles synthesized using plant extracts show strong antibacterial activity. *IET Nanobiotechnol* **9**, 142-152.

Lamfon, H., Porter, S.R., McCullough, M. and Pratten, J. (2003) Formation of Candida albicans biofilms on non-shedding oral surfaces. *Eur J Oral Sci* **111**, 465-471.

Lu, Z., Rong, K., Li, J., Yang, H. and Chen, R. (2013) Size-dependent antibacterial activities of silver nanoparticles against oral anaerobic pathogenic bacteria. *J Mater Sci Mater Med* **24**, 1465-1471.

Manarelli, M.M., Delbem, A.C.B., Báez-Quintero, L.C., de Moraes, F.R.N., Cunha, R.F. and Pessan, J.P. (2017) Fluoride varnishes containing sodium trimetaphosphate reduce enamel demineralization *in vitro*. *Acta Odontol Scand* **75**, 376-378.

Manasathien, J., Indrapichate, K. and Intarapichet, O.K. (2012) Antioxidant activity and bioefficacy of pomegranate Punica granatum Linn peel and seed extracts. *Global J Pharmacol* **6**, 131-141.

Matsubara, V.H., Igai, F., Tamaki, R., Tortamano Neto, P., Nakamae, A.E. and Mori, M. (2015) Use of silver nanoparticles reduces internal contaminantion of external hexagon implants by *Candida albicans*. *Braz Dent J* **26**, 458-462.

McGaughey, C. and Stowell, E.C. (1977) Effects of polyphosphates on the solubility and mineralization of HA: relevance to a rationale for anticaries activity. *J Dent Res* **56**, 579-587.

Melo, M.A., Cheng, L., Zhang, K., Weir, M.D., Rodrigues, L.K. and Xu, H.H. (2013) Novel dental adhesives containing nanoparticles of silver and amorphous calcium phosphate. *Dent Mater* **29**, 199-210.

Miceli, M.H., Bernardo, S.M. and Lee, S.A. (2009) *In vitro* analyses of the combination of high-dose doxycycline and antifungal agents against *Candida albicans* biofilms. *Int J Amtimicrob Agents* **34**, 326-332.

Miranda, M., Fernández, A., Lopez-Esteban, S., Malpartida, F., Moya, J.S. and Torrecillas, R. Ceramic/metal biocidal nanocomposites for bone-related applications. *J Mater Sci Mater Med* **23**, 1655-1662.

Monteiro, D.R., Silva, S., Negri, M., Gorup, L.F., de Camargo, E.R., Oliveira, R., Barbosa, D.B. and Henriques, M. (2013) Antifungal activity of silver nanoparticles in combination with nystatin and chlorhexidine digluconate against *Candida albicans* and *Candida glabrata* biofilms. *Mycoses* **56**, 672-680.

Monteiro, D.R., Feresin, L.P., Arias, L.S., Barão, V.A., Barbosa, D.B. and Delbem, A.C. (2015) Effect of tyrosol on adhesion of *Candida albicans* and *Candida glabrata* to acrylic surfaces. *Med Mycol* **53**, 656-665.

Monteiro, D.R., Arias, L.S., Fernandes, R.A., Straioto, F.G., Barros Barbosa, D., Pessan, J.P. and Delbem A.C.B. (2017) Role of tyrosol on *Candida albicans*, *Candida glabrata* and *Streptococcus mutans* biofilms developed on different surfaces. *Am J Dent* **30**, 35-39.

Monteiro, D.R., Arias, L.S., Fernandes, R.A., Deszo da Silva, L.F., de Castilho, M.O.V.F., da Rosa, T.O., Vieira, A.P.M., Straioto, F.G., Barbosa, D.B. and Delbem, A.C.B. (2017) Antifungal activity of tyrosol and farnesol used in combination against *Candida* species in the planktonic state or forming biofilms. *J Appl Microbiol* **123**, 392-400.

Muthusamy, G., Thangasamy, S., Raja, M., Chinnappan, S. and Kandasamy, S. (2017) Biosynthesis of silver nanoparticles from Spirulina microalgae and its antibacterial activity. *Environ Sci Pollut Res Int* **24**, 19459-19464.

Nuñez-Anita, R.E., Acosta-Torres, L.S., Vilar-Pineda, J., Martínez-Espinosa, J.C., de la Fuente-Hernández, J. and Castaño, V.M. (2014) Toxicology of antimicrobial nanoparticles for prosthetic devices. *Int J Nanomedicine* **9**, 3999-4006.

Patil, M.P. and Kim, G.D. (2017) Eco-friendly approach for nanoparticles synthesis and mechanism behind antibacterial activity of silver and anticancer activity of gold nanoparticles. *Appl Microbiol Biotechnol* **101**, 79-92.

Rizzello, L. and Pompa, P.P. (2014) Nanosilver-based antibacterial drugs and devices: mechanisms, methodological draebacks, and guidelines. *Chem Soc Rev* **43**, 1501-1518.

Santos, V.E. Jr., Vasconcelos Filho, A., Targino, A.G., Flores, M.A., Galembeck, A., Caldas, A.F. Jr. and Rosenblatt, A. (2014) A new "silver-bullet" to treat caries in children – nano silver fluoride: a randomized clinical trial. *J Dent* **42**, 945-951.

Shanmughapriya, S., Sornakumari, H., Lency, A., Kavitha, S. and Natarajaseenivasan, K. (2014) Synergistic effect of amphotericin B and tyrosol on biofilm formed by *Candida krusei* and *Candida tropicalis* from intrauterine device users. *Med Mycol* **52**, 853-861.

Shimada, A., Noda, M., Matoba, Y., Kumagai, T., Kozai, K. and Sugiyama, M. Oral lactic acid bacteria related to the occurrence and/or progression of dental caries in Japanese preschool children. *Biosci Microbiota Food Health* **34**, 29-36.

Souza, J.A., Barbosa, D.B., Silva, A.A., do Amaral, J.G., Gorup, L.F., de Souza Neto, F.N., Fernandes, R.A., Fernandes, G.L., Camargo, E.R., Agostinho, A.M. and Delbem, A.C. (2018) Green synthesis of silver nanoparticles combined to calcium glycerophosphate: antimicrobial and antibiofilm activities. *Future Microbiol* **13**, 345-357.

Struzycka, I. (2014) The oral microbiome in dental caries. *Pol J Microbiol* **63**, 127-135.

Takahashi, N. and Nyvad, B. (2011) The role of bacteria in the caries process: ecological perspectives. *J Dent Res* **90**, 294-303.

Takamiya, A.S., Monteiro, D.R., Bernabé, D.G., Gorup, L.F., Camargo, E.R., Gomes-Filho, J.E., Oliveira, S.H. and Barbosa, D.B. (2016) *In Vitro* and *In Vivo* Toxicity Evaluation of Colloidal Silver Nanoparticles Used in Endodontic Treatments. *J Endod* **42**, 953-960.

Tian, B., Chen, W., Dong, Y., Marymont, J.V., Lei, Y., Ke, Q., Guo, Y. and Zhu Z. (2016) Silver nanoparticle-loaded hydroxyapatite coating: structure, antibacterial properties, and capacity for osteogenic induction in vitro. *RSC Adv* **6**, 8549-8562.

Tippayawat, P., Phromviyo, N., Boueroy, P. and Chompoosor, A. Green synthesis of silver nanoparticles in aloe vera plant extract prepared by a hydrothermal method and their synergistic antibacterial activity. *PeerJ* **4**, e2589.

Tiveron, A.R., Delbem, A.C., Gaban, G., Sassaki, K.T. and Pedrini, D. (2015) *In vitro* enamel remineralization capacity of composite resins containing sodium trimetaphosphate and fluoride. *Clin Oral Investig* **19**, 1899-1904.

Turkevich, J., Stevenson, P.C. and Hillier, J. (1951) A study of the nucleation and growth processes in the synthesis of colloidal gold. *Discuss Faraday Soc* **11**, 55-75.

Sengottaiyan, A., Aravinthan, A., Sudhakar, C. Selvam, K., Srinivasan, P., Govarthanan, M., Manoharan, K. and Selvankumar, T. (2016) Synthesis and

characterization of Solanum nigrum-mediated silver nanoparticles and its protective effect on alloxan-induced diabetic rats. *J Nanostruct Chem* **6**, 41-48.

Solgi, M. and Taghizadeh, M. (2012) Silver nanoparticles eco-friendly synthesis by two medicinal plants. *Int J Nanomater Biostruct* **2**, 60-64.

Wei, G.X. and Bobek, L.A. (2004) *In vitro* synergic antifungal effect of MUC7 12-mer with histatin-5 12-mer or miconazole. *J Antimicrob Chemother* **53**, 750-758.

Zhang, L., Weir, M.D., Chow, L.C., Antonucci, J.M., Chen, J. and Xu, H.H. (2016) Novel rechargeable calcium phosphate dental nanocomposite. *Dent Mater* **32**, 285-293.

Tables

Table 1. Minimum inhibitory concentration (MIC) of tyrosol (TYR) and nanocompounds obtained by chemical (C) and '*green*' (G) routes against *Streptococcus mutans* and *Candida albicans*, and Fractional Inhibitory Concentration Index (FICI)

Groups	MIC (µg/mL)		FICI	
	S. mutans	*C. albicans*	*S. mutans*	*C. albicans*
C	800.0	800.0	-	-
TYR	12434.4	6908.0	-	-
G	1560.2	1560.2	-	-
C+TYR	100.0/172.7	200.0/345.4	0.14	0.30
G+ TYR	>624.8/2763.2	390.0/172.7	-	0.27

∗The association was considered as synergistic when FICI ≤ 0.5; indifferent when 0.5 < FICI < 4, and antagonistic when FICI > 4.0.

Figures

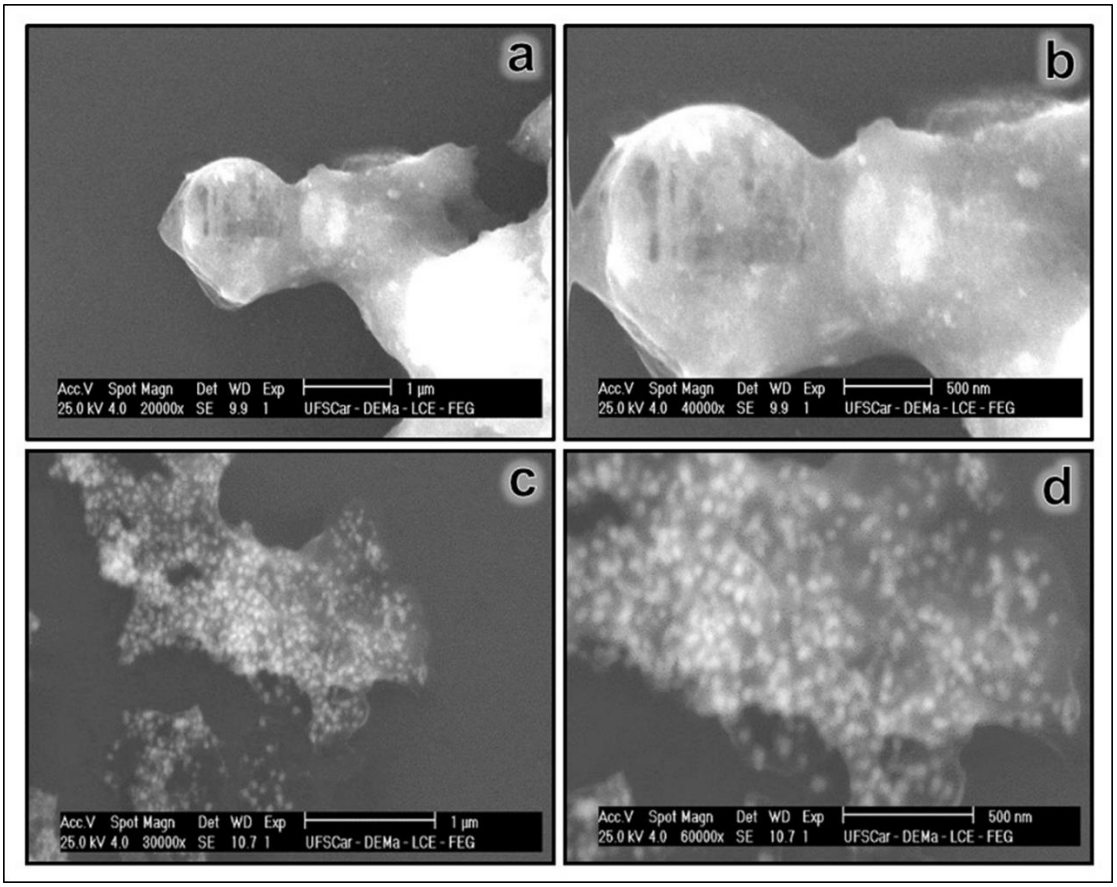

Figure 1. Scanning electron microscopy images of the AgNPs/CaGP nanocompounds: **a** and **b**) Compound obtained by the chemical process (C); **c** and **d**) Compound obtained by the '*green*' process (G). Magnification: 20000x (**1a**), 40000x (**1b**), 30000x (**1c**) and 60000x (**1d**).

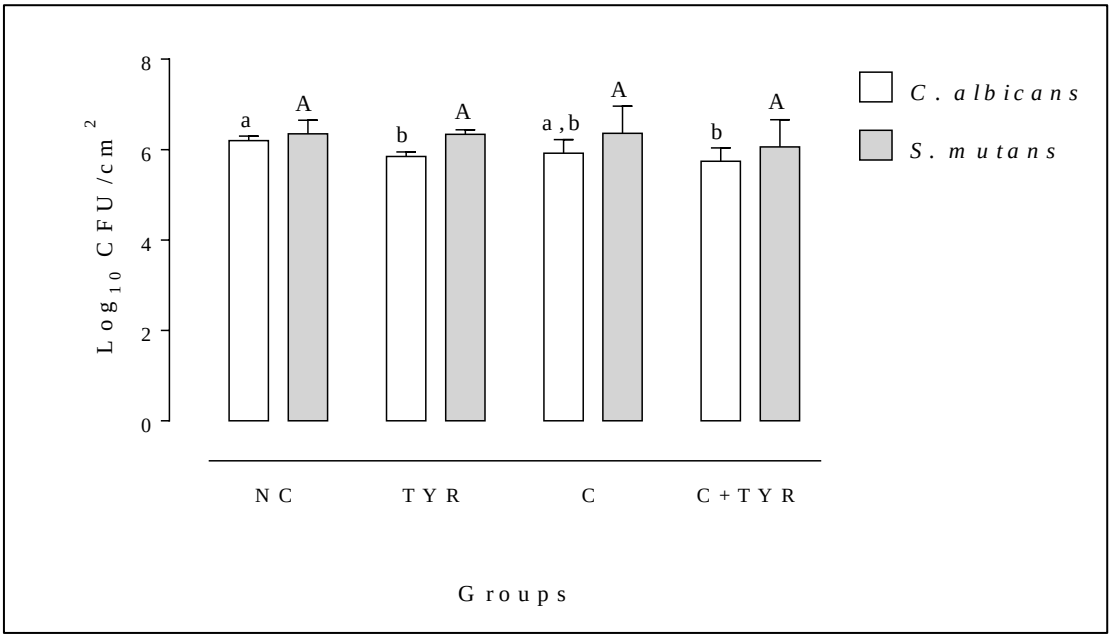

Figure 2. Mean values (±SD) of the logarithm of colony forming units per cm^2 (log_{10} CFU/cm^2) for single biofilms of *C. albicans* and *S. mutans*. NC = negative control; C = nanocompound obtained by the chemical process; TYR = tyrosol. Concentrations tested for *C. albicans*: C at 4,000 µg/mL and TYR at 6,908 µg/mL. For *S. mutans*: C at 1,000 µg/mL and TYR at 1,727 µg/mL. Different lowercase and uppercase letters indicate significant differences among the treatments for *C. albicans* ($p<0.05$; Kruskall-Wallis test followed by the Tukey test) and *S. mutans* ($p<0.05$; Kruskall-Wallis test followed by the Tukey test) biofilms, respectively.

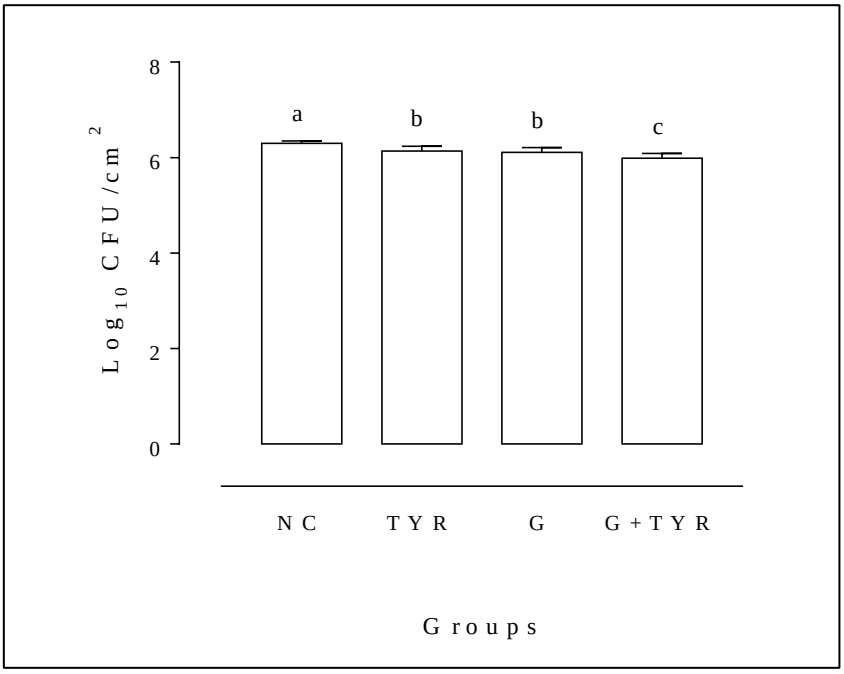

Figure 3. Mean values (±SD) of the logarithm of colony forming units per cm^2 (log_{10} CFU/ cm^2) for single biofilms of *C. albicans*. NC = negative control; G = nanocompound obtained by '*green*' route at 7810 µg/mL; TYR = tyrosol at 3454 µg/mL; G+TYR = 7810 µg/mL of G and 3454 µg/mL of TYR. Different lowercase letters indicate significant differences among the treatments ($p<0.05$; Kruskall-Wallis test followed by the Student-Newman-Keuls test).

CAPÍTULO 4

'*Green*' silver nanoparticles combined with tyrosol as potential oral antimicrobial therapy *

***** *Artigo nas normas do periódico Journal of Applied Microbiology*

'*Green*' silver nanoparticles combined with tyrosol as potential oral antimicrobial therapy

Running Head: Silver nanoparticles and tyrosol

José Antonio Santos Souza[1], Debora Barros Barbosa[1], Jackeline Gallo do Amaral[1], Aline Satie Takamiya[1], Douglas Roberto Monteiro[2], Luiz Fernando Gorup[4], Francisco Nunes de Souza Neto[3], Renan Aparecido Fernandes[5], Gabriela Lopes Fernandes[1], Emerson Rodrigues Camargo[3], Alessandra Marçal Agostinho[6], Sandra Helena Penha Oliveira[1], Alberto Carlos B. Delbem[1]

[1]São Paulo State University (UNESP), School of Dentistry, Araçatuba, São Paulo, Brazil.
[2]Graduate Program in Dentistry (GPD – Master's Degree), University of Western São Paulo (UNOESTE), Presidente Prudente, São Paulo, Brazil.
[3]Federal University of São Carlos, São Carlos, São Paulo, Brazil.
[4]Federal University of Grande Dourados, Dourados, Mato Grosso do Sul, Brazil.
[5]University Center of Adamantina (UNIFAI), Adamantina, São Paulo, Brazil.
[6]Michigan State University, East Lansing, Michigan, USA.

[*]Corresponding author:
Alberto Carlos Botazzo Delbem
São Paulo State University (UNESP), School of Dentistry
Department of Pediatric Dentistry and Public Health
Rua José Bonifácio, 1193.
16015-050 Araçatuba – SP
Brazil
Tel. +55 18 3636 3314
Fax +55 18 3636 3332
Email: alberto.delbem@unesp.br

'*Green*' silver nanoparticles combined with tyrosol as potential oral antimicrobial therapy

Abstract

Aim: The aim of this study was to evaluate *in vitro* activity of silver nanoparticles (AgNPs) associated or not to the tyrosol (TYR) against *Streptococcus mutans* and *Candida albicans* in planktonic and biofilms states. Furthermore, cytotoxicity effect of the AgNPs associated or not to TYR on fibroblast cells was investigated.

Methods and Results: AgNPs were produced using pomegranate (*Punica granatum L.*) peel extract and characterized by UV-visible, X-ray diffraction and scanning electron microscopy. Minimum inhibitory concentration (MIC) of each drug and their combinations were determined by microdilution method. The effect of drug association against planktonic cells was assessed by the fractional inhibitory concentration index. Single biofilms of *C. albicans* and *S. mutans* were developed during 24 h and then treated with AgNPs and TYR alone or in combination for 24 h. After, the number of cultivable cells was quantified. L929 was exposed to AgNPs associated or not to TYR, and 3-(4,5-dimethylthiazol-2-yl)-2,5-diphenyltetrazolium bromide was performed after 24, 48 and 72 hours. Culture medium was used as the control. The results were statistically analyzed by ANOVA, Kruskall-Wallis test and Bonferroni correction ($p < 0.05$). In general, AgNPs showed higher antimicrobial activity than TYR. Combination of both antimicrobial agents was effective against both microorganisms at low concentrations and was not toxic to fibroblast cells L929 except to the highest association. However, synergistic activity was noted only against *C. albicans* planktonic cells. Regarding biofilm susceptibility, an expressively density reduction of 4.62 $\log_{10}$ was observed for *S. mutans* biofilm cells treated with AgNPs. However, the addition of TYR to AgNPs did not improve their action against its biofilm cells. AgNPs in combination with TYR showed a synergistic effect against *C. albicans* biofilms.

Conclusion: These findings suggest the potential use of AgNPs with or without TYR against representative oral pathogens.

Keywords: Biosynthesis, Silver nanoparticles, Quorum sensing, *Candida albicans*, *Streptococcus mutans*.

Introduction

In the last years, the use of nanoparticles has been expanded considerably, since these molecules possess potential applications in industry, medicine and therapeutics. Silver nanoparticles (AgNPs) have proven antimicrobial action against a broad spectrum of microorganisms such as bacteria (Perveen *et al*. 2018; Pérez-Díaz *et al*. 2015; Reidy *et al*. 2013), fungi (Soares *et al*. 2018; Kim *et al*. 2012) and viruses (Khandelwal *et al*. 2014), and present antioxidant, anti-inflammatory, anticancer and antiangiogenic activities (Akhtar *et al*. 2015). Moreover, its anti-biofilm activity has been reported (Souza *et al*. 2018; Monteiro *et al*. 2014; Freire *et al*. 2014; Velazquez-Velazquez *et al*. 2015). Environmentally friendly protocols, as using plant or fruit extract have been proposed to synthesize these nanoparticles, since physical and chemical methods (laser ablations, pyrolysis, chemical or physical vapor deposition) are generally costly and/or toxic (Patil *et al*. 2017; de Matos and Courrol 2016). Recently, pomegranate (*Punica granatum L*.) peel extract was employed and reported to obtain AgNPs (Fernandes *et al*. 2018; Souza *et al*. 2018). *Punica granatum L*. peel may contains different phenolic compounds i.e. ellagic acid and its derivatives like punicalagin that participate in the process of reduction of silver ions as well as in the nanoparticles stabilization (Nasiriboroumand *et al*. 2018; Singh *et al*. 2018); AgNPs have been utilized in association to conventional therapies and to other novel antimicrobials with promising results. Longhi *et al*. (2016) showed that AgNPs combined with fluconazole cause a significant dose-dependent decrease in the viability of mature biofilm of fluconazole-resistant *Candida albicans*.

Tyrosol (TYR) is a quorum-sensing molecule secreted by *C. albicans* which plays a role in morphogenesis, biofilm development and is important for the infectious process (Wongsuk *et al*. 2016). This molecule has been investigated as antimicrobial agent against fungal and bacterial pathogens, including *C. albicans*, *C. glabrata*, *Streptococcus mutans* (Monteiro *et al*. 2017; Arias *et al*. 2016) and *Pseudomonas aeruginosa* (Abdel-Rhman *et al.* 2015).

It has been known that biofilms, which are well-structured microbial communities surrounded by extracellular polymeric substance (EPS) (Mathé and Van Dijck 2013), are more resistant than planktonic cell to many antibiotics and antifungals. For this reason, the combination between different antimicrobials has been investigated. For instance, TYR in combination with amphotericin B showed a synergistic effect (90% reduction in *C. tropicalis* biofilm) when 80 µM TYR was co-administered with 4 mg/L amphotericin

B (Shanmughapriya *et al*. 2014). TYR alone is able to inhibit mature biofilms, but when associated with azoles there is an increase in the anti-biofilm effect (Cordeiro *et al*. 2015).

S. mutans and *C. albicans* are important pathogens of the oral cavity widely described in the literature. *S. mutans*, a gram-positive bacterium, is considered the major responsible for the caries lesions, and the extracellular matrix surrounding its biofilm make them resistant to antimicrobial therapies (Broadbent *et al*. 2013). *C. albicans* is a commensal but opportunistic yeast found in different parts of the human body. Their ability to form biofilm on both biotic and abiotic substrates becomes this dimorphic fungus a relevant focus of attention in some oral diseases (O'Donell *et al*. 2017). Studies suggest that this yeast may have a cariogenic potential still not established (Nikawa H *et al*. 2003). Some studies revealed that *C. albicans* is frequently detected in plaque biofilms of children with early childhood caries in association to high levels of *S. mutans* (De Carvalho *et al*. 2006; Raja *et al*. 2010). In a study conducted by Ghasempour *et al*. (2011), 60% of the children with proximal caries and 100% with cervical caries were positive for *C. albicans*.

Considering all above-mentioned aspects, this study aimed: to synthesize and characterize AgNPs obtained by a '*green*' process and to evaluate their effect associated to TYR against planktonic and sessile biofilm cells of two clinically oral relevant pathogens (*S. mutans* and *C. albicans*). Furthermore, cytotoxicity effect of the AgNPs associated or not to TYR on fibroblast cells was investigated.

Materials and methods

Synthesis and Characterization of silver nanoparticles

Synthesis and characterization of the AgNPs solution was performed at the Interdisciplinary Laboratory of Electrochemistry and Ceramics (LIEC) Department of Chemistry, Federal University of São Carlos (UFSCar - São Carlos, São Paulo, Brazil). AgNPs were produced through the reduction of silver ions by a '*green*' route using extract of pomegranate peels (*Punica granatum L*.), as previously reported by Fernandes *et al*. (2018) and Souza *et al*. (2018). For this, silver nitrate ($AgNO_3$, Merck, Darmstadt, Germany) at 0.232 mM was dissolved in 10 mL of deionized water and heated to 90° C in a volumetric flask. Following, a surfactant (ammonium salt of polymethacrylic acid (NH-PM), Polysciences, Inc., Warrington, USA) at 0.128 mM and an aqueous solution of pomegranate peel extract at 7 mg/mL were added to the flask and kept at 95° C for 10 minutes under constant agitation. The resultant solution was stored in dark bottles at 4° C

and, was characterized by UV-visible absorption spectroscopy (UV-Vis) (spectrophotometer Shimadzu MutiSpec-1501, Shimadzu Corporation, Tokyo, Japan) and X-ray diffraction (XRD) (Diffractometer Rigaku DMax-2000PC, Rigaku Corporation, Tokyo, Japan). The particles morphology was characterized by scanning electron microscopy (SEM) using a Zeiss Supra 35VP microscope (S-360 microscope, Leo, Cambridge, USA) with field emission gun electron effect (FEG-SEM) operating at 10 kV.

Antimicrobial activity

Minimum inhibitory concentration (MIC)

AgNPs combined or not to TYR (Sigma-Aldrich, CAS 501-94-0, St. Louis, MO, USA) were tested against planktonic cells of *C. albicans* ATCC 10231 and *S. mutans* ATCC 25175 by the broth microdilution method, as previously reported (Arias *et al*. 2016). Briefly, a stock solution containing 6.2 mg Ag/mL (AgNPs) and 200 mM of TYR was prepared and diluted, sequentially, to a final concentration ranging from 1:2 to 1:512.

Based on the minimum inhibitory concentration (MIC) values, the fractional inhibitory concentration (FIC) was calculated. This index evaluates the drug synergism or antagonism based on MIC values for each compound and its association. To calculate the FIC index (FICI) the formula: $\Sigma FIC = FIC_A + FIC_B$, where $FIC_A = MIC_A$ in combination / MIC_A alone, and $FIC_B = MIC_B$ in combination / MIC_B alone, was used. $\Sigma FIC \leq 0.5$ indicates synergism; ΣFIC between 0.5 and 4.0, no interaction; and $\Sigma FIC > 4$, antagonism (Wei and Bobek 2004). MIC and FICI were performed in triplicate on three different occasions.

Biofilm killing

Twenty-four-old hours biofilms of *C. albicans* ATCC 10231 and *S. mutans* ATCC 25175 were grown using artificial saliva (Lamfon *et al*. 2003) in 96-well microtiter plates (Costar, Tewksbury, USA) and treated for 24 h with each drug (AgNPs and TYR) and its combination (AgNP+TYR). Previously, the drugs at ½ MIC, MIC, 10 and 100 x MIC values were tested in combination (pilot study), and the concentrations selected were 100 x MIC for *C. albicans* and ½ MIC for *S. mutans*: 244 µg Ag/mL (AgNP) and 7.8 mM (TYR), and 39.05 µg Ag/mL (AgNP) and 1.25 mM (TYR) respectively for each microorganism. After the treatments, biofilms were scraped from the bottom of the wells, serially diluted in phosphate-buffered saline and plated on Sabouraud Dextrose Agar

(Difco, Le Pont de Claix, France) (for *C. albicans*) or Brain Heart Infusion Agar (Difco) (for *S. mutans*) and, the sessile cells (after incubation at 37º C, 24-48 h) were counted and the Log_{10} per unit area was calculated (Log_{10} CFU/cm^2).

The effect of drug's combination against the biofilms was interpreted according to Miceli *et al*. (2009). When the drug combination (AgNP+TYR) showed a significant Log_{10} CFU/cm^2 reduction compared to AgNP or TYR alone ($p < 0.05$), the association was considered synergistic. When the combination showed a Log_{10} CFU/cm^2 lower than that observed for each drug alone, but no significant difference was observed ($p > 0.05$), the effect was classified as additive. An antagonistic effect was observed when the drugs alone (AgNPs and TYR) shower a lower Log_{10} CFU/cm^2 than the combinations tested ($p < 0.05$).

2.3. Cell culture

L929 mouse fibroblasts were cultured in Dulbecco's modified Eagle's medium (DMEM supplemented with 10% fetal bovine serum, 1% antibiotic/antimycotic cocktail (300 units/mL penicillin, 5 µg/mL amphotericin B), and L-glutamine 0.3 g/L. All of them were purchased from GIBCO BRL (Gaithersburg, Maryland, USA). Cells were maintained under standard cell culture conditions at 37º C in a humidified atmosphere of 95% air and 5% CO_2. Cells were routinely passaged using 0.25% trypsin (Sigma-Aldrich, St. Louis, Missouri, USA).

2.4. *In Vitro* Cytotoxicity Protocol

MTT assay was used to measure the cell viability as previously described by Bedran *et al*. (2014). Briefly, L929 fibroblasts were seeded into 24-well plates (1×10^4 cells/mL of medium/ well). After that, the cells were incubated at 37º C, in a humidified air atmosphere of 5% CO_2 for 24 h. The exposure of the cells to AgNPs+TYR was initiated at ~100% of cell confluence, and the assay was done in DMEM. Concentrations of the combination used in this study were: AgNPs – 39.05; 9.76 and 2.44 µg/mL combined with TYR – 1.25; 0.31 and 0.08 mM. Compounds also were evaluated alone. Three wells were used for each dose and substance tested. Tween 20 and culture medium were used as controls. The exposures of cell cultures were stopped by the discarding of the exposure medium after 24, 48 and 72 h. Viable cells were stained with formazan dye (3-[4,5-dimethylthiazol-2-yl]-2,5-diphenyltetrazolium bromide) (MTT) (Sigma Chemical Co, St. Louis, Missouri, USA). MTT was dissolved in PBS at 5 mg/L, filtered

in order to sterilize and remove small amounts of insoluble residues and after the times of cells exposure to AgNPs+TYR, AgNPs and TYR, stock MTT solution (20 µL per 180 µL of culture medium) was added to all wells of the assay, and plates were incubated at 37º C for 4 h. The MTT solution was then discarded and 200 µL of isopropyl alcohol were added to each well and mixed for 30 min to dissolve the dark blue crystals. The blue solution was then transferred to a 96-well plate and the optical density (OD) was read in a micro plate reader (Spectra Max 190; Molecular Devices, Sunnyvale, California, USA) at 570 nm wavelength. Viability was calculated as the ratio of mean of OD obtained for each condition compared to the control conditions. All laboratory assays were carried out at least three times.

3. Statistical Analysis

Sigma Plot 12.0 software (Systat Software Inc., San Jose, CA, USA) was used for statistical analysis, and the significance level was set at 5%. For *C. albicans* biofilms, results were analyzed applying one-way ANOVA followed by Student-Newman-Keuls *post hoc* test. For *S. mutans* biofilms, the CFU results did not pass normality test; thus, Kruskal-Wallis test was performed followed by Tukey's test. Cytotoxicity data were analyzed statistically by ANOVA and Bonferroni correction.

Results

Synthesis and characterization of AgNPs

UV-Vis presented a plasmon band between 420 and 450 nm (Fig. 1A), indicating the formation of nanoparticles. The XRD pattern of the AgNPs (Fig. 1B) showed diffraction peaks which correspond to (111), (200), (220) and (311) planes of pure Ag with face-centered cubic system (PDF № 04-0783). SEM image (Fig. 1C) demonstrated the formation of spherical nanoparticles and regular distribution with size of approximately 50 nm (Souza *et al*. 2018).

Antimicrobial evaluation

In the planktonic state, AgNPs were more effective against *S. mutans* (78.1 µg/mL) than *C. albicans* (312.5 µg/mL). For both microorganisms, the combination tested (AgNP+TYR) showed MICs substantially lower than those found for each compound alone. However, a synergistic effect was only observed against *C. albicans* (FICI = 0.008) (Table 1). In relation to effect on biofilms, for *C. albicans*, when AgNPs

were coupled with TYR, there was a significant reduction in the number of biofilm cells in comparison with negative control (NC) and with each drug alone ($p < 0.001$), showing a synergistic effect. For *S. mutans*, at a sub-inhibitory concentration (39.05 µg/mL), AgNPs were able to reduce 4.62 $\log_{10}$ the number of viable cells of the biofilm ($p < 0.001$). However, the addition of TYR to AgNPs did not improve their action against *S. mutans* biofilm (Figure 2).

In Vitro Cytotoxicity

The MTT assay was used to measure the cytotoxicity of AgNPs, TYR and AgNPs+TYR to cell line L929 after exposure for 24, 48 and 72 hours. As observed in Figure 3, the cytotoxicity of the compounds to L929 occurred in a dose-dependent manner for all periods analyzed. MTT conversion by cells significantly decreased after AgNPs+TYR treatment at 39.05 µg/mL (AgNPs) / 1.25 mM (TYR) ($p < 0.001$) compared with the control at 24, 48 and 72 hours. On the other hand, the others tested combinations were not toxic to fibroblast cells. For some concentrations of the compounds evaluated, there was a reduction in the cell viability at initial periods (24 and 48 h) ($p < 0.001$). However, after 72 h, the viability did not differ from the control group with exception of the TYR (1.25 mM) and AgNPs (39.05 µg/mL) / TYR (1.25 mM).

Discussion

A great effort has been put into developing metal nanoparticles synthesized using eco-friendly natural sources such as plant extracts, fruits, fungi, honey and microorganisms (Philip 2010) especially because they have lower cytotoxicity compared to conventional synthesis (Rajora *et al*. 2016). In this study, AgNPs were produced following the protocol described by Fernandes *et al*. (2018) and Souza *et al*. (2018), where the reduction agent used was pomegranate peel extract. Polyphenols such ellagic tannins and gallic and ellagic acids are commonly found in peel extracts of pomegranate (Singh *et al*. 2018) and participate in the reduction process of silver nanoparticles (Goudarzi *et al*. 2016).

In our study each microorganism responded differently to the nanoparticles. This fact may be due to the charge present on the outer membrane of *S. mutans* and cell wall of *C. albicans* as well as the thick of the membranes of both microorganisms. Although the external surface as *S. mutans* (Malanovic and Lohner 2016) as *C. albicans* is negatively charged (Lipke and Ovalle 1998), the main components are distinct. Gram

positive bacteria exhibit as the main component lipoteichoic acid crossing by peptidoglycan (Malanovic and Lohner 2016) whereas glucosamine polymer chitin and ß-glucan are present in the fungi cell wall (Lipke and Ovalle 1998), and it might afford different interactions of AgNPs with each site of outer surface of the microorganisms. Moreover, similarly with mechanism of action of some antimicrobials, AgNPs could interfere in the synthesis of some compounds of the membranes and disturb its integrity. It could alter the external charge of the microorganisms and consequently its susceptibility to the drug tested. For instance, AgNPs lead to leakage of the bacteria membrane through reducing the production of sugars by bacteria and hence its death (Li *et al*. 2013). In addition, gram positive bacteria exhibit about one third of the membrane thickness (60-80 nm) compared with fungi membrane (200 nm), which would favor the effect of AgNPs into the bulk of cell.

TYR had no effect on biofilm cells quantification. This fact may be due the low concentration of TYR proposed in this study (7.8 and 1.25 mmol/L respectively for *C. albicans* and *S. mutans*) when compared with concentration values used by Arias *et al*. (200 mmol/L for both microorganisms) (Arias *et al*. 2016). However, when used in combination with AgNPs against planktonic cells there was an expressively reduction of TYR concentration to affect *C. albicans* (625 times) and *S. mutans* (72 times). The synergism probably occurred in planktonic cells state due to their fragility, differently when they are in sessile form in biofilms, in which the presence of extracellular matrix and the expression of other biofilms defense mechanisms can prevent the penetration and action of the compounds studied (Kuhn and Ghannoum 2004). Also, AgNPs concentrations were considerably decreased when associated to TYR, notably for *C. albicans* which was almost 130 times lower than AgNPs alone. Furthermore, tested combinations were not toxic to fibroblast cells L929 in the different evaluated times, except to the highest association (AgNPs – 39.05 µg/mL + TYR – 1.25 mM).

In view of the foregoing results, the use of AgNPs associated with TYR may be an alternative for the prevention of denture stomatitis since its association caused an expressive reduction of *C. albicans* planktonic cells at very low concentrations. Noteworthy it was also noted AgNPs actively kill the biofilm cells of 4.62 $\log_{10}$ for *S. mutans* when exposed to sub-inhibitory concentration being nontoxic to fibroblast cells. Our results to indeed stimulate novel studies to further understand the biological basis of the action of those drugs in combination as well the sub-inhibitory doses of AgNPs against pathogenic biofilms. Moreover, considering the lack of antimicrobial disposable

options to control and treat chronic oral infection as denture stomatitis and caries disease, naturally derived AgNPs could be an attractive choice, particularly due to the phenolic compounds, which may offer advantages over chemically produced ones considering their anti-inflammatory and antioxidant activities and diminished toxicity against mammalian cells.

Acknowledgments

This study was supported by São Paulo Research Foundation (FAPESP), as PhD scholarship (Process 2015/00825-5) to the first author, and CAPES Foundation, Ministry of Education of Brazil (Processes 88881.030455/2013-01 and 88887.068358/2014-00).

Conflict of Interest

None to declare.

References

Perveen, S., Safdar, N., Chaudhry, G.E. and Yasmin, A. (2018) Antibacterial evaluation of silver nanoparticles synthesized from lychee peel: individual versus antibiotic conjugated effects. *World J Microbiol Biotechnol* **34(8)**, 118. doi: 10.1007/s11274-018-2500-1.

Pérez-Díaz, M.A., Boegli, L., James, G., Velasquillo, C., Sánchez-Sánchez, R., Martínez-Martínez, R.E., Martínez-Castañon, G.A. and Martinez-Gutierrez, F. (2015) Silver nanoparticles with antimicrobial activities against Streptococcus mutans and their cytotoxic effect. *Mater Sc. Eng C Mater Biol Appl* **55**, 360-366.

Reidy, B., Haase, A., Luch, A., Dawson, K.A. and Lynch, I. (2013) Mechanisms of silver nanoparticle release, transformation and toxicity: a critical review of current knowledge and recommendations for future studies and applications. *Materials (Basel)* **6(6)**, 2295-2350.

Soares, M.R.P.S., Corrêa, R.O., Stroppa, P.H.F. Marques, F.C., Andrade, G.F.S., Corrêa, C.C., Brandão, M.A.F. and Raposo, N.R.B. (2018) Biosynthesis of silver nanoparticles using *Caesalpinia ferrea* (Tul.) Martius extract: physicochemical characterization, antifungal activity and cytotoxicity. *PeerJ* **6**:e4361. doi: 10.7717/peerj.4361.

Kim, S.W., Jung, J.H., Lamsal, K., Kim, Y.S., Min, J.S. and Lee, Y.S. (2012) Antifungal effects of silver nanoparticles (AgNPs) against various plant pathogenic fungi. *Mycobiology* **40(1)**, 53-58.

Khandelwal, N., Kaur, G., Kumar, N. and Tiwari, A. (2014) Application of silver nanoparticles in viral inhibition: A new hope for antivirals. *Dig J Nanomater Biostructures* **9(1)**, 175-186.

Akhtar, M.S., Swamy, M.K., Umar, A. and Al Sahli, A.A. (2015) Biosynthesis and characterization of silver nanoparticles from methanol leaf extract of Cassia didymobotyra and assessment of their antioxidant and antibacterial activities. *J Nanosci Nanotechno* **15(12)**, 9818-9823.

Souza, J.A., Barbosa, D.B., Berretta, A.A., do Amaral, J.G., Gorup, L.F., de Souza Neto, F.N., Fernandes, R.A., Fernandes, G.L., Camargo, E.R., Agostinho, A.M. and Delbem, A.C. (2018) Green synthesis of silver nanoparticles combined to calcium glycerophosphate: antimicrobial and antibiofilm activities. *Future Microbiol* **13**, 345-357.

Monteiro, D.R., Negri, M., Silva, S., Gorup, L.F., de Camargo, E.R., Oliveira, R., Barbosa, D.B. and Henriques, M. (2014) Adhesion of Candida biofilm cells to human epithelial cells and polystyrene after treatment with silver nanoparticles. *Colloids Surf B Biointerfaces* **114**, 410-412.

Freire, P.L., Stamford, T.C. and Albuquerque, A.J. (2015) Action of silver nanoparticles towards biological systems: cytotoxicity evaluation using hen's egg test and inhibition of Streptococcus mutans biofilm formation. *Int J Antimicrob Agents* **45(2)**, 183-187.

Velázquez-Velázquez, J.L., Santos-Flores, A., Araujo-Meléndez, J., Sánchez-S-anchez, R., Velasquillo, C., González, C., Martínez-Castañon, G. and Martinez-Gutierrez, F. (2015) Anti-biofilm and cytotoxicity activity of impregnated dressings with silver nanoparticles. *Mater Sci Eng C Mater Bio. Appl* **49**, 604-611.

Patil, M.P. and Kim, G.D. (2017) Eco-friendly approach for nanoparticles synthesis and mechanism behind antibacterial activity of silver and anticancer activity of gold nanoparticles. *Appl Microbiol Biotechnol* **101(1)**, 79-92.

de Matos, R.A. and Courrol, L.C. (2016) Biocompatible silver nanoparticles prepared with amino acids and a green method. *Amino Acids* **49(2)**, 379-388.

Fernandes, R.A., Berretta, A.A., Torres, E.C., Buszinski, A.F.M., Fernandes, G.L., Mendes-Gouvêa, C.C., de Souza-Neto, F.N., Gorup, L.F., de Camargo, E.R. and

Barbosa, D.B. (2018) Antimicrobial potential and cytotoxicity of silver nanoparticles phytosynthesized by pomegranate peel extract. *Antibiotics (Basel)* **7(3)**. pii: E51. doi: 10.3390/antibiotics7030051.

Nasiriboroumand, M., Montazer, M. and Barani, H. (2018) Preparation and characterization of biocompatible silver nanoparticles using pomegranate peel extract. *J Photochem Photobiol B* **179**, 98-104.

Singh, B., Singh, J.P., Kaur, A. and Singh, N. (2018) Phenolic compounds as beneficial phytochemicals in pomegranate (Punica granatum L.) peel: A review. *Food Chem*. **261**, 75-86.

Moteriya, P. and Chanda, S. (2016) Synthesis and characterization of silver nanoparticles using Caesalpinia pulcherrima flower extract and assessment of their in vitro antimicrobial, antioxidant, cytotoxic, and genotoxic activities. *Artif Cells Nanomed Biotechnol* **45(8)**, 1556-1567.

Longhi, C., Santos, J.P., Morey, A.T., Marcato, P.D., Durán, N., Pinge-Filho, P., Nakazato, G., Yamada-Ogatta, S.F. and Yamauchi, L.M. (2016) Combination of fluconazole with silver nanoparticles produced by Fusarium oxysporum improves antifungal effect against planktonic cells and biofilm of drug-resistant Candida albicans. *Med Mycol* **54(4)**, 428-432.

Wongsuk, T., Pumeesat, P. and Luplertlop, N. (2016) Fungal quorum sensing molecules: Role in fungal morphogenesis and pathogenicity. *J. Basic Microbiol* **56(5)**, 440-447.

Monteiro, D.R., Arias, L.S., Fernandes, R.A., Straioto, F.G., Barros Barbosa, D., Pessan, J.P. and Delbem, A.C.B. (2017) Role of tyrosol on Candida albicans, Candida glabrata and Streptococcus mutans biofilms developed on different surfaces. *Am J Dent* **30(1)**, 35-39.

Arias, L.S., Delbem, A.C., Fernandes, R.A., Barbosa, D.B. and Monteiro, D.R. (2016) Activity of tyrosol against single and mixed-species oral biofilms. *J Appl Microbiol* **120(5)**, 1240-1249.

Abdel-Rhman, S.H., El-Mahdy, A.M. and El-Mowafy, M. (2015) Effect of Tyrosol and Farnesol on Virulence and Antibiotic Resistance of Clinical Isolates of Pseudomonas aeruginosa. *Biomed Res. Int.* **2015**, 456463. doi: 10.1155/2015/456463.

Mathé, L. and Van Dijck, P. (2013) Recent insights into Candida albicans biofilm resistance mechanisms. *Curr Genet* **59(4)**, 251-264.

Shanmughapriya, S., Sornakumari, H., Lency, A., Kavitha, S. Natarajaseenivasan, K. (2014) Synergistic effect of amphotericin B and tyrosol on biofilm formed by Candida krusei and Candida tropicalis from intrauterine device users. *Med Mycol* **52(8)**, 853-861.

Cordeiro Rde, A., Teixeira, C.E., Brilhante, R.S., Castelo-Branco, D.S., Alencar, L.P., de Oliveira, J.S., Monteiro, A.J., Bandeira, T.J., Sidrim, J.J., Moreira, J.L. and Rocha, M.F. (2015) Exogenous tyrosol inhibits planktonic cells and biofilms of Candida species and enhances their susceptibility to antifungals. *FEMS Yeast Res* **15(4)**, fov012. doi: 10.1093/femsyr/fov012.

Broadbent, J.M., Foster Page, L.A., Thomson, W.M. and Poulton, R. (2013) Permanent dentition caries through the first half of life. *Br Dent J* **215(7)**, E12. doi: 10.1038/sj.bdj.2013.991.

O'Donnell, L.E., Alalwan, H.K., Kean, R. Calvert, G., Nile, C.J., Lappin, D.F., Robertson, D., Williams, C., Ramage, G. and Sherry, L. (2017) Candida albicans biofilm heterogeneity does not influence denture stomatitis but strongly influences denture cleansing capacity. *J Med Microbiol* **66(1)**, 54-60.

Nikawa, J., Yamashiro, H., Makihira, S. Nishimura, M., Egusa, H., Furukawa, M., Setijanto, D. and Hamada, T. (2003) In vitro cariogenic potential of Candida albicans. *Mycoses* **46(11-12)**, 471-478.

De Carvalho, F.G., Silva, D.S., Hebling, J., Spolidorio, L.C. and Spolidorio, D.M. (2006) Presence of mutans streptococci and Candida spp. in dental plaque/dentine of carious teeth and early childhood caries. *Arch Oral Biol* **51(11)**, 1024-1028.

Raja, M., Hannan, A. and Ali, K. (2010) Association of oral candida carriage with dental caries in children. *Caries Res* **44(3)**, 272-276.

Ghasempour, M., Sefidgar, S.A., Eyzadian, H. and Gharakhani, S. (2011) Prevalence of Candida albicans in dental plaque and caries lesion of early childhood caries (ECC) according to sampling site. *Caspian J Intern Med* **2(4)**, 304-308.

Kim, J.S., Kuk, E., Yu, K.N., Kim, J.H., Park, S.J., Lee, H.J., Kim, S.H., Park, Y.K., Park, Y.H., Hwang, C.Y., Kim, Y.K., Lee, Y.S., Jeong, D.H. and Cho, M.H. (2007) Antimicrobial effects of silver nanoparticles. *Nanomedicine* **3(1)**, 95-101.

Wei, G.X. and Bobek, L.A. (2004) In vitro synergic antifungal effect of MUC7 12-mer with histatin-5 12-mer or miconazole. *J Antimicrob Chemother* **53(5)**, 750-758.

Miceli, M.H., Bernardo, S.M. and Lee, S.A. (2009) *In vitro* analyses of the combination of high-dose doxycycline and antifungal agents against *Candida albicans* biofilms. *Int J Amtimicrob Agents* 34, 326-332.

Bedran, T.B., Mayer, M.P., Spolidorio, D.P. and Grenier, D. (2014) Synergistic anti-inflamatory activity of the antimicrobial peptidies human beta-defensin-3 (hBD3) and cathelicidin (LL-37) in a three-dimensional co-culture model of gingival epithelial cells and fibroblasts. *PLoS One* **9(9)**, e106766. doi: 10.1371/journal.pone.0106766.

Philip, D. (2010) Rapid green synthesis of spherical gold nanoparticles using Mangifera indica leaf. *Spectrochim. Acta A Mol Biomol Spectrosc* **77(4)**, 807-810.

Rajora, N., Kaushik, S., Jyoti, A. and Kothari, S.L. (2016) Rapid synthesis of silver nanoparticles by Pseudomonas stutzeri isolated from textile soil under optimised conditions and evaluation of their antimicrobial and cytotoxicity properties. *IET Nanobiotechnol* **10(6)**, 367-373.

Goudarzi, M., Mir, N., Mousavi-Kamazani, M., Bagheri, S. and Salavati-Niasiri, M. (2016) Biosynthesis and characterization of silver nanoparticles prepared from two novel natural precursors by facile thermal decomposition methods. *Sci Rep* **6**, 32539.

Gorup, L.F., Longo, E., Leite, E.R. and Camargo, E.R. (2011) Moderating effect of ammonia on particle growth and stability of quasi-monodisperse silver nanoparticles synthesized by the Turkevich method. *J Colloid Interface Sci* **360(2)**, 355-358.

Ben Nasr, C., Ayed, N. and Metche, M. (1996) Quantitative determination of the polyphenolic content of pomegranate peel. *Z Lebensm Unters Forsch* **203(4)**, 374-378.

Singh, R.P., Chidambara Murthy, K.N. and Jayaprakasha, G.K. (2002) Studies on the antioxidant activity of pomegranate (Punica granatum) peel and seed extracts using in vitro models. *J Agric Food Chem* **50(1)**, 81-86.

Malanovic, N. and Lohner, K. (2016) Gram-positive bacterial cell envelopes: The impact on the activity of antimicrobial peptides. *Biochim Biophys Acta* **1858(5)**, 936-946.

Lipke, P.N. and Ovalle, R. (1998) Cell wall architecture in yeast: new structure and new challenges. *J Bacteriol* **180(15)**, 3735-3740.

Li, J., Rong, K., Zhao, H., Li, F., Lu, Z. and Chen, R. (2013) Highly selective antibacterial activities of silver nanoparticles against Bacillus subtilis. *J Nanosci Nanotechnol* **13(10)**, 6806-6813.

Kuhn, D.M. and Ghannoum, M.A. (2004) Candida biofilms: antifungal resistance and emerging therapeutic options. *Curr Opin Investig Drugs* **5(2)**, 186-197.

Tables

Table 1. Minimum inhibitory concentration (MIC) of silver nanoparticles (AgNP) and tyrosol against *Streptococcus mutans* and *Candida albicans* and fractional inhibitory concentration (FIC).

Microorganism	Treatments			ΣFICI
	AgNP (µg/mL)	*Tyrosol* (mM)	*AgNP/Tyrosol*	
C. albicans	312.5	50	2.44/0.08	0.008
S. mutans	78.1	90	39.05/1.25	0.63

∗The association was considered as synergistic when FICI ≤ 0.5; indifferent when 0.5 < FICI < 4, and antagonistic when FICI >4.0.

Figures

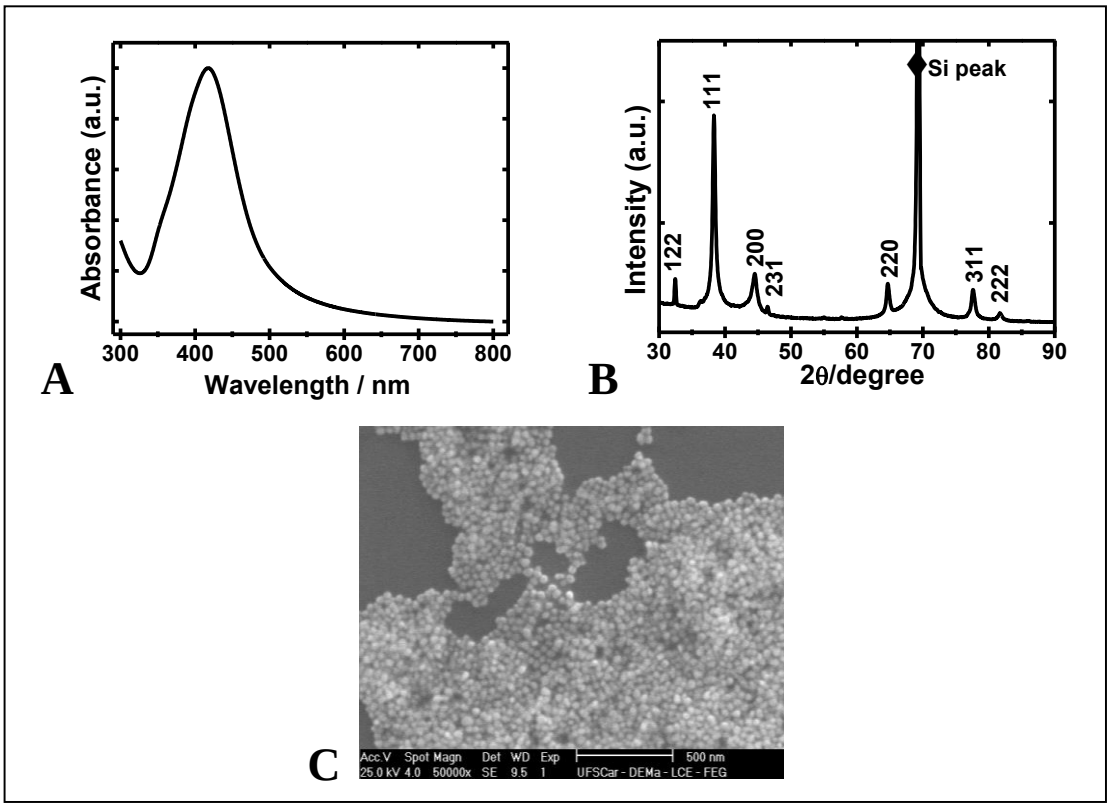

Figure 1. UV-Visible spectrum (A), XRD pattern and (C) SEM micrograph of the AgNPs. XRD: X-ray diffraction; SEM: Scanning electron microscopy; AgNPs: silver nanoparticles.

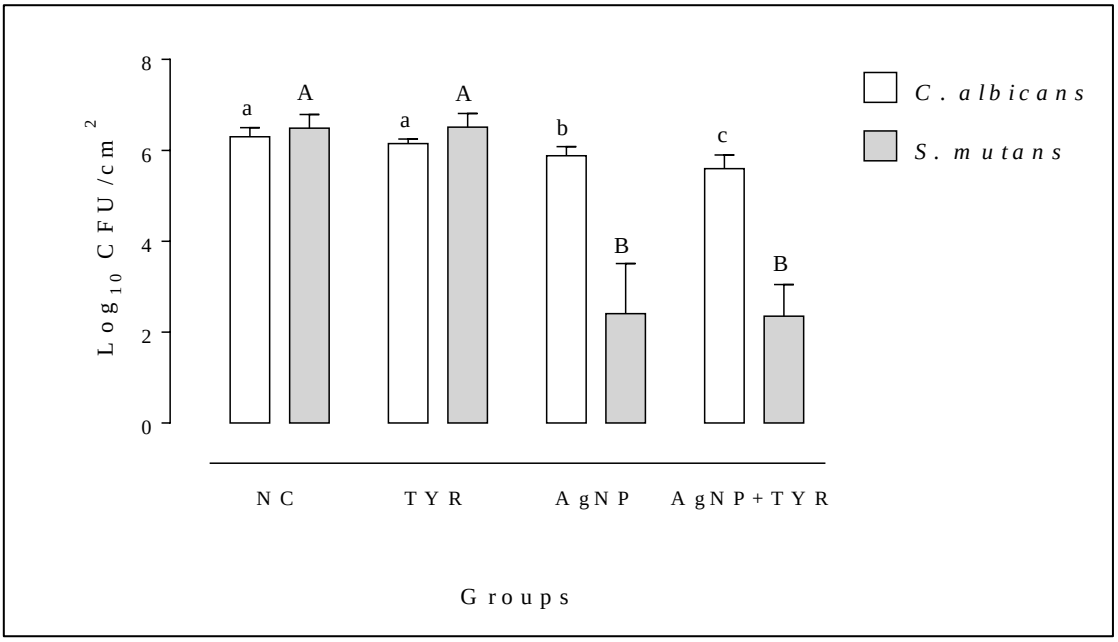

Figure 2. Mean values (±SD) of the logarithm of colony forming units per cm^2 (log_{10} CFU/cm^2) for *C. albicans* and *S. mutans* single biofilms. NC = negative control (artificial saliva); TYR (tyrosol) at 7.8 mM and 1.25 mM; AgNP (silver nanoparticles) at 244 µg/mL and 39.05 µg/mL for *C. albicans* and *S. mutans*, respectively. Different lowercase letters indicate significant difference among the treatments for *C. albicans* biofilm ($p<0.05$; Student-Newman-Keuls test) and capital letters for *S. mutans* biofilm ($p<0.05$, Tukey test).

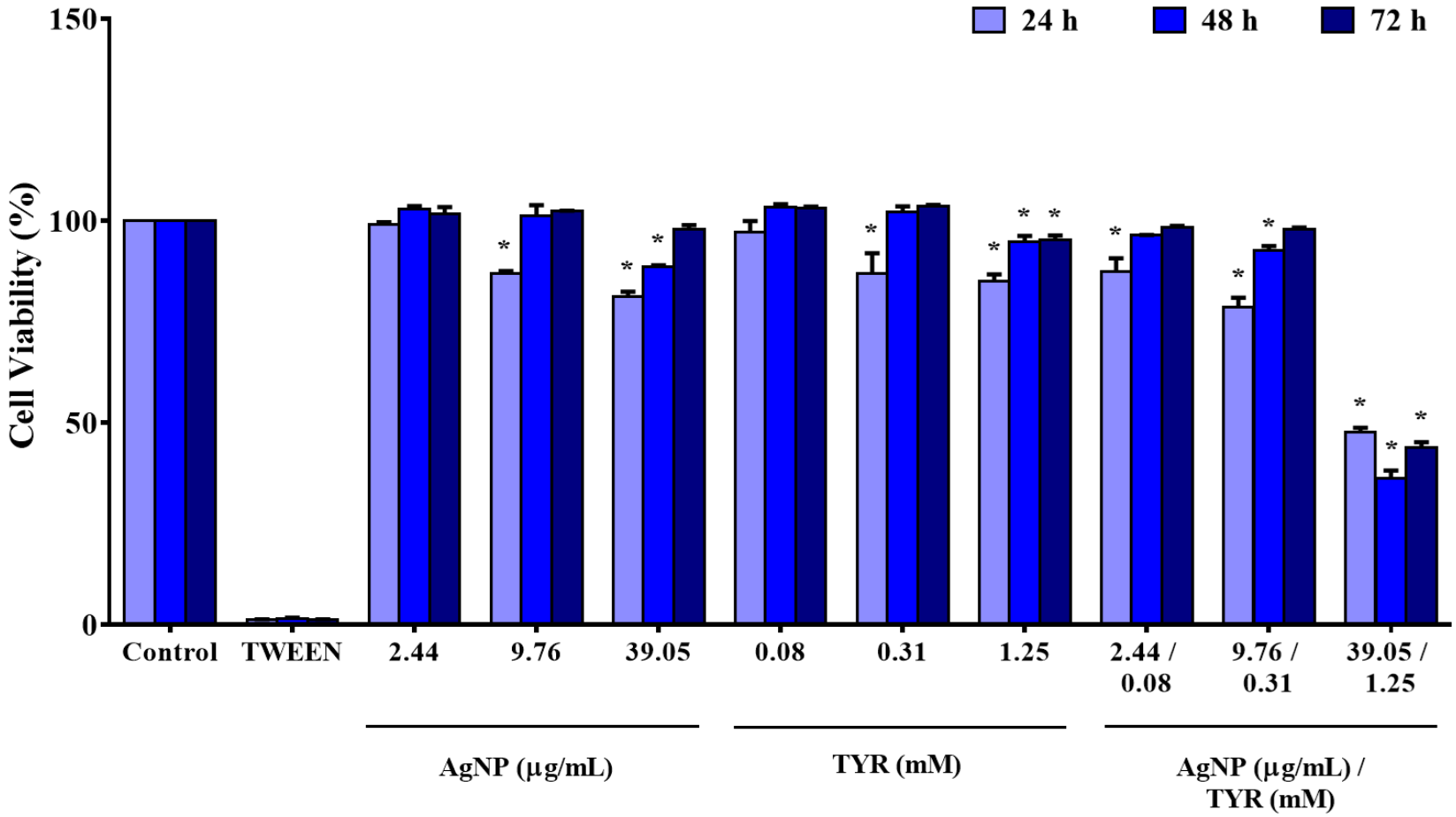

Figure 3. Cytotoxicity of AgNPs, TYR and AgNPs+TYR to fibroblasts (L929) after 24, 48, and 72 hours of treatment expressed as a percentage. Error bars indicate the standard deviations of the means. *Significant diference ($p < 0.001$) compared with the control group using ANOVA with the Bonferroni correction.

CAPÍTULO 5

'*Green*'-synthesized silver nanoparticles inhibit growth, filamentation and biofilm formation prompted by *Candida albicans* and *Candida glabrata* *

***** *Artigo nas normas do periódico Medical Micology*

'*Green*'-synthesized silver nanoparticles inhibit growth, filamentation and biofilm formation prompted by *Candida albicans* and *Candida glabrata*

Short-title: *In vitro* antifungal activity of '*green*'-synthesized silver nanoparticles

José Antonio Santos Souza[1], Marta M. Alves[2], Débora Barros Barbosa[1], Mª Manuel Lopes[3], Alberto Carlos B. Delbem*[1], Nuno Pereira Mira*[4]

[1]São Paulo State University (UNESP), School of Dentistry, Araçatuba, São Paulo, Brazil.
[2]Centro de Química Estrutural, Instituto Superior Técnico, Universidade de Lisboa, Lisbon, Portugal.
[3]Faculdade de Farmácia da Universidade de Lisboa, Departamento de Microbiologia e Imunologia, Av. Prof. Gama Pinto, 1649-003 Lisbon.
[4]iBB, Institute for Bioengineering and Biosciences, Instituto Superior Técnico – Department of Bioengineering, Universidade de Lisboa, Lisbon, Portugal.

*Corresponding author: Prof. Nuno Pereira Mira, iBB, Institute for Bioengineering and Biosciences, Instituto Superior Técnico – Department of Bioengineering, Universidade de Lisboa, Av. Rovisco Pais, 1049-001, Lisboa, Portugal; email: nuno.mira@tecnico.ulisboa.pt; Tel. +351-218419181; Fax +351-218489199; Alberto Carlos Botazzo Delbem, São Paulo State University (UNESP), School of Dentistry, Department of Pediatric Dentistry and Public Health, Rua José Bonifácio, 1193, 16015-050 Araçatuba – SP, Brazil, Tel. +55 18 3636 3314, Fax +55 18 3636 3332, Email: alberto.delbem@unesp.br.

Keywords: '*Green*' synthesis of silver nanoparticles, Oral candidiasis, *Candida albicans*, *Candida glabrata*, Biofilms.

Abstract

The aim of this study has been to analyze the antimicrobial efficacy of '*green*'-synthesized silver nanoparticles (AgNPs) against 57 strains of *Candida* spp. (two standard and 55 oral isolates) as well as evaluate the ability of AgNPs to synergize with fluconazole, nystatin and amphotericin B against the fluconazole-resistant *C. albicans* strains. Antibiofilm effect of AgNPs against *Candida* strains also was investigated. AgNPs were synthesized using peel extract of pomegranate. Minimum inhibitory concentration (MIC_{50}) of AgNPs alone or in combination with different antifungal agents was assessed through microdilution method recommended by EUCAST. Filamentation form inhibition also was determined. The effect of AgNPs on *Candida* biofilms was assessed through PrestoBlue, quantification of colony-forming units (CFUs) and scanning electron microscopy (SEM). Only two isolates of *C. albicans* were resistant to fluconazole, and these susceptible to '*green*'-AgNPs. *C. glabrata* oral isolates presented the lowest MIC_{50} values for AgNPs when compared with *C. albicans* isolates. AgNPs were able to inhibit *C. albicans* and *C. glabrata* biofilm formation; SEM images showed a reduction in the formation of hyphae (in *C. albicans*) and alterations in the cell morphology (in both biofilms). Nanoparticles were effective against early (12 h) and mature (24 h) *C. glabrata* biofilms. Also, a synergistic activity of AgNPs with tested antifungals was observed. '*Green*'-AgNPs are a potent antifungal agent with effect on *C. albicans* and *C. glabrata* oral clinical isolates, including fluconazole-resistant strains and *C. glabrata* biofilms in different formation phases. Nanoparticles also presented synergistic activity against fluconazole-resistant clinical isolates when associated to antifungal agents used in clinical practice.

1. Introduction

Candida species are microbes commonly found in the microflora of the oral cavity, of the skin and of the gastrointestinal, respiratory or genitourinary tracts of humans.[1] Under certain conditions these commensal populations can overgrow causing infections (generally referred as candidiasis) that range from mild rushes to deathly disseminated mycoses.[2] Oral candiadiasis is one of the more common forms of superficial candidiasis and varies from point pseudomembrane infections (thrush) causing inflammation and soreness, to more serious cases where chronic mucositis is observed with consequent appearance of erythroplakic and leukoplakic lesions.[3] Although the incidence of oral candidiasis in healthy individuals is sporadic, in some groups where immunosuppression is observed, the incidence reaches levels as high as 90%, as it is the case of AIDS patients.[4-6] Besides causing a significant burden for healthcare systems due to the large amount of resources spent in prophylactic and active therapies, prolonged infections caused by *Candida* in the oral mucosa have also been linked with the development of more serious pathologies, such as progressive periodontal diseases, dental caries and, more rarely, cancer.[3, 7] Oral candidiasis was also found to be a relevant risk factor for the development of systemic candidiasis since the colonizing oral population can serve as a reservoir for subsequent dissemination in the bloodstream.[3] *Candida albicans* is the most relevant ethiological agent causative of oral candiadiasis, but the number of infections caused by non-*Candida albicans Candida* species (usually known as NCAC) is increasing, with emphasis on infections caused by *C. glabrata*.[8-10] This shift in the pattern of infecting *Candida* species in the oral tract is also observed in other infection sites[11, 12] and is believed to result from the massive use of fluconazole, either in active treatments and in prophylaxis, that resulted in the selection of more tolerant strains/species. Indeed, *C. glabrata* is well known for its intrinsically high resilience to fluconazole and other azoles, specially when compared with *C. albicans*.[9] Part of the success of *C. albicans* and *C. glabrata* as oral pathogens relies on their ability to easily adhere to both biotic (such as oral epithelial cells or the teeth) and abiotic surfaces (such as dentures or orthodontic appliances) found in the oral cavity.[3, 13] After an initial stage of adherence, *Candida* cells keep further developing on the different surfaces as biofilms, in which the cells form a complex community embedded in a self-secreted extracellular matrix.[14] Growth in the form of a biofilm confers *Candida* cells a highly protected environment that provides protection against the activity of the host immune system or to environmental stressors, including antifungals.[14, 15] In line with this, studies show that

Candida cells are much more tolerant to azoles, echinocandins or polyenes when growing in a biofilm than during planktonic growth, as reviewed by Silva et al. (2017).[15] Besides high adhesiveness, other factors attributable to *C. albicans* virulence in the oral tract include the ability to trigger filamentation and the secretion of extracellular proteases that facilitate penetration to the inner layers of oral epithelium.[16] Compared to *C. albicans*, the mechanisms underlying *C. glabrata* virulence in the oral niche remain far less understood, being observed that this yeast species does not undergo the yeast-hyphae transition and it also does not appear to secrete proteases as a mean to colonize oral epithelial cells.[9]

The increase in the emergence of *C. albicans* and *C. glabrata* strains resistant to currently used oral antifungals (in particular, to fluconazole) has been paving the way for the search of alternative anti-*Candida* agents. Ideally, these new agents should have a different biological target than those targeted by azoles to assure a higher efficacy even against azole-resistant strains. In the recent years, silver nanoparticles (AgNPs), synthesized either by conventional chemical reduction methods or by different biological entities, have been highlighted as interesting antimicrobial agents showing activity against bacteria, virus and fungi, including *Streptococcus mutans*,[17-19] *Staphylococcus aureus*,[20] *C. albicans*, *C. glabrata*, *C. krusei* and *C. guilliermondii*.[18, 21-25] The advantages of AgNPs include the simplicity of the synthesis process and the possibility of being incorporated on dental materials, medical devices and surgical textile fabrics thereby reducing the risk of infection.[26, 27] Recently, we have reported the successful synthesis of AgNPs through a '*green*' process using extracts of different parts of the fruit *Punica granatum*.[18] Comparing with chemical methods to synthesize AgNPs, '*green*' processes are more environmental friendly, more cost effective, easier to scale up and more biocompatible.[28] The pomegranate peel is characterized by having a high phenolic content largely composed by ellagic and gallic acid, that are believed to serve as reducing agents for Ag^{+} ions as well as to contribute for stabilization of AgNPs.[29-31] Previous work from Souza et al. (2018)[18] showed that the AgNPs synthesized by this '*green*' process exhibit activity against *S. mutans* and *C. albicans*, showing the potential to inhibit growth of these species when they grow planktonically or in a biofilm. Notably, the efficacy of the greenly synthesized AgNPs against *S. mutans* was comparable or even above the one exhibited by chlorhexidine, a commonly used oral antimicrobial agent.[18] More recently, it was also shown that spray formulations containing the '*green*' synthesized AgNPs maintain a robust activity against *C. albicans* and *S. aureus*.[20] In the

present study we aimed at keep fostering the utilization of '*green*' AgNPs as anti-*Candida* agents and therefore the activity of the AgNPs synthesized from the pomegranate peel of *Punica granatum* was tested against a set of oral clinical strains of *C. albicans* and of *C. glabrata* strains, including against strains shown to be resistant to fluconazole. We have also examined the existence of synergistic effects between the AgNPs synthesized from *Punica granatum* with traditional therapeutics used in treatment of oral candidiasis (fluconazole, nystatin and amphotericin B), as well as the effect of the '*green*' AgNPs as inhibitors of biofilm formation and filamentation, two factors known to underlie *C. albicans* and *C. glabrata* oral pathogenesis.

2. Materials and Methods

2.1. *Candida* strains and growth media

A total of 57 strains were used in this work including two reference strains (*C. albicans* SC5314 and *C. glabrata* CBS138) and 55 clinical isolates recovered from the oral tract of healthy individuals and patients with diagnosed prosthetic stomatitis. Yeasts were cultured on Yeast Peptone Dextrose (YPD) medium or in RPMI medium (adjusted to pH 7.0) depending on the assay. YPD contains, per liter, 20 g glucose (Merck Millipore, Portugal), 10 g of yeast extract (HiMedia Laboratories, Mumbai, India) and 20 g peptone (HiMedia Laboratories). RPMI contains, per liter, 20.8 g RPMI-1640 synthetic medium (Sigma), 36 g glucose (Merck Millipore), 0.3 g of L-glutamine (Sigma) and 0.165 mol/L of MOPS (3-(N-morpholino) propanesulfonic acid, Sigma). To obtain the solid media 2% agar were added to the corresponding liquid medium composition.

2.2. Preparation of '*green*' AgNPs

'*Green*' synthesis of AgNPs was performed according to Souza et al. (2018)[18] and Gorup et al. (2011)[32]. Briefly, 0.42 g of silver nitrate ($AgNO_3$, Merck KGaA) were dissolved in 100 mL of deionized water heated to 90º C. Next, 5 mL of ammonium salt of polymethacrylic acid was added followed by 0.7 g of aqueous extract of the peel of *P. granatum*. The reaction was kept under constant agitation at 95º C for 10 min. During the study, antimicrobial solution was stored in dark bottles at 4º C.

2.3. Assessment of *C. glabrata*/*C. albicans* strains susceptibility to fluconazole

Susceptibility of the isolates or of the reference strains to fluconazole (FLC) was performed using a standardized microdilution method to assess the minimum inhibitory

concentration (MIC_{50}), similar to the method recommended by the European Committee for Antimicrobial Susceptibility Testing (EUCAST) to test the inhibitory effect of azoles.[33] *C. glabrata* and *C. albicans* cells were cultivated for 17 h in YPD growth medium at 30º C with 250 rpm orbital agitation and then diluted in RPMI to obtain a cell suspension having an OD_{600nm} of 0.05. 100 µL of these cell suspensions were mixed in 96-well polystyrene plates (Costar) with 100 µL of fresh RPMI medium 2x concentrated (control) or with 100 µL of this same medium supplemented with FLC. The concentrations of FLC tested ranged from 0.125 to 64 mg/L. The stock solutions of FLC were prepared in DMSO and kept at -20º C until further use. The inoculated plates were incubated at 37º C for 24 h and, after this period, the optical density (OD_{530nm}) of the culture was measured in a microplate reader (SpectroStar Nano, BMG Labtech, Germany). MIC_{50} values were taken as being the first concentration of antifungal that reduced growth of the strains to half that registered in drug-free medium, as defined by EUCAST (2008).[33] The MIC_{50} values for each clinical strain were compared with the clinical breakpoint recommended by EUCAST (2017)[34] to classify the isolates as resistant, susceptible dose-dependent or susceptible. As such, *C. albicans* isolates were considered resistant to FLC when MIC_{50} values were above 4 mg/L and susceptible when the MIC_{50} values was equal or below 2 mg/L. For *C. glabrata*, isolates with MIC_{50} above of 32 mg/L were considered resistant, while those exhibiting a MIC_{50} equal or below 0.002 mg/L were considered susceptible and those with MIC_{50} values between 32 and 0.002 were considered susceptible dose-dependent. All the assays were performed in duplicate.

2.4. Assessment of the inhibitory effect of the '*green*' AgNPs against *C. albicans* and *C. glabrata*, alone or in combination with other antifungals

The effect of the '*green*' synthesized AgNPs in inhibiting growth of *C. albicans* and *C. glabrata* (reference or clinical strains) was based on the determination of the MIC_{50}, by a microdilution method similar to the one detailed in 2.3. Concentrations ranging between 1.22 to 1,024 mg/L of AgNPs were used. The existence of a synergistic effect between the '*green*' AgNPs and FLC, nystatin (NYT) or amphotericin B (AmB) was tested using a checkerboard method[35] in which the MIC_{50} for the different drugs (alone or in combination) is determined using a microdilution method similar to the one described in 2.3. The MIC_{50} value determined was afterwards used to calculate the fractional inhibitory concentration index (FICI), through the following formula: ΣFICI =

FIC_A + FIC_B, where FIC_A = MIC_A in combination / MIC_A alone, and FIC_B = MIC_B in combination / MIC_B alone. FICI values ≤ 0.5 indicate synergism; between 0.5–4.0, no interaction; > 4.0, antagonism.[36-38] Stock solutions of FLC or of AmB (Sigma) were prepared in DMSO while the stock solution of NYT (Bristol-Myers Squibb, Moreton, UK) was prepared in RPMI. The range of concentrations used for each antifungal was: AgNPs – 8 to 64 mg/L; FCL – 0.063 to 0.50 mg/L; nystatin – 0.125 to 0.50 mg/L and AmB – 0.016 to 0.125 mg/L.

2.5. Assessment of the presence of '*green*' AgNPs on filamentation and biofilm formation undertaken by *C. albicans* and *C. glabrata*

To assess the effect of the '*green*' AgNPs on the ability of *C. albicans* SC5314 to filament, cells were cultivated overnight in YPD medium and then diluted (to obtain a cell suspension having an OD_{600nm} of 0.05) in fresh RPMI supplemented or not with the AgNPs and with 10% fetal bovine serum (FBS, Sigma). The cells were further incubated at 30º C for 24 h, after which sets of microscopic images (taken with a Zeiss microscope equipped with a 1,000x magnification lense) were taken. The number of cells undergoing filamentation was compared with the total number of cells present in the pictures to assess the percentage of filamenting cells. The assays were performed in duplicate and more than 200 cells were used in each assay. For statistical analysis, the GraphPad Prism 7.0 (GraphPad Software, CA, USA) program was used, and the significance level was set at 5%; two-way analysis of variance (ANOVA) was applied followed by the Sidak's multiple comparisons test.

To assess the effect of the AgNPs on biofilm formation undertaken by *C. albicans* SC5314 and *C. glabrata* CBS138, the cells were cultivated in RPMI in 96-well polystyrene plates (Costar) in the presence or absence of AgNPs and using the same experimental setting described in 2.3. for the determination of MIC_{50}. In the case of *C. albicans*, the concentrations of AgNPs tested were 600, 700, 800 and 900 mg/L, while for *C. glabrata* 1.22; 2.44; 4.88; 9.76; 24.40 and 122.0 mg/L was used. After 24 h of incubation at 37º C, the supernatant was removed and the wells were washed twice with 100 µL of phosphate-buffered saline (PBS; 0.1 mol L^{-1}, pH 7). The remaining PBS was aspirated and the amount of biofilm formed was quantified by adding 100 µL of PrestoBlue™ Cell Viability Reagent (Invitrogen™, Carlsbad, CA, USA) diluted (1:10) in RPMI. The mixture was then incubated for 30 min at 37º C. After this, 80 µL from each well were transferred into a new 96-well plate for fluorescent readings at two

wavelengths (570 and 600 nm). The amount of biofilm formed by each strain in each condition tested was based on the A570 nm value normalized to the corresponding A600 nm value.[39] All the assays were performed in triplicate. In both cases, one-way ANOVA was applied followed by the Dunnett's multiple comparisons test.

To further characterize the effect of AgNPs in the structure of the biofilms formed, these were formed using the same experimental conditions described above with the difference that 5 mL polystyrene plates (Greiner Bio One, Germany) were used instead of the 96-microwell plates. After 24 h of incubation at 37º C, the supernatant was removed and the cells adhered to the surface of the plate were dehydrated using the following protocol: washing with distilled water, washing with 70% ethanol for 10 minutes; washing with 95% ethanol for 10 minutes; and washing with 100% ethanol for 20 minutes. Plates were then dried in a desiccator for 48 h, coated with gold and visualized by scanning electron microscope (SEM) with a JEOL-JSM7001F apparatus in different magnifications.[40]

2.6. Effect of AgNPs in mature biofilms *C. glabrata* CBS138

To assess the effect of AgNPs in mature biofilms formed by *C. glabrata* CBS138 on the surface of 96-multiwell polystyrene plates the same experimental setting used in 2.5 was employed. After 12 or 24 h, the medium was carefully removed from the 96-multiwell plates and replaced by fresh RPMI medium either or not supplemented with 2.44 mg/L of the '*green*' AgNPs. Incubation proceeded for another 24 h at 37º C, after which cellular viability of the biofilm-embedded was measured by staining with PrestoBlue. For this the same staining procedure described in 2.5 was used. For statistical analysis, two-way ANOVA followed by the Sidak post hoc test.

3. Results

3.1. Effect of '*green*' AgNPs against oral *C. albicans* isolates, including against fluconazole-resistant strains

Because reports in the literature show significant strain-to-strain variation among *C. albicans* species in what concerns resistance to antimicrobials, we have decided to assess whether the reported inhibitory effect of the '*green*' AgNPs against the SC5314 strain would be comparable with the one registered for clinical isolates recovered from the oral tract. For that we have explored a cohort of 50 isolates that were recovered from healthy donors and from patients with diagnosed prosthetic stomatitis during an

epidemiological survey undertaken in Portugal. The results obtained showed that the MIC_{50} of the '*green*' AgNPs for the *C. albicans* SC5314 strain was 600 mg/L (Fig. 1). A similar value was obtained for 5 of the oral strains tested (FFULORAL16, FFULORAL21, FFULORAL26, FFULORAL29 and FFULORAL34), while slightly higher values were obtained for the majority of the other oral strains: 700 mg/L for 14 strains, 800 mg/L for 19 strains and 900 mg/L for 12 strains (Fig. 1). We have also profiled the clinical strains in terms of their resistance to fluconazole being possible to identify in our cohort two *C. albicans* strains that could be considered resistant to fluconazole (MIC above 64 mg/L, compared with the resistance breakpoint of 4 mg/L), FFULORAL1 and FFULORAL2 (Supplementary Figure S1). The MIC_{50} of the '*green*' AgNPs for these two strains was 800 mg/L for FFULORAL1 and 700 mg/L for FFULORAL2, thus being in the average of those obtained for the overall cohort of strains tested and indicating that the azole-resistance phenotype did not influenced tolerance to the AgNPs.

3.2. Assessment of the effect of '*green*' AgNPs against *C. albicans* in combination with other antifungals

To assess whether the efficacy of the '*green*' AgNPs against *C. albicans* and *C. glabrata* could be improved when used in combination with other antifungals used to treat oral candidiasis, we have assessed the corresponding MIC_{50} value in the presence of FLC, NYT and AmB. Three *C. albicans* strains were used for this: the laboratory strain SC5314 and the fluconazole-resistant isolates (FFULORAL1 and FFULORAL2). The range of concentrations of the AgNPs or of the antifungals used was selected to have no significant inhibition when used alone (comparison of the first row and first column in the heat-map shown in Fig. 2; Supplementary Figure S2). The results obtained are schematically represented in the heat-map shown in Fig. 2 and in Table 1. In general, growth of the three strains of *C. albicans* tested in the presence of the two drugs (AgNPs and fluconazole/nystatin/amphotericin B) was always more inhibitory than the one observed in the presence of the drugs alone (heat-map in Fig. 2 and Supplementary Figure S2) which is somehow expected. To identify relevant synergistic interactions the fractional inhibitory concentration index (FICI) was calculated since this has used before with success to investigate synergistic drug interactions in *Candida*.[36-38] In all cases it was possible to identify a synergistic interaction of the '*green*' AgNPs with the three antifungals tested (Table 1 and Fig. 2). A relevant observation was the fact that this

synergistic interaction was observed not only in the laboratory strain SC5314 but also in the two fluconazole-resistant isolates, FFULORAL1 and FFULORAL2.

3.3. Exposure of *C. albicans* to '*green*' AgNPs reduces filamentation and biofilm formation

Since the ability to form biofilms and to trigger hyphae formation has been pinpointed as two relevant virulence factors underlying oral pathogenesis of *C. albicans*,[16] we have decided to investigate how these traits would be modulated by exposure to '*green*' AgNPs. To assess the impact in filamentation we have cultivated, at 37º C, *C. albicans* SC5314 cells in RPMI medium supplemented with FBS (a well-known inducer of filamentation in this species) and with AgNPs. The concentration of AgNPs used in this assay was the one identified as the MIC_{50} in the phenotypic screenings described above. In control conditions, during growth in RPMI (at pH 7) at 37º C around 80% of the observed *C. albicans* cells exhibited hyphae, this number increasing up to about 95% when FBS was further added to the medium (Fig. 4). The incubation in the presence of the '*green*' AgNPs drastically reduced the number of cells exhibiting hyphae, this effect being observed either in the presence or absence of FBS (Fig. 4). We have also examined the impact of the presence of AgNPs in biofilm formation on the surface of polystyrene undertaken by *C. albicans* along cultivation in RPMI medium. The amount of biofilm formed by *C. albicans* in the presence of 600 mg/L of '*green*' AgNPs was reduced by more than 50% the one formed in the absence of the nanoparticles, this reduction being further increased to more than 90% when the concentration of the AgNPs was increased to 900 mg/L (Fig. 4, panel A). Microscopic observation of the biofilms by SEM confirmed the reduced biofilm in the culture cultivated in the presence of the '*green*' AgNPs, also evidencing a much low number of hyphae embedded in the biofilm matrix (Fig. 4).

3.4. '*Green*' AgNPs inhibits growth and biofilm formation in *C. glabrata*

In this work we have also decided to test the effect of the '*green*' AgNPs obtained from *Punica granatum* against the emerging oral pathogen *C. glabrata*.[9] For this we have used the laboratory strain CBS138 and also a small cohort of oral clinical strains (Fig. 1). The determination of the AgNPs MIC_{50} against these strains was tested using the same methodology employed for *C. albicans*. Notably, the MIC_{50} value obtained for the laboratory strain *C. glabrata* CBS138 was of only 2.44 mg/L, which is more than 100-

fold lower the values obtained for *C. albicans* (Fig. 1). This much higher sensitivity of *C. glabrata* to the '*green*' AgNPs, compared with *C. albicans*, was also observed for the set of oral strains tested (Fig. 1), although in this case the MIC_{50} values were slightly higher reaching a maximum of 64 mg/L for the more resilient strain (FFULORAL52). Among the cohort of *C. glabrata* strains tested none could be considered resistant to fluconazole (MIC_{50} above 64 mg/L) (Supplementary Figure S1), however, FFULORAL51 presented a MIC_{50} value of 32 mg/L.

Similar to what was observed for *C. albicans*, biofilm formation prompted by *C. glabrata* cells on the surface of polystyrene along cultivation in RPMI medium was found to be reduced in the presence of the '*green*' AgNPs this being observed both by the PrestoBlue quantification that was observed and also by microscopic imaging of the biofilms (Fig. 5, panel A). This inhibitory effect of AgNPs against *C. glabrata* biofilm cells was observed even in mature biofilms (formed by 12 h and 24 h in the absence of the nanoparticles), being clearly visible a reduction in the viability of the biofilm-embedded cells as indicated by the reduced absorbance of the PrestoBlue reagent (Fig. 5, panel B).

4. Discussion

In the present study, '*green*' AgNPs presented antimicrobial activity against *C. albicans* and *C. glabrata* oral clinical isolates. Interestingly, *C. glabrata* strains were more susceptible to nanoparticles when compared to *C. albicans*. Rahisuddin et al. (2015)[41] also investigated the effect of the AgNPs produced by a '*green*' method against *Candida* species. For *C. glabrata*, MIC values were between 8 and 15 mg/L; whereas for *C. albicans*, these values were 40-60 mg/L. The absent of hyphal elements may have favored the action of AgNPs, since these cellular structures are more exuberant and hard to eradicate.[42] Also, *C. albicans* is able to form well-structured biofilms which contain yeast, pseudohyphae, hyphae and exopolysaccharides that prevent the entry of AgNPs.[43] On the other hand, Soares *et al*. (2018)[21] synthesized AgNPs using a *C. ferrea* seed extract as a reducing agent. For *C. albicans* and *C. glabrata*, MIC values were 312.5 mg/L and 1,250 mg/L, respectively.

In the recent years, resistance of *Candida* species to antifungal therapy has increased.[44, 45] In our study, two oral clinical isolates of *C. albicans* were classified as resistant to the FLC (CA1 and CA2). Our results showed that AgNPs were effective against both strains as well as to isolates considered sensitives to this antifungal agent.

However, a high concentration of AgNPs was necessary (600 mg/L). There are few studies in the literature that evaluated the effect of AgNPs against resistant clinical isolates to azoles. In a study conducted by Longhi *et al*. (2016)[46], AgNPs produced by an eco-friendly method exhibited an antifungal effect with MIC values ranging from 1.74 to 4.35 mg/L; in addition, these concentrations were not cytotoxic to mammalian cells. It is known that physical and chemical properties of AgNPs – including size, size distribution, particle morphology and type of reducing agents used for synthesis – are much important for determination of cytotoxicity.[47] Studies suggest that smaller size particles could cause more toxicity to microorganisms than larger.[48] AgNPs synthesized in this study presented spherical shape and regular distribution with size of approximately 50 nm.[18]

Some studies have demonstrated that antifungal agents – FLC, NYT, AmB or chlorhexidine digluconate – showed synergistic or enhanced activity in combination with AgNPs against *C. albicans*.[49-52] The combination of antimicrobial agents can increase the drug efficacy and reduce the adverse effects these drugs. One of the goals of this study was evaluated the effect of AgNPs in combination with different antifungals (FLC, NYT and AmB) against FFULORAL1, FFULORAL2 (FLC-resistant strains) and SC5314 (reference strain). In relation to FLC-AgNPs, some combinations were more effective than drugs alone to all tested microorganisms. FLC is an azole antifungal used against *C. albicans* infections. In Dentistry, it is the drug of choice since it is effective, better tolerated compared to topic and intravenous therapies and more convenient.[53] Longhi *et al*. (2016)[46] also observed a reduction in the FLC-MIC values of resistant clinical isolates when combined to AgNPs. It's known that AgNPs can alter the permeability of the cell membrane[54, 55], suggesting that they may facilitate the entry of FLC, which interferes with ergosterol biosynthesis. In addition, FLC can also target the fungal cell membrane, which further promotes the adhesion of AgNPs to fungal membrane and, consequently, enhance the action of AgNPs on *C. albicans* cell membrane.[50] Our results showed that combination of AgNPs with NYT and AmB also was effective against *C. albicans*. NYT and AmB are polyene macrolides that bind to membrane of fungal cells causing alteration of cell permeability and the formation of small diameter channels that lead to cell death.[56] NYT is frequently used as a topical agent in the treatment of oral candidiasis[57] and AmB is used to treat systemic fungal infections. In addition to changing the permeability of cell membrane, AgNPs interact with cell wall, release toxic ions, penetrate inside the cells, cause DNA damage, etc.[58] Thereby, the effect of the NYT and

AmB on cell membrane can have facilitated the entry of AgNPs into the cytoplasm, where these particles bind to their targets. In the studies conducted by Silva et al. (2013)[59] and Monteiro et al. (2013)[52], NYT-AgNPs exhibited inhibitory effects on biofilms of *C. albicans* and *C. glabrata*.

Some virulence factors, such as morphological transition and biofilm formation, have been associated to difficulties on treatment of the infections caused by *Candida* species.[60, 61] The formation of hyphae helps *C. albicans* to penetrate the host tissues leading to the establishment of infection (Sun et al. 2015);[62] moreover, their presence favors biofilm formation. In the present study, the ability of AgNPs to inhibit the formation of filamentous forms was evaluated, and the results revealed that AgNPs were able to reduce approximately 57% the formation of hyphae in the presence of FBS. This result reveals that nanoparticles can have an important role in the biofilm formation. To verify this, we also evaluated the effect of different concentrations of AgNPs to inhibit biofilm formation of *C. albicans* through PrestoBlue assay. There was a reduction in the biofilm formation in all tested concentrations, being dose-dependent (Fig. 4A); in the presence of 600 mg/L AgNPs, there was a decrease of approximately 50%. In our study, the morphology of cells within the biofilms, both in the absence and in the presence of AgNPs treatment, was studied using SEM technique. *C. albicans* cultures were treated with AgNPs at a concentration of 600 mg/L. As a result, we observed scarce biofilms, composed mostly of yeast cells and few filamentous forms. True hyphae were absent from these biofilms, as shown in Figs. 4C and 4D. These results suggested that AgNPs are able to inhibit filamentation and subsequent biofilm formation. In the Figs. 4C and 4D, it is possible to observe the nanoparticles on the cells. This reinforces the idea that AgNPs act by disturbing the membrane and creating pores provoking ion leakage, generating apoptosis and showing ultrastructural changes.[63]

In the last years, the number of infections caused by non-*Candida albicans Candida* (NCAC) species, namely due to *C. glabrata*, has increased significantly.[11, 64, 65] Furthermore, *C. glabrata* resistance to antifungal drugs has been reported.[66, 67] In this study, FLC-resistant *C. glabrata* clinical isolates were not founded. However, we investigated the effect of AgNPs on *C. glabrata* (reference strain) biofilms since there is not studies about it in the literature. Our results revealed that AgNPs are able to inhibit the *C. glabrata* biofilm formation even in low concentrations (2.44 to 9.76 mg/L), as showed in the Figs. 5A and 5C. *C. glabrata* cells size (1-4 µm) and the absence of hyphae and pseudohyphae[64] can explain this result. In relation to *C. albicans*, high

concentrations of AgNPs were required to reduce formation of the biofilm. In Fig. 5D, nanoparticles anchored to cells as well as alterations in the cellular membrane can be observed, indicating that AgNPs have any effect on cells, but more detailed analyzes are needed to confirm this affirmation. In 24 h-old *C. glabrata* biofilms, there was a significant reduction in the cell viability after treatment with 2.44 mg/L of AgNPs. *C. glabrata* presents the lowest metabolic activity in comparison with other *Candida* species, despite having the highest number of biofilm cultivable cells. Moreover, *C. glabrata* biofilms are constituted by multilayer with blastoconidia packed with total absence of pseudohyphae and hyphae.[64] These characteristics may facilitate the action of the nanoparticles.

In conclusion, this study showed that AgNPs are potent antifungal agents with effect on *C. albicans* and *C. glabrata* oral clinical isolates, including FLC-resistant strains. However, cytotoxicity studies on mammalian cells must be performed. Nanoparticles were also effective against *C. glabrata* mature biofilms. Thus, new studies with resistant *C. glabrata* clinical isolates must be done. Finally, AgNPs associated to different antifungal agents used in clinical practice (FLC, NYT and AmB) were effective against FLC-resistant *C. albicans* isolates at low concentrations.

5. Acknowledgments

This study was supported by the São Paulo Research Foundation (FAPESP, process 2016/22039-4).

6. Declaration of interest

The authors report no conflicts of interest.

7. References

1. Seed PC. The human mycobiome. *Cold Spring Harb Perspect Med* 2014; 5(5): a019810.

2. Hani U, Shivakumar HG, Vaghela R, Osmani RA, Shrivastava A. Candidiasis: a fungal infection--current challenges and progress in prevention and treatment. *Infect Disord Drug Targets* 2015; 15(1): 42-52.

3. Rautemaa R, Ramage G. Oral candidosis--clinical challenges of a biofilm disease. *Crit Rev Microbiol* 2011; 37(4): 328-36.

4. Korting HC, Ollert M, Georgii A, Froschl M. In vitro susceptibilities and biotypes of Candida albicans isolates from the oral cavities of patients infected with human immunodeficiency virus. *J Clin Microbiol* 1988; 26(12): 2626-31.

5. Palmer GD, Robinson PG, Challacombe SJ, *et al.* Aetiological factors for oral manifestations of HIV. *Oral Dis* 1996; 2(3): 193-7.

6. Phelan JA, Saltzman BR, Friedland GH, Klein RS. Oral findings in patients with acquired immunodeficiency syndrome. *Oral Surg Oral Med Oral Pathol* 1987; 64(1): 50-6.

7. Dongari-Bagtzoglou A, Dwivedi P, Ioannidou E, *et al.* Oral Candida infection and colonization in solid organ transplant recipients. *Oral Microbiol Immunol* 2009; 24(3): 249-54.

8. Miranda-Cadena K, Marcos-Arias C, Mateo E, *et al.* Prevalence and antifungal susceptibility profiles of Candida glabrata, Candida parapsilosis and their close-related species in oral candidiasis. *Arch Oral Biol* 2018; 95: 100-107.

9. Li L, Redding S, Dongari-Bagtzoglou A. Candida glabrata: an emerging oral opportunistic pathogen. *J Dent Res* 2007; 86(3): 204-15.

10. Mushi MF, Bader O, Taverne-Ghadwal L, *et al.* Oral candidiasis among African human immunodeficiency virus-infected individuals: 10 years of systematic review and meta-analysis from sub-Saharan Africa. *J Oral Microbiol* 2017; 9(1): 1317579.

11. Sadeghi G, Ebrahimi-Rad M, Mousavi SF, Shams-Ghahfarokhi M, Razzaghi-Abyaneh M. Emergence of non-Candida albicans species: Epidemiology, phylogeny and fluconazole susceptibility profile. *J Mycol Med* 2018; 28(1): 51-58.

12. Achkar JM, Fries BC. Candida infections of the genitourinary tract. *Clin Microbiol Rev* 2010; 23(2): 253-73.

13. Ramage G, Martinez JP, Lopez-Ribot JL. Candida biofilms on implanted biomaterials: a clinically significant problem. *FEMS Yeast Res* 2006; 6(7): 979-86.

14. Silva S, Negri M, Henriques M, *et al.* Adherence and biofilm formation of non-Candida albicans Candida species. *Trends Microbiol* 2011; 19(5): 241-7.

15. Silva S, Rodrigues CF, Araujo D, Rodrigues ME, Henriques M. Candida Species Biofilms' Antifungal Resistance. *J Fungi (Basel)* 2017; 3(1).

16. Moyes DL, Richardson JP, Naglik JR. Candida albicans-epithelial interactions and pathogenicity mechanisms: scratching the surface. *Virulence* 2015; 6(4): 338-46.

17. Fernandes GL, Delbem ACB, do Amaral JG, *et al.* Nanosynthesis of Silver-Calcium Glycerophosphate: Promising Association against Oral Pathogens. *Antibiotics (Basel)* 2018; 7(3).

18. Souza JA, Barbosa DB, Berretta AA, *et al.* Green synthesis of silver nanoparticles combined to calcium glycerophosphate: antimicrobial and antibiofilm activities. *Future Microbiol* 2018; 13: 345-357.

19. Perez-Diaz MA, Boegli L, James G, *et al.* Silver nanoparticles with antimicrobial activities against Streptococcus mutans and their cytotoxic effect. *Mater Sci Eng C Mater Biol Appl* 2015; 55: 360-6.

20. Fernandes RA, Berretta AA, Torres EC, *et al.* Antimicrobial Potential and Cytotoxicity of Silver Nanoparticles Phytosynthesized by Pomegranate Peel Extract. *Antibiotics (Basel)* 2018; 7(3).

21. Soares M, Correa RO, Stroppa PHF, *et al.* Biosynthesis of silver nanoparticles using Caesalpinia ferrea (Tul.) Martius extract: physicochemical characterization, antifungal activity and cytotoxicity. *PeerJ* 2018; 6: e4361.

22. Monteiro DR, Takamiya AS, Feresin LP, *et al.* Susceptibility of Candida albicans and Candida glabrata biofilms to silver nanoparticles in intermediate and mature development phases. *J Prosthodont Res* 2015; 59(1): 42-8.

23. Szweda P, Gucwa K, Kurzyk E, *et al.* Essential Oils, Silver Nanoparticles and Propolis as Alternative Agents Against Fluconazole Resistant Candida albicans, Candida glabrata and Candida krusei Clinical Isolates. *Indian J Microbiol* 2015; 55(2): 175-83.

24. Monteiro DR, Silva S, Negri M, *et al.* Silver nanoparticles: influence of stabilizing agent and diameter on antifungal activity against Candida albicans and Candida glabrata biofilms. *Lett Appl Microbiol* 2012; 54(5): 383-91.

25. Wady AF, Machado AL, Zucolotto V, *et al.* Evaluation of Candida albicans adhesion and biofilm formation on a denture base acrylic resin containing silver nanoparticles. *J Appl Microbiol* 2012; 112(6): 1163-72.

26. Hazer DB, Mut M, Dincer N, *et al.* The efficacy of silver-embedded polypropylene-grafted polyethylene glycol-coated ventricular catheters on prevention of shunt catheter infection in rats. *Childs Nerv Syst* 2012; 28(6): 839-46.

27. Monteiro DR, Gorup LF, Takamiya AS, *et al.* The growing importance of materials that prevent microbial adhesion: antimicrobial effect of medical devices containing silver. *Int J Antimicrob Agents* 2009; 34(2): 103-10.

28. Kumari A, Guliani A, Singla R, Yadav R, Yadav SK. Silver nanoparticles synthesised using plant extracts show strong antibacterial activity. *IET Nanobiotechnol* 2015; 9(3): 142-52.

29. Nasiriboroumand M, Montazer M, Barani H. Preparation and characterization of biocompatible silver nanoparticles using pomegranate peel extract. *J Photochem Photobiol B* 2018; 179: 98-104.

30. Goudarzi M, Mir N, Mousavi-Kamazani M, Bagheri S, Salavati-Niasari M. Biosynthesis and characterization of silver nanoparticles prepared from two novel natural precursors by facile thermal decomposition methods. *Sci Rep* 2016; 6: 32539.

31. Meena Kumari M, Jacob J, Philip D. Green synthesis and applications of Au-Ag bimetallic nanoparticles. *Spectrochim Acta A Mol Biomol Spectrosc* 2015; 137: 185-92.

32. Gorup LF, Longo E, Leite ER, Camargo ER. Moderating effect of ammonia on particle growth and stability of quasi-monodisperse silver nanoparticles synthesized by the Turkevich method. *J Colloid Interface Sci* 2011; 360(2): 355-8.

33. Subcommittee on Antifungal Susceptibility Testing of the EECfAST. EUCAST definitive document EDef 7.1: method for the determination of broth dilution MICs of antifungal agents for fermentative yeasts. *Clin Microbiol Infect* 2008; 14(4): 398-405.

34. *European Committee on Antimicrobial Susceptibility Testing. Antifungal Agents. Breakpoint tables for interpretation of MICs, version 8.1*.

35. Sun L, Sun S, Cheng A, *et al.* In vitro activities of retigeric acid B alone and in combination with azole antifungal agents against Candida albicans. *Antimicrob Agents Chemother* 2009; 53(4): 1586-91.

36. Nishi I, Sunada A, Toyokawa M, Asari S, Iwatani Y. In vitro antifungal combination effects of micafungin with fluconazole, voriconazole, amphotericin B, and flucytosine against clinical isolates of Candida species. *J Infect Chemother* 2009; 15(1): 1-5.

37. Chaturvedi V, Ramani R, Ghannoum MA, *et al.* Multilaboratory testing of antifungal combinations against a quality control isolate of Candida krusei. *Antimicrob Agents Chemother* 2008; 52(4): 1500-2.

38. Chaturvedi V, Ramani R, Andes D, *et al.* Multilaboratory testing of two-drug combinations of antifungals against Candida albicans, Candida glabrata, and Candida parapsilosis. *Antimicrob Agents Chemother* 2011; 55(4): 1543-8.

39. Montelongo-Jauregui D, Srinivasan A, Ramasubramanian AK, Lopez-Ribot JL. An In Vitro Model for Oral Mixed Biofilms of Candida albicans and Streptococcus gordonii in Synthetic Saliva. *Front Microbiol* 2016; 7: 686.

40. Fernandes RA, Monteiro DR, Arias LS, *et al.* Biofilm formation by Candida albicans and Streptococcus mutans in the presence of farnesol: a quantitative evaluation. *Biofouling* 2016; 32(3): 329-38.

41. Rahisuddin, Al-Thabaiti SA, Khan Z, Manzoor N. Biosynthesis of silver nanoparticles and its antibacterial and antifungal activities towards Gram-positive, Gram-negative bacterial strains and different species of Candida fungus. *Bioprocess Biosyst Eng* 2015; 38(9): 1773-81.

42. Monteiro DR, Arias LS, Fernandes RA, *et al.* Antifungal activity of tyrosol and farnesol used in combination against Candida species in the planktonic state or forming biofilms. *J Appl Microbiol* 2017; 123(2): 392-400.

43. Shafreen RM, Muthamil S, Pandian SK. Inhibition of Candida albicans virulence factors by novel levofloxacin derivatives. *Appl Microbiol Biotechnol* 2014; 98(15): 6775-85.

44. Mahmoudi M, Serpooshan V. Silver-coated engineered magnetic nanoparticles are promising for the success in the fight against antibacterial resistance threat. *ACS Nano* 2012; 6(3): 2656-64.

45. Pfaller MA. Antifungal drug resistance: mechanisms, epidemiology, and consequences for treatment. *Am J Med* 2012; 125(1 Suppl): S3-13.

46. Longhi C, Santos JP, Morey AT, *et al.* Combination of fluconazole with silver nanoparticles produced by Fusarium oxysporum improves antifungal effect against planktonic cells and biofilm of drug-resistant Candida albicans. *Med Mycol* 2016; 54(4): 428-32.

47. Zhang XF, Liu ZG, Shen W, Gurunathan S. Silver Nanoparticles: Synthesis, Characterization, Properties, Applications, and Therapeutic Approaches. *Int J Mol Sci* 2016; 17(9).

48. Sriram MI, Kalishwaralal, K., Barathmanikanth, S., Gurunathani, S. Size-based cytotoxicity of silver nanoparticles in bovine retinal endothelial cells. *J Neurosci Methods* 2012; 1: 56-77.

49. Ahmad A, Wei Y, Syed F, *et al.* Amphotericin B-conjugated biogenic silver nanoparticles as an innovative strategy for fungal infections. *Microb Pathog* 2016; 99: 271-281.

50. Sun L, Liao K, Li Y, *et al.* Synergy Between Polyvinylpyrrolidone-Coated Silver Nanoparticles and Azole Antifungal Against Drug-Resistant Candida albicans. *J Nanosci Nanotechnol* 2016; 16(3): 2325-35.

51. Dar MA, Ingle A, Rai M. Enhanced antimicrobial activity of silver nanoparticles synthesized by Cryphonectria sp. evaluated singly and in combination with antibiotics. *Nanomedicine* 2013; 9(1): 105-10.

52. Monteiro DR, Silva S, Negri M, *et al.* Antifungal activity of silver nanoparticles in combination with nystatin and chlorhexidine digluconate against Candida albicans and Candida glabrata biofilms. *Mycoses* 2013; 56(6): 672-80.

53. Pfaller MA, Diekema DJ, Procop GW, Rinaldi MG. Comparison of the Vitek 2 yeast susceptibility system with CLSI microdilution for antifungal susceptibility testing of fluconazole and voriconazole against Candida spp., using new clinical breakpoints and epidemiological cutoff values. *Diagn Microbiol Infect Dis* 2013; 77(1): 37-40.

54. Hwang IS, Lee J, Hwang JH, Kim KJ, Lee DG. Silver nanoparticles induce apoptotic cell death in Candida albicans through the increase of hydroxyl radicals. *FEBS J* 2012; 279(7): 1327-38.

55. Kim KJ, Sung WS, Suh BK, *et al.* Antifungal activity and mode of action of silver nano-particles on Candida albicans. *Biometals* 2009; 22(2): 235-42.

56. Dos Santos AG, Marques JT, Carreira AC, *et al.* The molecular mechanism of Nystatin action is dependent on the membrane biophysical properties and lipid composition. *Phys Chem Chem Phys* 2017; 19(44): 30078-30088.

57. Williams D, Lewis M. Pathogenesis and treatment of oral candidosis. *J Oral Microbiol* 2011; 3.

58. Dakal TC, Kumar A, Majumdar RS, Yadav V. Mechanistic Basis of Antimicrobial Actions of Silver Nanoparticles. *Front Microbiol* 2016; 7: 1831.

59. Silva S, Pires P, Monteiro DR, *et al.* The effect of silver nanoparticles and nystatin on mixed biofilms of Candida glabrata and Candida albicans on acrylic. *Med Mycol* 2013; 51(2): 178-84.

60. Martins N, Ferreira IC, Barros L, Silva S, Henriques M. Candidiasis: predisposing factors, prevention, diagnosis and alternative treatment. *Mycopathologia* 2014; 177(5-6): 223-40.

61. Pierce CG, Srinivasan A, Uppuluri P, Ramasubramanian AK, Lopez-Ribot JL. Antifungal therapy with an emphasis on biofilms. *Curr Opin Pharmacol* 2013; 13(5): 726-30.

62. Sun L, Liao K, Wang D. Effects of magnolol and honokiol on adhesion, yeast-hyphal transition, and formation of biofilm by Candida albicans. *PLoS One* 2015; 10(2): e0117695.

63. Lara HH, Romero-Urbina DG, Pierce C, *et al.* Effect of silver nanoparticles on Candida albicans biofilms: an ultrastructural study. *J Nanobiotechnology* 2015; 13: 91.

64. Rodrigues CF, Silva S, Henriques M. Candida glabrata: a review of its features and resistance. *Eur J Clin Microbiol Infect Dis* 2014; 33(5): 673-88.

65. Silva S, Negri M, Henriques M, *et al.* Candida glabrata, Candida parapsilosis and Candida tropicalis: biology, epidemiology, pathogenicity and antifungal resistance. *FEMS Microbiol Rev* 2012; 36(2): 288-305.

66. Wiederhold NP. Antifungal resistance: current trends and future strategies to combat. *Infect Drug Resist* 2017; 10: 249-259.

67. Amirrajab N, Badali H, Didehdar M, *et al.* In Vitro Activities of Six Antifungal Drugs Against Candida glabrata Isolates: An Emerging Pathogen. *Jundishapur J Microbiol* 2016; 9(5): e36638.

Tables

Table 1. Effect of fluconazole (FLC), nystatin (NYT) and amphotericin B (AmB) alone or in combination with '*green*' silver nanoparticles (AgNPs) against FLC-resistant *Candida albicans* oral clinical isolates and reference strain SC5314.

Drug in combination and stain	MIC_{50}[a] (in mg/L)				FICI[b]	INT[c]
	Alone		In combination			
	Antifungal	AgNPs	Antifungal	AgNPs		
FLC						
SC5314	0.25	600	0.063	32	0.303	SYN
			0.125	16	0.527	IND
			0.125	32	0.553	IND
FFULORAL1	> 64	800	0.063	16	0.021	SYN
			0.063	32	0.041	SYN
			0.125	16	0.022	SYN
			0.125	32	0.042	SYN
FFULORAL2	> 64	700	0.063	16	0.024	SYN
			0.063	32	0.047	SYN
			0.125	16	0.025	SYN
			0.125	32	0.048	SYN
NYT						
SC5314	0.50	600	0.125	16	0.277	SYN
			0.125	32	0.303	SYN
			0.25	16	0.527	IND
			0.25	32	0.553	IND
FFULORAL1	0.50	800	0.125	16	0.27	SYN
			0.125	32	0.29	SYN
			0.25	16	0.52	IND
			0.25	32	0.54	IND
FFULORAL2	0.50	700	0.125	16	0.273	SYN
			0.125	32	0.296	SYN
			0.25	16	0.523	IND
			0.25	32	0.546	IND
AmB						
SC5314	0.063	600	0.016	32	0.303	SYN
			0.031	16	0.527	IND
			0.031	32	0.553	IND
FFULORAL1	0.50	800	0.031	16	0.083	SYN
			0.031	32	0.103	SYN
			0.063	16	0.145	SYN
			0.063	32	0.165	SYN
FFULORAL2	1.00	700	0.063	32	0.108	SYN
			0.125	16	0.148	SYN
			0.125	32	0.171	SYN

Note: [a]MIC_{50}, minimum inhibitory concentration. [b]FICI, faction inhibited concentration index. [c]SYN, synergism; ANT, antagonism; IND, indifference. Synergism was defined as a FICI of ≤0.5, antagonism was defined as a FICI of >4.0, and indifference was defined as a FICI of >0.5 to 4 (i.e., no interaction).

Figures

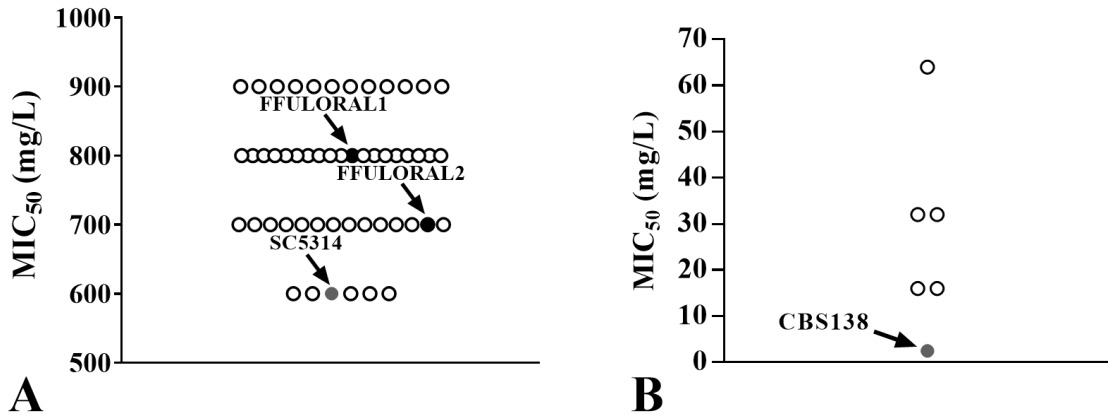

Figure 1. MIC_{50} values for the '*green*' AgNPs against the reference (gray) and the oral isolates of *C. albicans* (A) and *C. glabrata* (B). FLC-resistant isolates are in black, while FLC-sensitives isolates are in white. AgNP – silver nanoparticles and FLC – fluconazole.

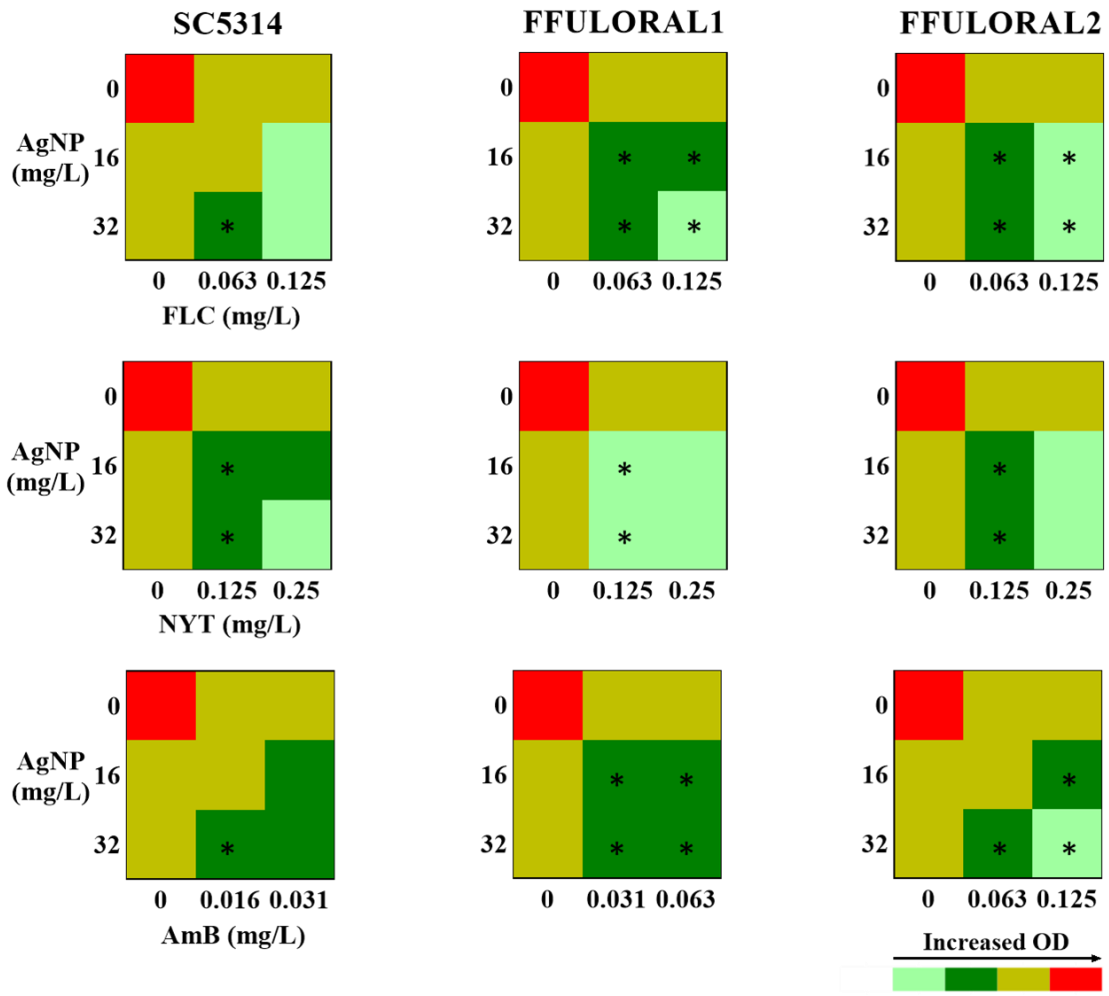

Figure 2. Heat map representing the effect of 'green' AgNPs alone or in combination with FLC, NYT and AmB against *C. albicans* SC5314 or against the two identified FLC-resistant *C. albicans* isolates. *Combinations considered synergistic according to the fractional inhibitory concentration index (FICI).

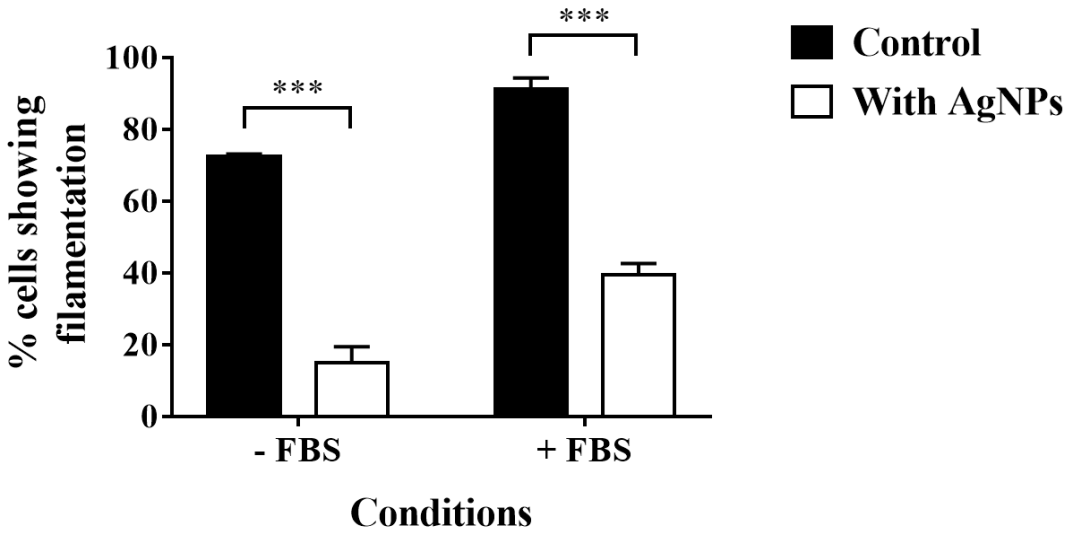

Figure 3. Effect of AgNPs in filamention of *C. albicans* SC5314. *C. albicans* cells were cultivated in RPMI growth medium supplemented or not with 10% FBS in the presence or absence of the '*green*' AgNPs (at 600 mg/L) at 37º C during 24 h, after which the percentage of cells undergoing filamentation was quantified as detailed in Materials and Methods. FBS – Fetal Bovine Serum; two-way ANOVA followed by the Sidak's multiple comparisons test, $p < 0.05$.

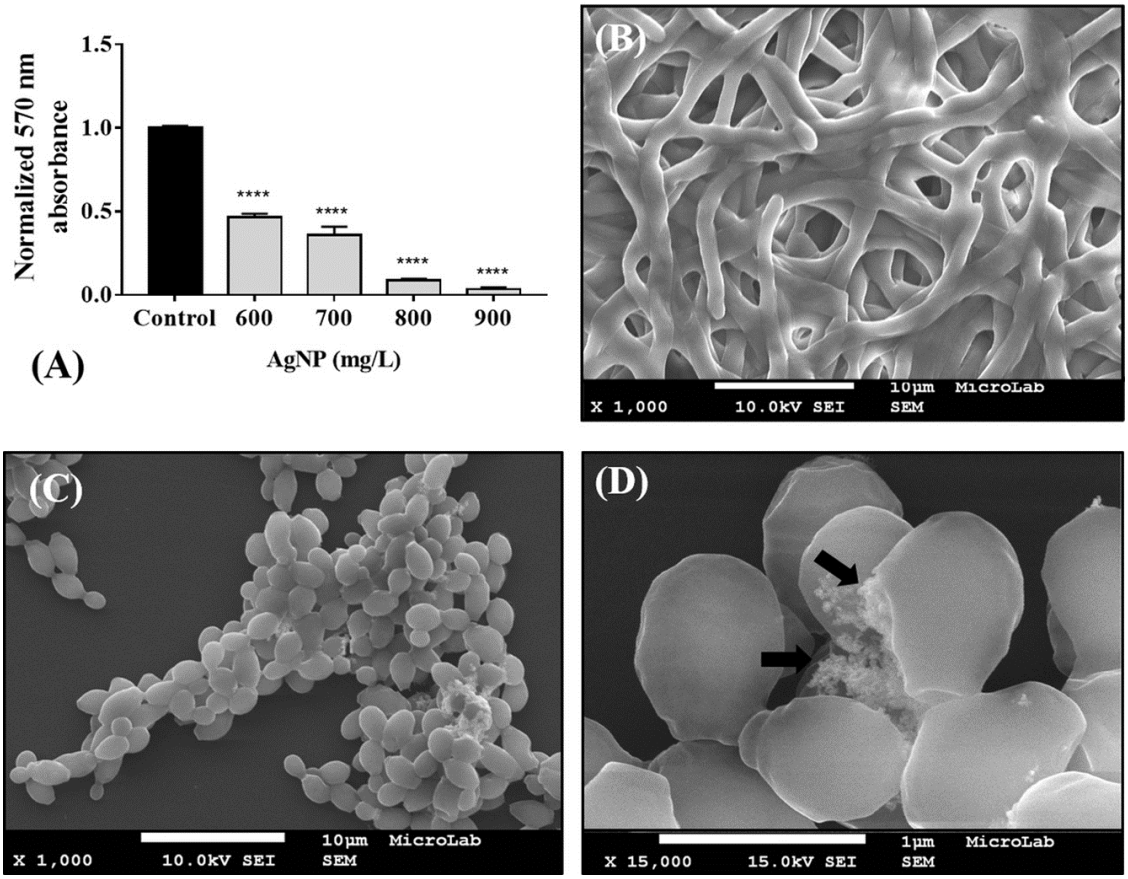

Figure 4. Effect of '*green'* AgNPs in biofilm formation prompted by *C. albicans* SC5314. (A) The biofilm formed by *C. albicans* SC5314 cells on the surface of polystyrene after 24 h of cultivation in RPMI medium supplemented or not with increasing concentrations of AgNPs was compared using the PrestoBlue assay, as described in Materials and Methods. In panels B, C and D are shown pictures obtained by SEM of the biofilm formed under the conditions described above in the absence (B) or presence of 600 mg/L of '*green'* AgNPs; ****-*p*-value below 0.05.

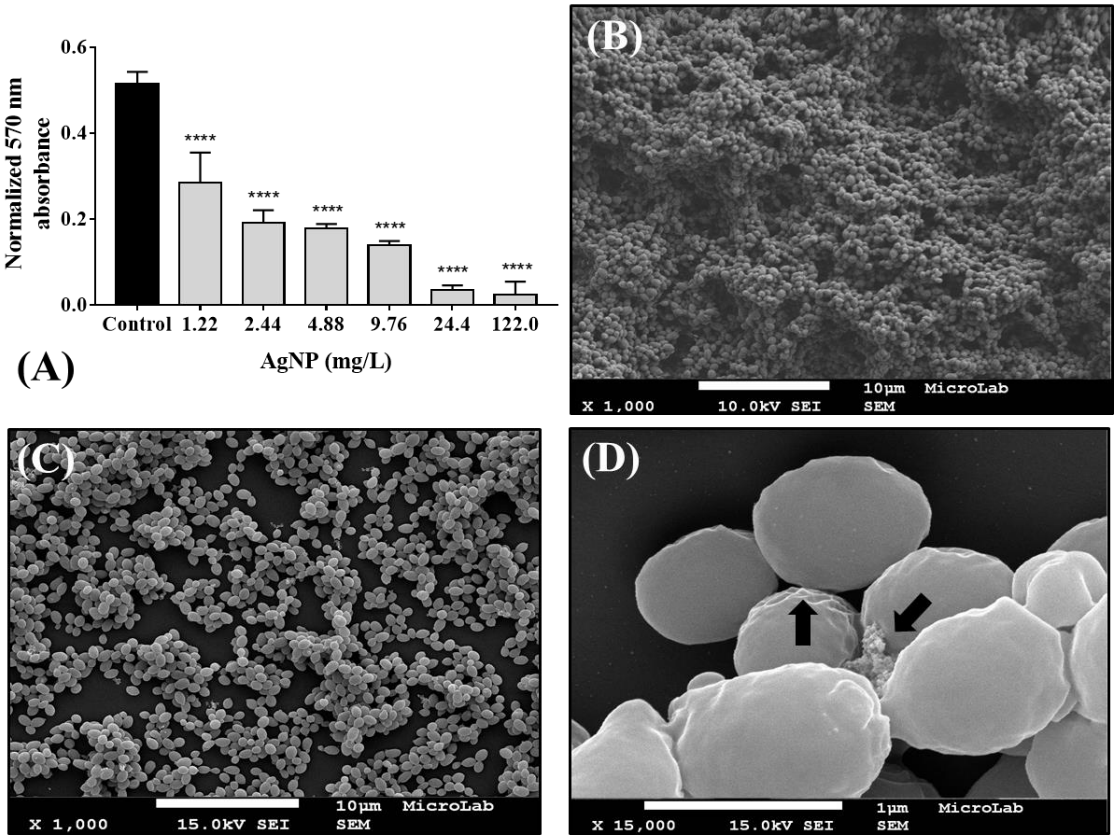

Figure 5. Effect of '*green'* AgNPs in biofilm formation prompted by *C. glabrata* CBS138. (A) The biofilm formed by *C. glabrata* CBS138 cells on the surface of polystyrene after 24 h of cultivation in RPMI medium supplemented or not with increasing concentrations of AgNPs was compared using the PrestoBlue assay, as described in Materials and Methods. In panels B, C and D are shown pictures obtained by SEM of the biofilm formed under the conditions described above in the absence (B) or presence of 2.44 mg/L of '*green'* AgNPs; ****-*p*-value below 0.05.

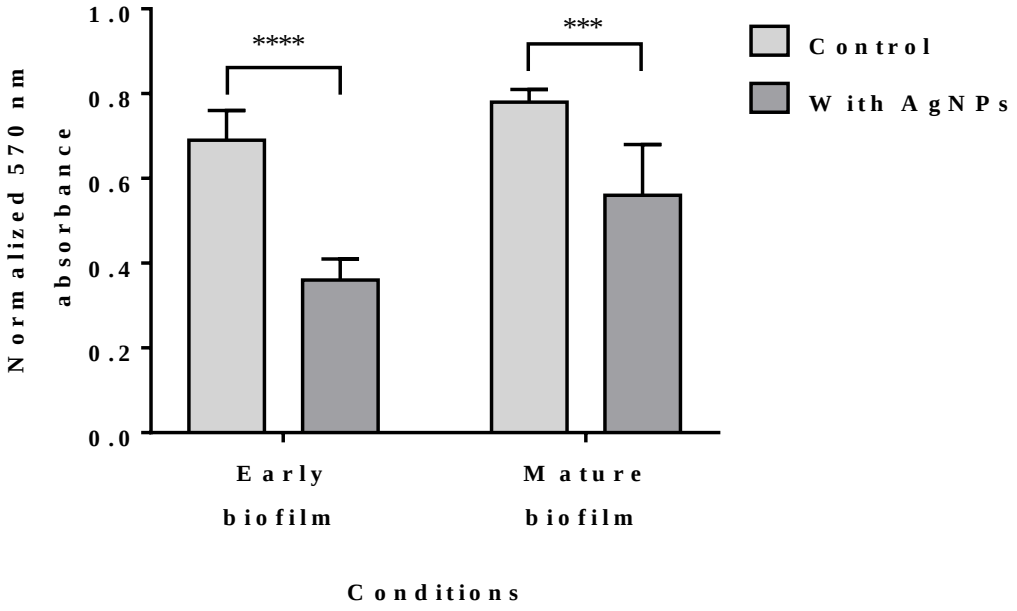

Figure 6. Relative absorbance obtained with the PrestoBlue assay for biofilms *C. glabrata* CBS138 formed by 12 h (Early biofilm) and 24 h (Mature biofilm) and treated with '*green*' AgNPs at 2.44 mg/L for 24 h. Error bars display standard deviation of the means. *Indicates significant differences ($p < 0.05$ – two-way ANOVA followed by the Sidak post hoc test) between Control and AgNPs groups in the different conditions. AgNPs – silver nanoparticles.

Supplementary Material

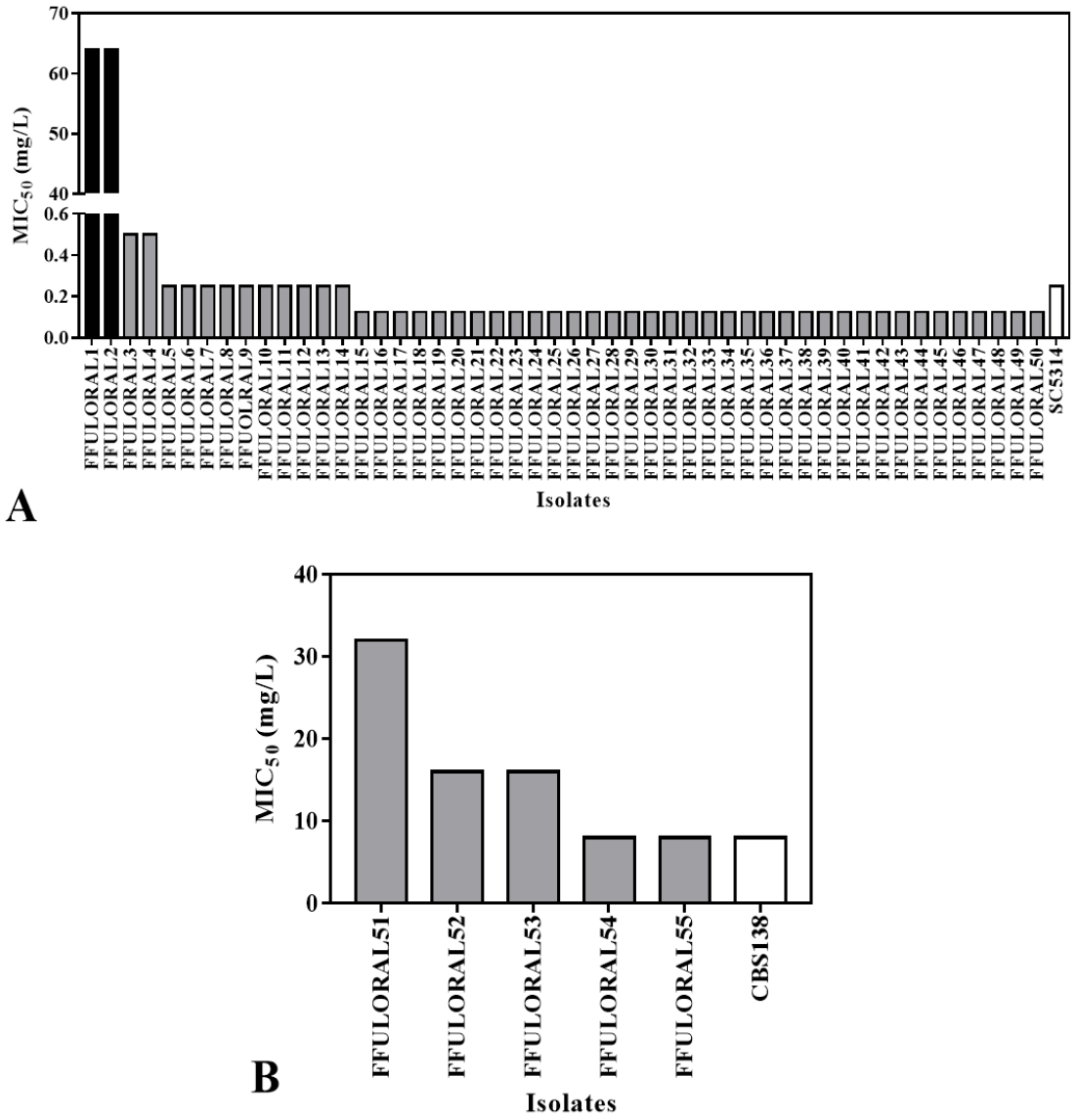

Figure S1. MIC_{50} values for the FLC against the reference (white) and the oral isolates of *C. albicans* (A) and *C. glabrata* (B). FLC-resistant isolates are in black, while FLC-sensitives isolates are in gray. FLC – fluconazole.

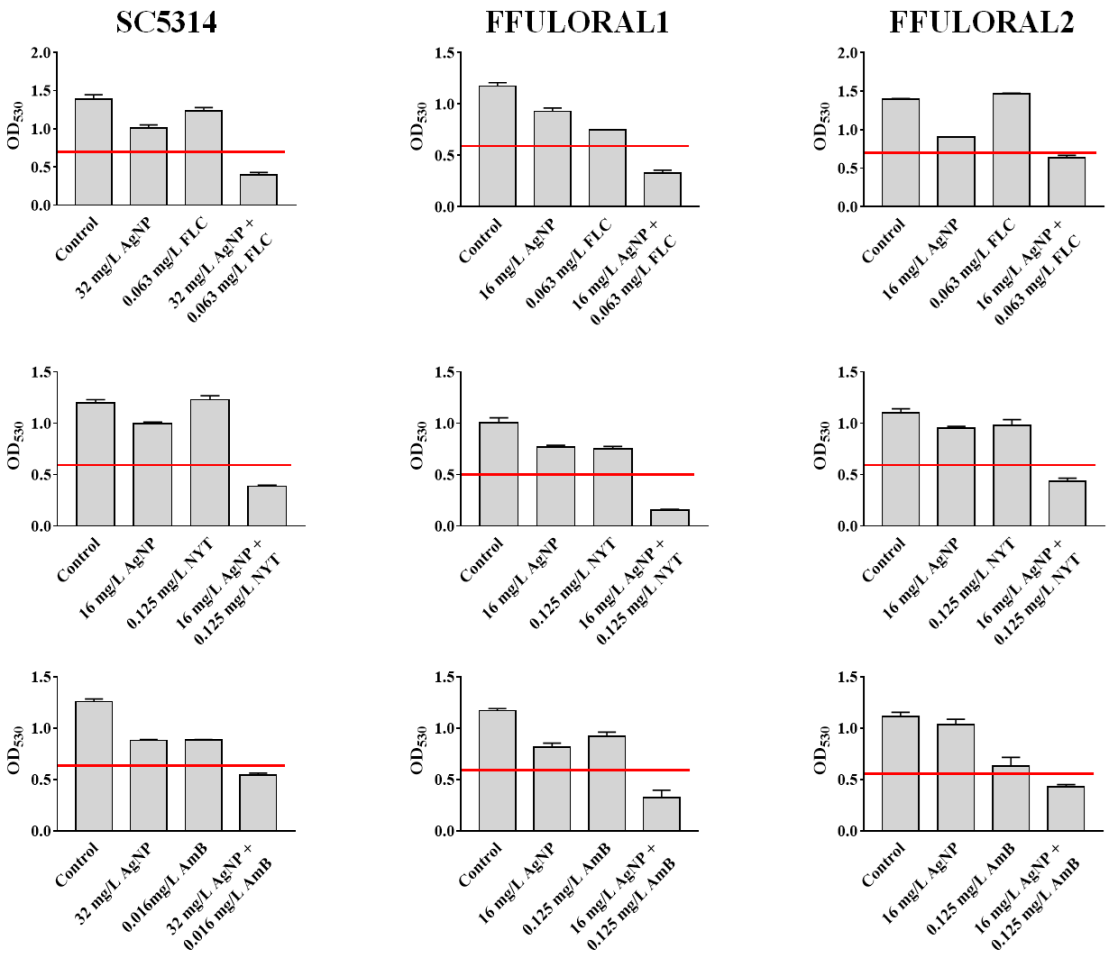

Figure S2. The effect of '*green*' AgNPs alone or in combination with FLC, NYT and AmB against *C. albicans* SC5314 or against the two identified FLC-resistant *C. albicans* isolates (FFULORAL1 and FFULORAL2). Combinations considered synergistic according to the fractional inhibitory concentration index (FICI).

CAPÍTULO 6

Resposta transcritômica de *Candida glabrata* após exposição às nanopartículas de prata sintetizadas por uma via '*green*'

Resposta transcriptômica de *Candida glabrata* após exposição às nanopartículas de prata sintetizadas por uma via '*green*'

Resumo

O objetivo deste estudo foi avaliar, comparativamente, as alterações do transcriptoma de células de *C. glabrata* CBS138 após exposição às nanopartículas de prata (NPsAg) obtidas pela síntese '*green*' (no estado planctônico e formando biofilmes) e ao íon prata (formando biofilmes). Inicialmente, soluções de nitrato de prata ($AgNO_3$ – Íon Ag^+) e de NPsAg (utilizando extrato da casca da romã) foram sintetizadas. A concentração inibitória mínima (CIM_{50}) da solução de Íon Ag^+ e das NPsAg foi determinada utilizando o método de microdiluição. O número de Unidades Formadoras de Colônias foi quantificado após 24 h de formação do biofilme de *C. glabrata* na presença do Íon Ag^+ ou das NPsAg. A resposta transcriptômica das células de *C. glabrata* frente às NPsAg foi determinada em duas situações: nos estados planctônico (após 2 h de exposição) e formando biofilmes (após 24 h). A resposta transcriptômica das células expostas às NPsAg formando biofilmes foi comparada com a do íon Ag^+. Os valores de CIM_{50} para Íon Ag^+ e NPsAg foram 1,22 e 2,44 mg/L, respectivamente. Houve uma redução de aproximadamente 93% na formação do biofilme quando os biofilmes de *C. glabrata* foram formados na presença do Íon Ag^+ e das NPsAg. No estado planctônico, os genes relacionados com a biossíntese de metionina e de lisina estão mais expressos, enquanto que os genes relacionados com o transporte transmembrana estão menos expressos; e, as células expostas às NPsAg responderam de forma distinta em relação ao Íon Ag^+, na formação do biofilme de *C. glabrata*. Diante desses resultados, pode-se concluir que, as NPsAg exercem o seu efeito na membrana citoplasmática da célula fúngica. Além disso, nós observamos efeitos distintos entre o Íon Ag^+ e as NPsAg na formação do biofilme.

Palavras-chaves: Prata. Nanotecnologia. Toxicidade. Análise em Microsséries.

1. Introdução

Nos últimos anos, a Nanotecnologia tem sido utilizada para controlar a formação de biofilmes através da incorporação de nanopartículas em diversos materiais (Monteiro *et al*. 2011). Neste contexto, as nanopartículas de prata (NPsAg) estão se destacando nas áreas da Medicina, Biologia, Química e Física (Song *et al*. 2009). As NPsAg tem sido incorporadas em diferentes materiais odontológicos, tais como: resinas compostas, cimento de ionômero de vidro, adesivos, cimentos endodônticos e ortodônticos, implantes dentários, resina acrílica, entre outros (Bapat *et al*. 2018). Na forma nanoparticulada, a prata possui uma maior área de superfície por volume (esta característica aumenta a interação das nanopartículas com o microrganismo), o que a torna potencialmente mais reativa (Chairuangkitti *et al*. 2013; Prabhu & Poulose, 2012; Wei *et al*. 2010).

Além disso, NPsAg possuem comprovada atividade antimicrobiana contra um amplo espectro de microrganismos, bactérias gram-positivas, gram-negativas, fungos (como por exemplo, *Candida albicans* e *C. glabrata*) e vírus, incluindo cepas resistentes às drogas que são habitualmente usadas para tratar infecções causadas por estes microrganismos (Rudramurthy *et al*. 2016; Zhang *et al*. 2016). Cerca de 650 espécies causadoras de doenças já se verificaram serem sensíveis à ação das AgNPs (Monteiro *et al*. 2012; Monteiro *et al*. 2011; Braydich-Stolle *et al*. 2010; Kim *et al*. 2009), o que torna estas nanopartículas muito atrativas como potenciais agentes terapêuticos (Ahamed *et al*. 2010). No entanto, as técnicas convencionais utilizadas para a síntese dessas nanopartículas podem afetar o meio ambiente e o sistema biológico (Ali *et al*. 2016), porque envolvem o uso de substâncias químicas tóxicas. Nesse sentido, a síntese '*green*' tem emergido como uma alternativa amplamente aceita para sintetizar NPsAg, por utilizar sistemas biológicos como por exemplo, bactérias, fungos e extratos de plantas (Arumai Selvan *et al*. 2018; Malik *et al*. 2014; Park *et al*. 2011). Alguns estudos mostram o envolvimento de compostos fenólicos presentes em plantas na redução de íons metálicos o que excluiria o uso de substâncias químicas (Kumari *et al*. 2015; Ahmad *et al*. 2012). Assim, extrato da casca de *Punica granatum L.* (romã) tem sido utilizado como agente redutor para os íons prata (Fernandes *et al*. 2018; Souza *et al*. 2018), devido à alta quantidade de compostos fenólicos – ácido elágico, elagitaninas e punicalagina – e por apresentarem também propriedades antioxidantes (Heber 2011).

Apesar deste efeito antimicrobiano amplamente reportado das NPsAg, pouco se sabe sobre o mecanismo molecular pelo qual estas nanopartículas exercem toxicidade contra as diferentes espécies de microrganismos (Bapat *et al*. 2018). O mecanismo de

ação mais comum das NPsAg está relacionado com a liberação de íons prata (Ag^+), que podem causar danos na membrana citoplasmática (sabe-se que nanopartículas formam pequenos poros na parede celular de microrganismos gram-negativos causando um aumento na permeabilidade celular) e consequentemente levar à perda de viabilidade celular (Yang *et al*. 2012). A liberação de íons Ag^+ é maior quando NPsAg menores que 10 nm são utilizadas comparadas com nanopartículas maiores (Roco, 2004). Outros efeitos reportados incluem a interrupção na produção de ATP pela célula e a inibição da replicação do DNA (Rizzello & Pompa, 2014). No entanto, permanecem por esclarecer de forma mais definitiva quais as respostas celulares quando expostas a NPsAg obtidas por uma via '*green*' e se essas respostas são idênticas às produzidas após exposição ao íon Ag^+.

Diante do exposto acima, o objetivo deste estudo foi avaliar comparativamente as alterações do transcriptoma de células de *C. glabrata* CBS138 após exposição às nanopartículas de prata (NPsAg) obtidas pela síntese '*green*' (no estado planctônico e formando biofilmes) e ao íon prata (formando biofilmes), a fim de compreender melhor o mecanismo de ação das NPsAg e verificar se o efeito das NPsAg sobre as células de *Candida* é diferente do íon Ag^+.

2. Materiais e métodos

2.1. Síntese das soluções experimentais

As soluções experimentais utilizadas neste estudo foram: Soluções de nitrato de prata ($AgNO_3$ – Íon Ag^+) e de nanopartículas de prata (NPsAg) sintetizadas por um método '*green*' utilizando extrato da casca da romã. As concentrações finais de cada composto foram: para a solução de Íon Ag^+ - 1000 mg/L e para a solução de NPsAg – 2500 mg/L.

2.1.1. Preparo das nanopartículas de prata

A síntese '*green*' das NPsAg foi realizada de acordo com Souza *et al*. (2018) e Gorup *et al*. (2011). Inicialmente, 0,42 g de nitrato de prata ($AgNO_3$, Merck KGaA, Alemanha) foram dissolvidos em 100 mL de água deionizada aquecida a 90º C. Depois, 5 mL de sal de amônio de ácido polimetacrílico foi adicionado seguido de 0,7 g de extrato aquoso da casca da *P. granatum*. A reação foi mantida sob agitação constante a 95º C por 10 minutos. Durante o estudo, a solução antimicrobiana foi estocada em frascos âmbar a 4º C. Os resultados prévios da microscopia eletrônica de varredura mostraram formato

esférico e distribuição regular com tamanho de aproximadamente 50 nm, que foram utilizados neste estudo.

2.1.2. Preparo da solução de nitrato de prata

Para a solução de Íon Ag^+, 1,57 g de $AgNO_3$ (Merck KGaA) foi dissolvido em 1000 mL de água deionizada. A solução também foi mantida em frascos âmbar a 4º C.

2.2. Microrganismos e Condições de Crescimento

C. glabrata CBS138 foi cultivada em Yeast Peptone Dextrose (YPD) suplementado com 2% de ágar por 24 h a 30º C. YPD contém, por litro, 20 g de sacarose (Merck Millipore, Portugal), 10 g de extrato de levedura (HiMedia Laboratories, Mumbai, Índia) e 20 g de peptone (HiMedia Laboratories). Nos ensaios antimicrobianos, meio RPMI ajustado a um pH 7.0 (com NaOH) foi utilizado. RPMI contém, por litro, 20,8 g de meio sintético RPMI-1640 (Sigma), 36 g de sacarose (Merck Millipore), 0,3 g de L-glutamina (Sigma) e 0,165 mol/L de MOPS (3-(N-morfolino) ácido propanosulfônico, Sigma).

2.3. Determinação da Concentração Inibitória Mínima (CIM_{50}) e de Unidades Formadoras de Colônias (UFCs/mL)

A concentração inibitória mínima (CIM_{50}) da solução de Íon Ag^+ e das NPsAg foi determinada usando o método da microdiluição recomendado pelo Comitê Europeu de Testes de Susceptibilidade Antimicrobiana (Rodriguez-Tudela *et al*. 2008). Para isso, células de *C. glabrata* CBS138 foram cultivados por 17 h em meio de crescimento YPD a 30º C com agitação orbital de 250 rpm. Na sequência, as células foram diluídas em meio RPMI (Sigma) para obter uma suspensão de células tendo uma densidade óptica (DO_{600nm}) de 0,05. A partir destas suspensões, alíquotas de 100 µL foram misturadas na placa de poliestireno de 96 poços (Costar) contendo 100 µL de meio RPMI (controle) ou com 100 µL deste mesmo meio suplementado com solução de Íon Ag^+ ou NPsAg. As concentrações de Íon Ag^+ e NPsAg testadas variaram de 0,005 a 2,44 mg/L e 0,08 a 39,06 mg/L, respectivamente. A concentração final do inóculo foi de 0,5 – 2,5 x 10^5 UFC/mL. As placas foram incubadas a 37º C por 24 h e, depois deste período, a densidade óptica (DO_{530nm}) foi mensurada em um leitor de microplaca (SpectroStar Nano, BMG Labtech, Germany). Valores de CIM_{50} foram tomados como sendo a primeira concentração do antifúngico que reduziu o crescimento dos microrganismos a metade que registrada no

meio sem a droga (controle), como definido pelo Comitê Europeu de Testes de Susceptibilidade Antimicrobiana (Rodriguez-Tudela *et al*. 2008).

Após o período de incubação (24 h), os biofilmes formados na presença e na ausência das do Íon Ag^+ e das AgNPs foram raspados com raspadores de células, diluídos em PBS e plaqueados em YPD ágar para determinar a quantidade de UFCs/mL. Estes experimentos foram realizados em triplicata.

2.4. Curva de Crescimento

Células de *C. glabrata* CBS138 foram inicialmente cultivadas em YPD a 30º C com agitação orbital de 250 rpm por 17 h. NPsAg na concentração da CIM_{50} (2,44 mg/L) foram diluídas em RPMI para um volume final de 100 mL em Erlenmeyer. A concentração final do inóculo foi de 0,5 – 2,5 x 10^5 UFC/mL. Os tempos avaliados foram: 0, 2, 4, 6, 8, 10, 12, 24, 48 e 72 horas. Após cada período experimental, a densidade óptica foi determinada em um comprimento de onda de 600 nm. Além disso, uma alíquota em cada tempo experimental também foi diluída em PBS, plaqueado em YPD ágar para determinar a UFCs/mL. Os experimentos foram realizados em triplicata.

2.5. Análise transcriptômica

Com o propósito de aprofundar o conhecimento do impacto das NPsAg sobre a fisiologia de *C. glabrata*, uma análise transcriptômica foi realizada a fim de avaliar quais genes estão mais ou menos expressos como resposta à exposição a esta solução antimicrobiana. A resposta transcriptômica das células de *C. glabrata* CBS138 frente às NPsAg foi determinada em duas situações: nos estados planctônico e formando biofilmes. A resposta transcriptômica das células expostas às NPsAg formando biofilmes foi comparada com a do íon Ag^+.

2.5.1. Estado Planctônico

Células de *C. glabrata* foram expostas às NPsAg (em uma concentração de 2,44 mg/L) por 2 h sob agitação constante (250 rpm) a 37º C. Após esse período, as células de *C. glabrata* foram coletadas por meio de centrifugação para a experiência dos '*microarrays*'. As células foram, então, armazenadas a -80º C para posterior extração do RNA. Os ensaios foram realizados em triplicata.

2.5.2. Formando biofilmes

Biofilmes de *C. glabrata* CBS138 foram formados na ausência e na presença das NPsAg (em uma concentração de 2,44 mg/L) e do íon Ag^+ (em uma concentração de 1,22 mg/L) em placas de 6 poços (Greiner Bio One, Alemanha) por 24 h. Após esse período, os biofilmes foram coletados, centrifugados (8200 rpm, por 5 min) e, as células foram armazenadas a -80º C para posterior extração do RNA. Os ensaios foram realizados em triplicata.

2.5.3. Extração do RNA

Em ambas situações (no estado planctônico e formando biofilmes), a extração do RNA foi realizada utilizando o kit RiboPure RNA Isolation (Ambion, Life Technologies, CA) de acordo com as instruções do fabricante. A concentração, qualidade e os níveis de integridade das amostras de RNA foram controlados usando um Agilent 2100 Bioanalisador (Agilent) de acordo com as instruções do fabricante. Apenas as amostras com razões 28S/18S rRNA entre 1,6 e 2,2 e mostrando uma ausência de degradação foram utilizadas nas análises subsequentes.

2.5.4. Experiência de '*Microarray*'

Os chips de DNA utilizados para a análise de '*microarray*' foram manufaturados pela Agilent usando um design para *C. glabrata* (Rossignol *et al*. 2007). Inicialmente, os cDNAs foram sintetizados a partir do RNA total extraído das células que foram expostas às soluções experimentais nas diferentes condições. As amostras foram preparadas por hibridização (*Agilent's Two-Color Microarray-Based Gene Expression Protocol*). Os '*microarrays*' hibridizados foram escaneados com um Axon 4000B scanner (Axon Instruments) e os dados foram adquiridos com GenePix Pro 5.1 software (Axon Instruments). Os dados resultantes foram processados usando o programa BRB-Array Tools em associação com o Excel e os 'fold-changes' foram estimados utilizando a normalização Lowess. Posteriormente, os genes com 'fold-changes' maior ou igual a 1,5 e menor ou igual a -1,5 foram categorizados utilizando o Banco de Dados de Catalógo Funcional MIPS (http://mips.helmholtz-muenchen.de/funcatDB/) e o Banco de Dados PathoYeastract de *C. glabrata* (http://pathoyeastract.org/cglabrata/rankbygo.php).

3. Resultados e Discussão

3.1. Concentração Inibitória Mínima (CIM_{50}), UFCs/mL e Curva de Crescimento

Para que a análise transcritômica fosse significativa e pudesse ser utilizada para comparar o íon Ag^+ com as NPsAg, um efeito tóxico equivalente nas diferentes condições testadas era necessário. Assim, decidimos estudar o efeito de cada estresse individualmente de forma a escolher concentrações que levassem a um idêntico nível de toxicidade, sobre as quais, posteriormente, seria possível tirar conclusões do ponto de vista comparativo. A Figura 1 mostra os valores de CIM_{50} para Íon Ag^+ (A) e NPsAg (B) e número de células viáveis (UFCs/mL) (C) após exposição às soluções experimentais. Os valores de CIM_{50} para Íon Ag^+ e NPsAg foram 1,22 e 2,44 mg/L, respectivamente. Houve uma redução de aproximadamente 93% na formação do biofilme quando os biofilmes de *C. glabrata* CBS138 foram formados na presença do íon Ag^+ e das NPsAg (as concentrações utilizadas foram baseadas nos valores de CIM_{50}).

A Figura 2 nos mostra a curva de crescimento de *C. glabrata* CBS138 (DO_{600nm} e UFC/mL) na presença ou na ausência de 2,44 mg/L de NPsAg. Na presença das NPsAg, houve uma redução na viabilidade celular de *C. glabrata* nos tempos avaliados em ambos experimentos (densidade óptica (DO_{600nm}) e UFCs/mL.

3.2. Análise transcriptômica

3.2.1. Estado Planctônico

Nós decidimos fazer a comparação em condições planctônicas visto que é uma forma mais direta de ver o efeito das '*green*'-NPsAg sobre a fisiologia de *C. glabrata*.

No estado planctônico, as células de *C. glabrata* tratadas ou não com NPsAg por 2 h foram recolhidas e, o RNA foi extraído para a análise transcriptômica. No total, 295 genes foram encontrados ser '*up-regulated*' e 52 genes foram encontrados ser '*down-regulated*' (acima de 1,5-vezes) (com $p < 0.05$). Em ambas as regulações (*up* ou *down*), os genes foram agrupados de acordo com a sua função biológica, usando o Banco de Dados do Catálogo Funcional MIPS, e as classes funcionais enriquecidas ($p < 0,05$) foram selecionadas (Figura 3). Pode-se observar que as principais funções *up-regulated* em *C. glabrata* após exposição às NPsAg foram 'Amino acid metabolism' e 'C-compound and carbohydrate metabolism'. Além disso, verificou-se que as principais funções *down-regulated* como resposta às NPsAg foram 'Homeostasis of cations' e 'Cellular import'.

Em relação ao 'Amino acid metabolism' e 'C-compound and carbohydrate metabolism', os genes relacionados à biossíntese da metionina e da lisina foram os mais representativos (Tabela 1). A superexpressão dos genes MET e LYS pode ser explicada pelo fato de que as NPsAg podem induzir uma alteração no conteúdo lipídico da

membrana plasmática, o que pode ter efeitos na importação de aminoácidos. Foi demonstrado que o transporte de metionina e de lisina é reduzido em células com maior conteúdo de ergosterol e é aumentado em células com menor conteúdo de ergosterol (Singh *et al*. 1979). Portanto, é provável que as células tratadas com as NPsAg tenham menores teores de ergosterol, o que poderia predizer um aumento no nível de importação de metionina e de lisina.

Os genes envolvidos na função 'Homeostasis of cations (prótons e íons metálicos)' estão sub-expressos em células de *C. glabrata* tratadas com NPsAg por 2 h (Tabela 2). A transição de metais é essencial para muitos processos metabólicos e sua homeostase é de fundamental importância para a manutenção dos principais mecanismos fisiológicos e, consequentemente, para a viabilidade celular (Nelson, 1999). No entanto, como isso também os torna potencialmente tóxicos, as células usam vários mecanismos para controlar a toxicidade deste elemento, incluindo um rígido controle do transporte de metais transmembrana. O transporte transmembrana mantém um equilíbrio entre a quantidade de metal necessária para processos biológicos e a quantidade que pode ser tóxica (Askwith e Kaplan, 1998). Desta forma, a repressão destes genes, como resultado da exposição às AgNPs, pode indicar que as células percebem o aumento na concentração de metal devido à presença das nanopartículas e tentam assim impedir a sua passagem através da membrana. Isto pode funcionar como uma ferramenta para manter a homeostase do metal dentro das células, enquanto, por sua vez, funciona como um mecanismo de resistência contra as NPsAg.

Quando as células de *Candida* são expostas a estresses ambientais, como os antifúngicos, geralmente, genes envolvidos com transporte de glicose são sobre-expressos como um meio de garantir que as células tenham energia suficiente para superar o estresse que estão sendo submetidas (Pais et al. 2016; Ng et al. 2015). No entanto, o contato das células de *C. glabrata* com as NPsAg desencadeou uma resposta oposta, resultando na desativação dos transportadores de membrana ('Cellular import' e 'C-compound and carbohydrate metabolism' – CAGL0D02640g, FPS2 e HXT1) (Tabela 2). Este resultado divergente pode estar relacionado com o mecanismo de ação ainda não completamente descrito das NPsAg, no entanto, é promissor reconhecer que este composto parece agir através de um mecanismo diferente quando comparado com os antifúngicos utilizados atualmente, dado que desencadeia uma atividade celular distinta.

3.2.2. Formando biofilmes

Nesta parte do estudo, nós investigamos se a resposta celular frente às NPsAg é diferente ou idêntica àquela produzida pelo íon Ag^+. Inicialmente, biofilmes de *C. glabrata* CBS138 foram formados na ausência e na presença das soluções antimicrobianas (íon Ag^+ - 1,22 mg/L e NPsAg – 2,44 mg/L) por 24 h. Após esse período, as células foram recolhidas para extração do RNA e para posterior análise transcriptômica. Na Figura 4, nós sumarizamos o número de genes *up-* ou *down-regulated* (acima de 1,5 vezes) em resposta aos estímulos. Pode-se observar que, 276 genes *up-regulated* e 274 genes encontrados serem *down-regulated* são exclusivos para as NPsAg. De acordo com o Banco de Dados do Catálogo Funcional MIPS, algumas funções foram específicas às NPsAg em relação ao íon Ag^+ tanto nos genes sobre- ou sub-expressos (*up-* ou *down-regulated*) (Fig. 5).

Células de *Candida* desenvolvem estratégias para crescer e sobreviver em diferentes ambientes desfavoráveis. No presente estudo, nós observamos que *C. glabrata* adquire dois mecanismos de proteção para permitir que o patógeno cresça e sobreviva sob estresse das NPsAg: através do aumento da síntese endógene de esteróis ou através da importação de esteróis exógenos. Nossos dados revelaram que a expressão dos genes reguladores da biossíntese de ergosterol e do metabolismo do esterol, bem como os genes transportadores do influxo de esterol, estão significativamente aumentados em *C. glabrata* sob estresse com as NPsAg (Tabela 3). Essa característica não foi observada nas células tratadas com o íon Ag^+. Da mesma forma, os genes transportadores do influxo de esteróis (AUS1, UPC2 e TIR3) e os genes biossintéticos do ergosterol (ERG1, ERG11, ERG3 e ERG25) são marcadamente regulados positivamente em leveduras quando a biossíntese do ergosterol é suprimida em hipóxia ou devido a síntese de esterol defeituosa. (Li et al. 2018). Além disso, as células de *C. glabrata* CBS138 expostas às NPsAg por 24 h apresentaram uma sobre-expressão de genes relacionados com o efluxo de drogas, tais como: CDR1 e PDR1 (função: 'Detoxification') (Tabela 3). Esse é o mecanismo predominante pelo qual *C. glabrata* medeia a resistência a uma ampla gama de azóis e outros compostos antifúngicos (Fonseca *et al*. 2014). Genes que estão envolvidos na manutenção de processos metabólicos das células de *Candida* estão sobre-expressos, como por exemplo: os genes da função 'Siderophore-iron transport' (FET3, AFT1 e FTR1).

As principais funções que se apresentaram *down-regulated* após exposição às nanopartículas por 24 h foram: 'Cell cycle', 'Aerobic respiration', 'Transport facilities',

'Electron transport' e 'Mitochondrion' (Tabela 4). Assim, o provável mecanismo de ação das NPsAg pode estar envolvido com estas funções.

Conclusão

Diante dos nossos resultados, pode-se concluir que, as células de *Candida* no estado planctônico podem responder de diferentes formas frente às NPsAg. Além disso, as células de *C. glabrata* responderam de forma diferente frente às NPsAg quando comparado com o íon Ag^{+}. Este fato pode nos ajudar a elucidar o mecanismo de ação destas nanopartículas e, também, nos ajuda na descoberta de novos alvos terapêuticos.

Referências

1. Monteiro, D.R., Gorup, L.F., Silva, S., Negri, M. et al (2011) Silver coloidal nanoparticles: antifungal effect against adhered cells and biofilms of Candida albicans and Candida glabrata. Biofouling 37, 711-719.
2. Song, J.Y. and Kim, B.S. (2009) Rapid biological synthesis of silver nanoparticles using plant leaf extracts. Bioprocess Biosyst Eng 32, 79-84.
3. Bapat RA, Chaubal TV, Joshi CP *et al*. An overview of application of silver nanoparticles for biomaterials in dentistry. *Mater Sci Eng C Mater Biol Appl*. 91, 881-898 (2018).
4. Chairuangkitti, P., Lawanprasert, S. et al (2013) Silver nanoparticles induce toxicity in A549 cells via ROSdependent and ROS-independent pathways. Toxicol In Vitro, 27, 330-338.
5. Prabhu S, Poulose EK. Silver nanoparticles: mechanism of antimicrobial action, synthesis, medical applications, and toxicity effects. *Int Nano Lett*. 2, 32 (2012). doi: 10.1186/2228-5326-2-32.
6. Wei, L., Tang, J., Zhang, Z. et al (2010) Investigation of the cytotoxicity mechanism of silver nanoparticles in vitro. Biomed Mater, 5, 044103.
7. Rudramurthy GR, Swamy MK, Sinniah UR, Ghasemzadeh A. Nanoparticles: Alternatives against drug-resistant pathogenic microbes. Molecules. 21(7), pii: E836 (2016). doi: 10.3390/molecules21070836.
8. Zhang XF, Liu ZG, Shen W, Gurunathan S. Silver nanoparticles: Synthesis, characterization, properties, applications, and therapeutic approaches. Int J Mol Sci. 17(9), pii: E1534 (2016). doi: 10.3390/ijms17091534.

9. Monteiro, D.R., Silva, S., Negri, M., Gorup, L.F. et al (2012) Silver nanoparticles: influence of stabilizing agent and diameter on antifungal activity against Candida albicans and Candida glabrata biofilms. Lett Appl Microbiol, 54, 383-391.
10. Braydich-Stolle, L.K., Lucas, B., Schrand, A. et al (2010) Silver nanoparticles disrupt GDNF/Fyn kinase signaling in spermatogonial stem cells. Toxicol Sci, 116, 577-589.
11. Kim, K.J., Sung, W.S., Suh, B.K. et al (2009) Antifungal activity and mode of action of silver nano-particles on Candida albicans. Biometals, 22, 235-242.
12. Ahamed, M., Alsalhi, M.S. and Siddiqui, M.K. (2010) Silver nanoparticle applications and human health. Clin Chim Acta, 411, 1841-1848.
13. Ali, M., Kim, B., Belfield, K.D. et al (2016) Green synthesis and characterization of silver nanoparticles using Artemisia absinthium aqueous extract – A comprehensive study. Mater Sci Eng C Mater Biol Appl, 58, 359-365.
14. Arumai Selvan D, Mahendiran D, Senthil Kumar R, Kalilur Rahiman A. Garlic, green tea and turmeric extracts-mediated green synthesis of silver nanoparticles: Phytochemical, antioxidant and in vitro cytotoxicity studies. J Photochem Photobiol B. 180, 243-252 (2018).
15. Malik P, Shankar R, Malik V, Sharma N, Mukherjee TK. Green chemistry based benign routes for nanoparticle synthesis. Journal of Nanoparticles. ID 302429 (2014) doi: 10.1155/2014/302429.
16. Park, Y., Hong, Y.N. Weyers, A. et al (2011) Polysaccharides and phytochemicals: a natural reservoir for the green synthesis of gold and silver nanoparticles. IET Nanobiotechnol, 5, 69-78.
17. Kumari, A., Guliani, A., Singla, R. et al (2015) Silver nanoparticles synthesized using plant extracts show strong antibacterial activity. IET Nanobiotechnol, 9, 142-152.
18. Ahmad, N., Sharma, Seema. and Rai, R. (2012) Rapid green synthesis of silver and gold nanoparticles using peels of Punica granatum. Adv Mat Lett 3, 376-380.
19. Fernandes RA, Berretta AA, Torres EC et al. Antimicrobial potential and cytotoxicity of silver nanoparticles phytosynthesized by pomegranate peel extract. Antibiotics (Basel). 7(3), pii: E51 (2018) doi: 10.3390/antibiotics7030051.
20. Souza JA, Barbosa DB, Berretta AA et al. Green synthesis of silver nanoparticles combined to calcium glycerophosphate: antimicrobial and antibiofilm activities. Future Microbiol. 13, 345-357 (2018).

21. Heber, D. (2011) Pomegranate ellagitannins. Herbal Medicine: Biomolecular and Clinical Aspects, 2nd edition.
22. Yang, X., Gondikas, A.P., Marinakos, S.M. et al (2012) Mechanism of silver nanoparticle toxicity is dependent on dissolved silver and surface coating in Caenorhabditis elegans. Environ Sci Technol 46, 1119-1127.
23. Roco MC. Science and technology integration for increased human potential and societal outcomes. Ann N Y Acad Sci. 1013, 1-16 (2004).
24. Rizzello, L. and Pompa, P.P. (2014) Nanosilver-based antibacterial drugs and devices: Mechanisms, methodological drawbacks, and guidelines. *Chem Soc Rev* 43, 1501-1518.
25. Rossignol T, Logue ME, Reynolds K, Grenon M, Lowndes NF, Butler G. Transcriptional response of *Candida parapsilosis* following exposure to farnesol. *Antimicrob. Agents Chemother*. 2007; 51(7): 2304-2312.
26. Saeed AI, Sharov V, White J, et al. TM4: a free, open-source system for microarray data management and analysis. *Biotechniques*. 2003; 34(2): 374-378.
27. Singh M, Jayakumar A, Prasad R. The effect of altered ergosterol content on the transport of various amino acids in Candida albicans. *Biochim Biophys Acta* 1979; 555:42-55.
28. Askwith C, Kaplan J. Iron and copper transport in yeast and its relevance to human disease. *Trends Biochem Sci* 1998; 23:135-138.
29. Nelson N, Harvery WR. Vacuolar and plasma membrane V-ATPases. *Phys Rev* 1999; 79:361-385.
30. Pais P, Costa C, Pires C, Shimizu K, Chibana H, Teixeira MC. Membrane proteome-wide response to the antifungal drug clotrimazole in Candida glabrata: Role of the transcription factor CgPdr1 and the Drug: H+ antiporters CgTpo1_1 and CgTpo1_2. *Mol Cell Proteomics* 2016; 15(1):57-72.
31. Ng TS, Mohd Desa MN, Sandai D, Chong PP, Than LT. Phylogenetic and transcripts profiling of glucose sensing related genes in Candida glabrata. *Jundishapur J Microbiol* 2015; 8(11):e25177. doi: 10.5812/jjm.25177.
32. Li QQ, Tsai HF, Mandal A, *et al*. Sterol uptake and sterol biosynthesis act coordinately to mediate antifungal resistance in Candida glabrata under azole and hypoxic stress. *Mol Med Rep* 2018; 17(5):6585-6597.

33. Fonseca E, Silva S, Rodrigues CF, Alves CT, Azeredo J, Henriques M. Effects of fluconazole on Candida glabrata biofilms and its relationship with ABC transporter gene expression. *Biofouling* 2014; 30(4):447-457.

Figuras

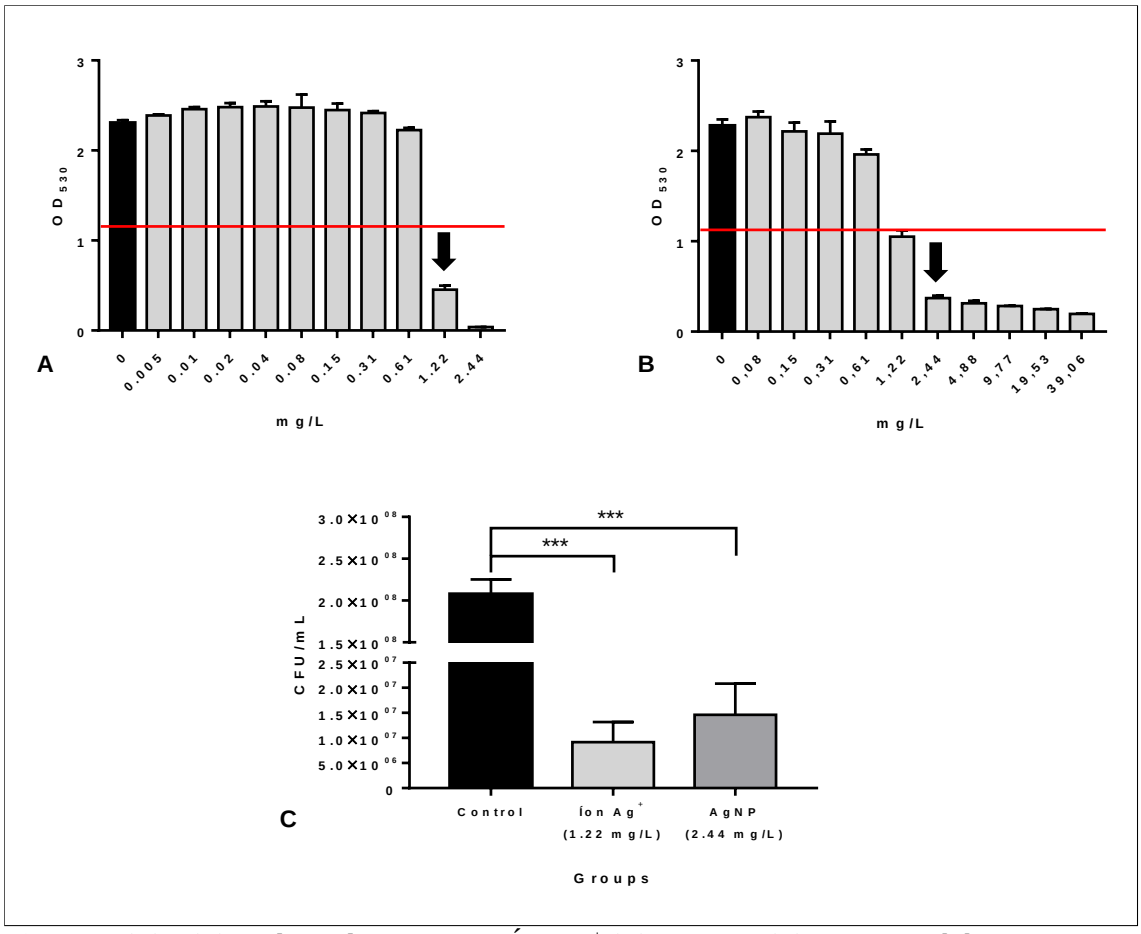

Figura 1. (A) e (B): Valores de CIM_{50} para Íon Ag^+ (A) e NPsAg (B) contra *C. glabrata* CBS138. A CIM foi determinada pelo método da microdiluição recomendado pelo EUCAST. Valores de CIM para cada composto está representado por uma seta. (C): Número de células cultiváveis dos biofilmes de *C. glabrata* CBS138 depois da formação do biofilme na presença ou na ausência do Íon Ag^+ e das NPsAg representado por UFCs/mL; as concentrações utilizadas foram baseadas nos valores de CIM_{50} (ANOVA 1-critério, seguido pelo teste de Dunnett, com $p < 0.05$).

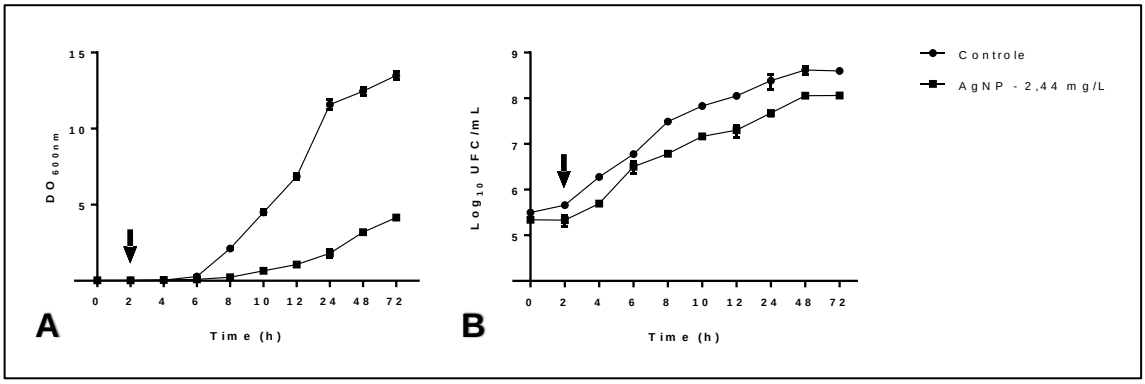

Figura 2. Curva de crescimento de *C. glabrata* CBS138 na presença ou na ausência das NPsAg (2,44 mg/L) expressa em densidade óptica (DO_{600nm}) (A) e número de unidades formadora de colônias por mL (Log_{10} UFCs/mL) (B). Seta mostrando o ponto que as amostras foram recolhidas para extração de RNA.

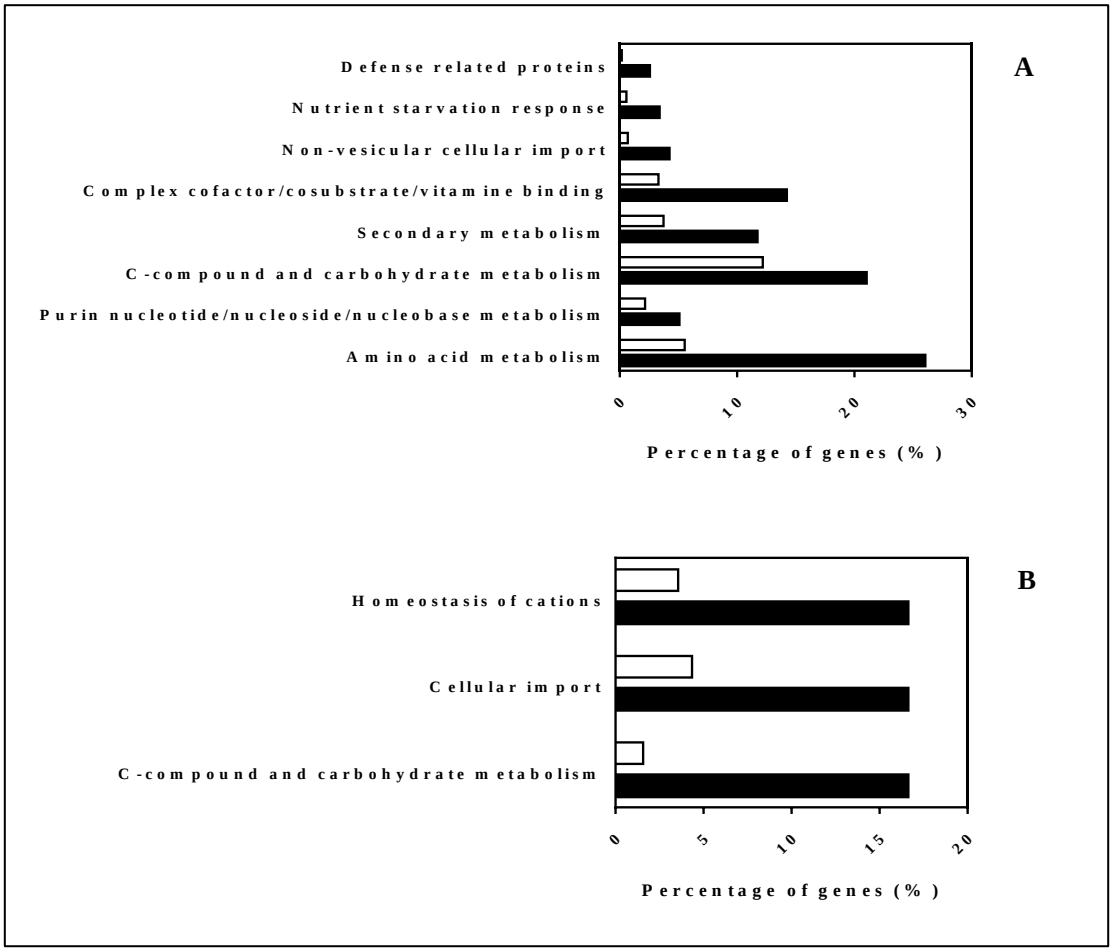

Figura 3. Agrupamento funcional de genes ativados em *C. glabrata* CBS138 (estado planctônico) em resposta às NPsAg por 2 h. Os genes encontrados ser *up*- (A) ou *down-regulated* (B) em resposta às NPsAg foram agrupados de acordo com a sua função biológica, usando o banco de dados do Catálogo Funcional MIPS (barras pretas), e as classes funcionais enriquecidas ($p < 0,05$) foram selecionadas. As barras brancas representam a porcentagem de genes agrupados em cada classe funcional, utilizando como conjunto de dados de entrada todo o genoma de *C. glabrata* CBS138.

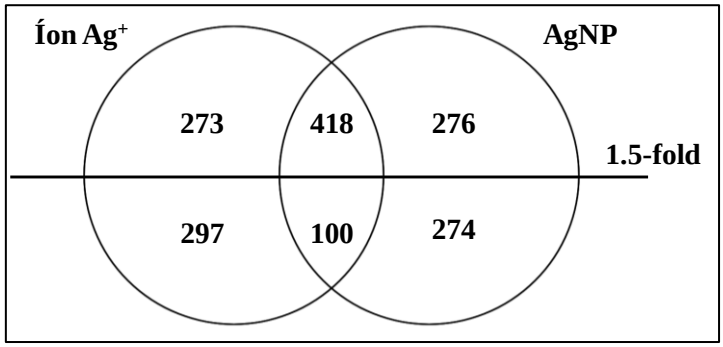

Figura 4. Diagrama de Venn resumindo o número de genes up- ou down-regulated (acima de 1,5 vezes (fold)) em resposta ao Íon Ag^+ e às NPsAg nas células de *C. glabrata* CBS138 formando biofilmes por 24 h.

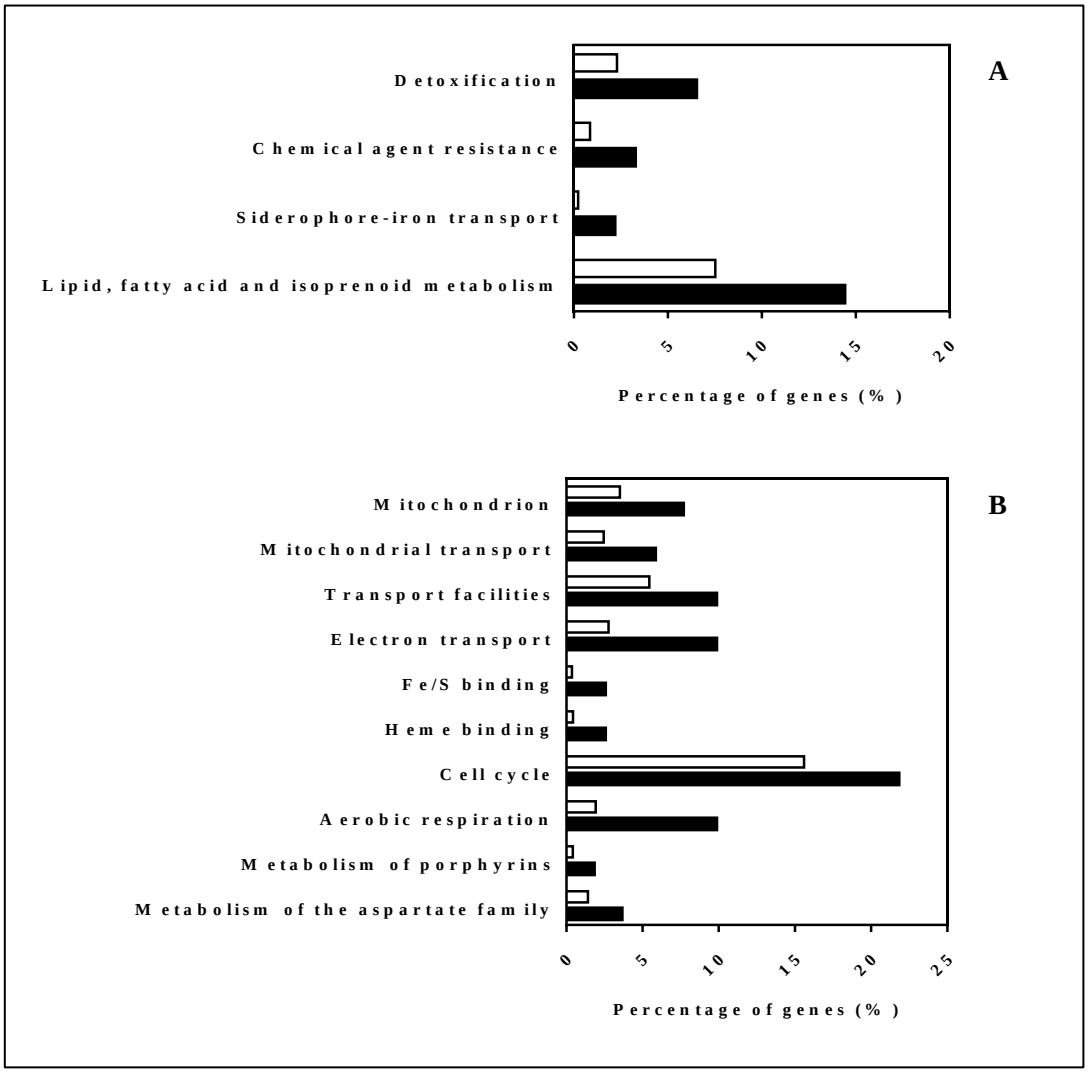

Figura 5. Agrupamento funcional de genes ativados em *C. glabrata* CBS138 (formando biofilmes) em resposta às NPsAg por 24 h. Os genes encontrados ser *up*- (A) ou *down-regulated* (B) em resposta às NPsAg foram agrupados de acordo com a sua função biológica, usando o banco de dados do Catálogo Funcional MIPS (barras pretas), e as classes funcionais enriquecidas ($p < 0,05$) foram selecionadas. As barras brancas representam a porcentagem de genes agrupados em cada classe funcional, utilizando como conjunto de dados de entrada todo o genoma de *C. glabrata* CBS138.

Tabelas

Tabela 1. Lista dos genes up-regulated em resposta às NPsAg por 2 h em *C. glabrata* CBS138 de acordo com os grupos funcionais obtidos pelo MIPS Functional (http://mips.helmholtz-muenchen.de/funcatDB/). A função biológica indicada foi baseada nas informações disponíveis em *Candida* Genome Database (http://candidagenome.org) e/ou na informação disponível para ortólogo *S. cerevisiae*.

ORF Name	Gene Name	Fold-Change	*p* value	Function
Amino Acid Metabolism				
CAGL0J06402g	(LYS20)	12.30	3.75E-03	Ortholog(s) have homocitrate synthase activity, role in DNA repair, histone displacement, lysine biosynthetic process via aminoadipic acid and nucleus localization
CAGL0F07029g	MET13	8.05	9.93E-03	Ortholog(s) have methylenetetrahydrofolate reductase (NAD(P)H) activity and role in methionine biosynthetic process, one-carbon metabolic process
CAGL0G02585g	LYS12	7.57	5.42E-03	Homo-isocitrate dehydrogenase
CAGL0K10978g	(LYS4)	6.41	2.55E-03	Ortholog(s) have homoaconitate hydratase activity, role in lysine biosynthetic process via aminoadipic acid and mitochondrion localization
CAGL0K07788g	(LYS2)	6.28	5.37E-03	Ortholog(s) have L-aminoadipate-semialdehyde dehydrogenase activity and role in lysine biosynthetic process via aminoadipic acid
CAGL0F06875g	(LYS1)	6.02	6.04E-03	Ortholog(s) have mRNA binding, saccharopine dehydrogenase (NAD+, L-lysine-forming) activity and role in lysine biosynthetic process via aminoadipic acid
CAGL0C03443g	LYS9	5.86	1.75E-03	Putative saccharopine dehydrogenase
CAGL0K06677g	MET8	5.77	3.33E-03	Putative bifunctional dehydrogenase and ferrochelatase; gene is upregulated in azole-resistant strain
CAGL0K08668g	MET28	5.03	1.52E-03	bZIP domain-containing protein
CAGL0D06402g	MET15	4.89	3.41E-03	O-acetyl homoserine sulfhydrylase (OAHSH), ortholog of S. cerevisiae MET17; required for utilization of inorganic sulfate as sulfur source; able to utilize cystine as a sulfur source while S. cerevisiae met15 mutants are unable to do so
CAGL0I04994g	MET6	4.86	4.03E-03	5-methyltetrahydropteroyltriglutamate homocysteine methyltransferase; protein abundance increased in ace2 mutant cells
C-compound and carbohydrate metabolism				
CAGL0J06402g	(LYS20)	12.30	3.75E-03	Ortholog(s) have homocitrate synthase activity, role in DNA repair, histone displacement, lysine biosynthetic process via aminoadipic acid and nucleus localization
CAGL0F07029g	MET13	8.05	9.93E-03	Ortholog(s) have methylenetetrahydrofolate reductase (NAD(P)H) activity and role in methionine biosynthetic process, one-carbon metabolic process
CAGL0G02585g	LYS12	7.57	5.42E-03	Homo-isocitrate dehydrogenase

CAGL0K10978g	(LYS4)	6.41	2.55E-03	Ortholog(s) have homoaconitate hydratase activity, role in lysine biosynthetic process via aminoadipic acid and mitochondrion localization
CAGL0M07612g	(FMS1)	3.71	4.85E-03	Ortholog(s) have polyamine oxidase activity and role in pantothenate biosynthetic process, spermine catabolic process
CAGL0J09240g	LYS21	3.68	1.07E-02	Homocitrate synthase; protein abundance increased in ace2 mutant cells

Tabela 2. Lista dos genes down- regulated em resposta às NPsAg por 2 h em *C. glabrata* CBS138 de acordo com os grupos funcionais obtidas pelo MIPS Functional (http://mips.helmholtz-muenchen.de/funcatDB/). A função biológica indicada foi baseada nas informações disponíveis em *Candida* Genome Database (http://candidagenome.org) e/ou na informação disponível para ortólogo *S. cerevisiae*.

ORF Name	Gene Name	Fold-Change	*p* value	Function
Cellular import				
CAGL0A01804g	HXT1	0.24	2.81E-02	Uncharacterized ORF; Ortholog(s) have fructose transmembrane transporter activity, pentose transmembrane transporter activity, role in glucose transmembrane transport, mannose transmembrane transport and plasma membrane localization
CAGL0E03894g	FPS2	0.27	2.69E-04	Verified ORF; Glycerol transporter; involved in flucytosine resistance; double fps1/fps2 mutant accumulates glycerol, has constitutive cell wall stress, is hypersensitive to caspofungin in vitro and in vivo
CAGL0D02640g	CAGL0D02640g	0.34	1.02E-02	Uncharacterized ORF; Has domain(s) with predicted transmembrane transporter activity, role in transmembrane transport and integral component of membrane, membrane localization
Homeostasis of cations				
CAGL0H10076g	CAGL0H10076g	0.28	7.88E-04	Uncharacterized ORF; Ortholog(s) have plasma membrane localization
CAGL0K07634g	GAT1	0.30	4.38E-03	Uncharacterized ORF; Ortholog(s) have sequence-specific DNA binding, transcription factor activity, RNA polymerase II transcription factor binding, transcriptional activator activity, RNA polymerase II proximal promoter sequence-specific DNA binding activity

CAGL0I07491g	(IZH4)	0.32	1.68E-03	Uncharacterized ORF; Ortholog(s) have role in cellular zinc ion homeostasis

Tabela 3. Lista dos genes up-regulated em resposta às NPsAg por 24 h, exclusivamente (diagrama de Venn), em *C. glabrata* CBS138 (formando biofilmes) de acordo com os grupos funcionais obtidas pelo MIPS Functional (http://mips.helmholtz-muenchen.de/funcatDB/). A função biológica indicada foi baseada nas informações disponíveis em *Candida* Genome Database (http://candidagenome.org) e/ou na informação disponível para ortólogo *S. cerevisiae*.

ORF Name	Gene Name	Fold Change	*p* value	Function
			Detoxification	
CAGL0A00451g	PDR1	4.35	0.004	Verified ORF; Zinc finger transcription factor, activator of drug resistance genes via pleiotropic drug response elements (PDRE); regulates drug efflux pumps and controls multi-drug resistance; gene upregulated and/or mutated in azole-resistant strains
CAGL0E04092g	SIT1	6.73	0.004	Verified ORF; Putative siderophore-iron transporter with 14 transmembrane domains; required for iron-dependent survival in macrophages; mRNA levels elevated under iron deficiency conditions; plasma membrane localized
CAGL0E04334g	ERG11	4.38	0.004	Verified ORF; Putative cytochrome P-450 lanosterol 14-alpha-demethylase; target enzyme of azole antifungal drugs; increased protein abundance in azole resistant strain
CAGL0F01419g	AUS1	49.18	0.0007	Verified ORF; ATP-binding cassette transporter involved in sterol uptake
CAGL0G08624g	QDR2	5.77	0.004	Verified ORF; Drug:H+ antiporter of the Major Facilitator Superfamily, confers imidazole drug resistance, involved in quinidine/multidrug efflux; gene is activated by Pdr1p; upregulated in azole-resistant strain
CAGL0I08019g	YOL075C	4.03	0.001	Uncharacterized ORF; Ortholog(s) have role in cellular response to drug and extrinsic component of fungal-type vacuolar membrane, plasma membrane localization
CAGL0J09944g	AQR1	8.88	0.009	Verified ORF; Plasma membrane drug:H+ antiporter involved in resistance to drugs and acetic acid

CAGL0K10714g	ROD1	4.14	0.041	Uncharacterized ORF; Ortholog(s) have ubiquitin protein ligase binding activity and role in adaptation of signaling pathway by response to pheromone involved in conjugation with cellular fusion, positive regulation of receptor internalization
CAGL0K07392g	COT1	3.20	0.01	Uncharacterized ORF; Ortholog(s) have zinc ion transmembrane transporter activity, role in cellular zinc ion homeostasis, filamentous growth and fungal-type vacuole localization
CAGL0L10912g	TPO4	7.16	0.033	Uncharacterized ORF; Ortholog(s) have spermidine transmembrane transporter activity, spermine transmembrane transporter activity, role in spermidine transport, spermine transport and fungal-type vacuole membrane, plasma membrane localization
CAGL0L02959g	ALY1	4.20	0.003	Uncharacterized ORF; Ortholog(s) have ubiquitin protein ligase binding activity, role in endocytosis, positive regulation of ubiquitin-dependent endocytosis, regulation of intracellular transport and early endosome, late endosome localization
CAGL0L02101g	BSD2	3.41	0.0097	Uncharacterized ORF; Ortholog(s) have role in metal ion transport, protein targeting to vacuole, ubiquitin-dependent protein catabolic process and endoplasmic reticulum, fungal-type vacuole membrane localization
CAGL0M01760g	CDR1	6.06	8.36E-04	Verified ORF; Multidrug transporter of ATP-binding cassette (ABC) superfamily, involved in resistance to azoles; expression regulated by Pdr1p; increased abundance in azole resistant strains; expression increased by loss of the mitochondrial genome
Lipid, fatty acid and isoprenoid metabolism				
CAGL0C03872g	TIR3	5.86	0.0004	Verified ORF; Putative GPI-linked cell wall protein involved in sterol uptake
CAGL0D05566g	YEH2	3.29	0.008	Uncharacterized ORF; Ortholog(s) have sterol esterase activity, role in sterol metabolic process and integral component of membrane, lipid droplet localization

CAGL0D05940g	ERG1	6.45	0.009	Verified ORF; Squalene epoxidase with a role in ergosterol synthesis; involved in growth under conditions of low oxygen tension
CAGL0E04334g	ERG11	4.38	0.004	Verified ORF; Putative cytochrome P-450 lanosterol 14-alpha-demethylase; target enzyme of azole antifungal drugs; increased protein abundance in azole resistant strain
CAGL0F01793g	ERG3	4.17	0.006	Verified ORF; Delta 5,6 sterol desaturase; C-5 sterol desaturase; predicted transmembrane domain and endolasmic reticulum (ER) binding motif; gene used for molecular typing of C. glabrata strain isolates
CAGL0F07865g	UPC2B	27.09	0.0013	Uncharacterized ORF; Putative Zn(2)-Cys(6) binuclear cluster transcriptional regulator of ergosterol biosynthesis
CAGL0I04246g	SUT1	10.78	0.016	Uncharacterized ORF; Putative transcription factor involved in sterol uptake; gene is upregulated in azole-resistant strain
CAGL0I00330g	SCS3	4.38	0.005	Uncharacterized ORF; Ortholog(s) have role in phospholipid biosynthetic process
CAGL0I07491g	IZH4	5.86	0.006	Uncharacterized ORF; Ortholog(s) have role in cellular zinc ion homeostasis
CAGL0K04477g	ERG25	3.51	0.011	Uncharacterized ORF; Ortholog(s) have C-4 methylsterol oxidase activity, role in ergosterol biosynthetic process and endoplasmic reticulum membrane, plasma membrane localization

Tabela 4. Lista dos genes down-regulated em resposta às NPsAg por 24 h, exclusivamente (diagrama de Venn), em *C. glabrata* CBS138 (formando biofilmes) de acordo com os grupos funcionais obtidas pelo MIPS Functional (http://mips.helmholtz-muenchen.de/funcatDB/). A função biológica indicada foi baseada nas informações disponíveis em *Candida* Genome Database (http://candidagenome.org) e/ou na informação disponível para ortólogo *S. cerevisiae*.

ORF Name	Gene Name	LogFC (wt AgNP 24 h/wt CTRL)	*p* value	Function
		Mitochondrion		
CAGL0B01815g	MRPL1	0.35	0.0006	Uncharacterized ORF; Ortholog(s) have structural constituent of ribosome activity and mitochondrial large ribosomal subunit localization
CAGL0B03663g	CIT1	0.32	0.02	Uncharacterized ORF; Ortholog(s) have citrate (Si)-synthase activity and peroxisome localization

CAGL0D05412g	MRPS5	0.35	0.005	Uncharacterized ORF; Ortholog(s) have structural constituent of ribosome activity and mitochondrial small ribosomal subunit localization
CAGL0E06314g	RSM22	0.32	0.005	Uncharacterized ORF; Ortholog(s) have structural constituent of ribosome activity and mitochondrial small ribosomal subunit localization
CAGL0F01243g	MDM38	0.29	0.016	Uncharacterized ORF; Ortholog(s) have ribosome binding activity
CAGL0G06402g	CIR2	0.23	0.00105	Uncharacterized ORF; Ortholog(s) have mitochondrion localization
CAGL0H08283g	HSP10	0.21	0.006	Uncharacterized ORF; Ortholog(s) have chaperone binding, unfolded protein binding activity, role in chaperone-mediated protein complex assembly, protein import into mitochondrial intermembrane space, protein refolding and mitochondrial matrix localization
CAGL0H05797g	MGR2	0.19	0.002	Uncharacterized ORF; Ortholog(s) have role in protein import into mitochondrial inner membrane, protein import into mitochondrial matrix and mitochondrial inner membrane presequence translocase complex, plasma membrane localization
CAGL0H06127g	TIM9	0.30	0.0105	Uncharacterized ORF; Ortholog(s) have protein transporter activity, role in protein import into mitochondrial outer membrane, regulation of growth rate and mitochondrial intermembrane space protein transporter complex localization
CAGL0H02123g	NAM8	0.22	0.0007	Uncharacterized ORF; Ortholog(s) have mRNA binding activity, role in mRNA splice site selection, positive regulation of mRNA splicing, via spliceosome and U1 snRNP, U2-type prespliceosome, commitment complex, cytoplasm localization
CAGL0H05137g	ALD6	0.30	0.005	Uncharacterized ORF; Ortholog(s) have aldehyde dehydrogenase [NAD(P)+] activity, role in NADPH regeneration, acetate biosynthetic process, response to salt stress and cytosol, mitochondrion localization
CAGL0I00748g	NDE1	0.08	0.005	Uncharacterized ORF; Ortholog(s) have NADH dehydrogenase activity, role in NADH oxidation, chronological cell aging, glycolytic fermentation to ethanol and mitochondrion, plasma membrane localization
CAGL0J09790g	GGC1	0.16	5.50E-05	Uncharacterized ORF; Ortholog(s) have guanine nucleotide transmembrane transporter activity and role in cellular iron ion homeostasis, guanine nucleotide transport, mitochondrial genome maintenance, transmembrane transport
CAGL0K04829g	RRG9	0.35	0.004	Uncharacterized ORF; Ortholog(s) have role in mitochondrial genome maintenance
CAGL0K06655g	NGR1	0.16	0.0008	Uncharacterized ORF; Ortholog(s) have mRNA binding activity, role in 3'-UTR-mediated mRNA destabilization, mitochondrion organization and P-

				body, cytoplasmic stress granule, perinuclear region of cytoplasm localization
CAGL0K02717g	MRP4	0.34	0.0006	Uncharacterized ORF; Ortholog(s) have structural constituent of ribosome activity and mitochondrial small ribosomal subunit localization
CAGL0K08184g	CCP1	0.18	0.002	Verified ORF; Cytochrome C peroxidase
CAGL0L02079g	CTP1	0.29	0.02	Uncharacterized ORF; Ortholog(s) have tricarboxylate secondary active transmembrane transporter activity, role in mitochondrial citrate transmembrane transport and plasma membrane localization
CAGL0L03289g	UTH1	0.25	0.0007	Uncharacterized ORF; Ortholog(s) have role in autophagy of mitochondrion, fungal-type cell wall biogenesis, fungal-type cell wall organization
CAGL0L00451g	MRPS17	0.32	0.00022	Uncharacterized ORF; Ortholog(s) have structural constituent of ribosome activity and mitochondrial small ribosomal subunit localization
CAGL0M07722g	CLU1	0.27	0.0021	Uncharacterized ORF; Ortholog(s) have role in cytoplasmic translational initiation and cytoplasmic stress granule, eukaryotic translation initiation factor 3 complex localization
Transport facilities				
CAGL0C01325g	COX5b	0.09	0.03412	Uncharacterized ORF; Ortholog(s) have cytochrome-c oxidase activity, nitrite reductase (NO-forming) activity, role in mitochondrial electron transport, cytochrome c to oxygen and mitochondrial respiratory chain complex IV localization
CAGL0F00209g	TNA1	0.17	0.00943	Uncharacterized ORF; Has domain(s) with predicted role in transmembrane transport and integral component of membrane localization
CAGL0F00231g	MIR1	0.1	1.25E-05	Uncharacterized ORF; Ortholog(s) have inorganic phosphate transmembrane transporter activity, role in phosphate ion transmembrane transport and integral component of mitochondrial inner membrane, plasma membrane localization
CAGL0G10131g	QCR2	0.07	0.0007	Uncharacterized ORF; Ortholog(s) have ubiquinol-cytochrome-c reductase activity and role in aerobic respiration, mitochondrial electron transport, ubiquinol to cytochrome c
CAGL0G10153g	QCR7	0.10	0.00068	Uncharacterized ORF; Ortholog(s) have mitochondrion localization
CAGL0G06402g	CIR2	0.23	0.00105	Uncharacterized ORF; Ortholog(s) have mitochondrion localization
CAGL0G03487g	TMN3	0.31	0.00034	Uncharacterized ORF; Ortholog(s) have role in cellular copper ion homeostasis, cellular response to drug, invasive growth in response to glucose limitation, pseudohyphal growth, vacuolar transport
CAGL0I01408g	CYC1	0.01	0.00384	Uncharacterized ORF; Ortholog(s) have electron transfer activity, role in mitochondrial electron transport, cytochrome c to oxygen, mitochondrial

				electron transport, ubiquinol to cytochrome c and mitochondrial intermembrane space localization
CAGL0I05918g	TIM17	0.23	0.002	Uncharacterized ORF; Ortholog(s) have protein transmembrane transporter activity, role in mitochondrial genome maintenance, protein import into mitochondrial matrix and mitochondrial inner membrane presequence translocase complex localization
CAGL0I05566g	TIM23	0.29	0.00059	Uncharacterized ORF; Ortholog(s) have mitochondrion targeting sequence binding, protein transmembrane transporter activity and role in protein import into mitochondrial matrix
CAGL0I06270g	QCR8	0.14	0.00114	Uncharacterized ORF; Ortholog(s) have ubiquinol-cytochrome-c reductase activity, role in aerobic respiration, mitochondrial electron transport, ubiquinol to cytochrome c and mitochondrial respiratory chain complex III, plasma membrane localization
CAGL0J06028g	MEP2	0.18	0.00178	Uncharacterized ORF; Ortholog(s) have high-affinity secondary active ammonium transmembrane transporter activity
CAGL0J00429g	COX6	0.08	0.00632	Uncharacterized ORF; Cytochrome c oxidase subunit VI
CAGL0J09790g	GGC1	0.16	5.50E-05	Uncharacterized ORF; Ortholog(s) have guanine nucleotide transmembrane transporter activity and role in cellular iron ion homeostasis, guanine nucleotide transport, mitochondrial genome maintenance, transmembrane transport
CAGL0L07766g	ATO2	0.30	0.03906	Uncharacterized ORF; Ortholog(s) have acetate transmembrane transporter activity, ammonium transmembrane transporter activity, role in ammonium transport, nitrogen utilization, plasma membrane acetate transport and plasma membrane localization
CAGL0L03828g	CYB5	0.35	0.00888	Uncharacterized ORF; Ortholog(s) have electron transfer activity, role in ergosterol biosynthetic process and endoplasmic reticulum membrane localization
			Cell cycle	
CAGL0A02596g	SPC110	0.24	0.04591	Uncharacterized ORF; Ortholog(s) have structural constituent of cytoskeleton activity
CAGL0B00616g	SPS2	0.22	0.00092	Uncharacterized ORF; Ecm33-family protein with a predicted role in cell wall biogenesis and organization; predicted GPI-anchor
CAGL0D02018g	HSK3	0.23	0.00224	Uncharacterized ORF; Ortholog(s) have microtubule plus-end binding activity
CAGL0D04620g	CLB2	0.13	0.00813	Uncharacterized ORF; Ortholog(s) have cyclin-dependent protein serine/threonine kinase activator activity

CAGL0D04268g	CTF18	0.22	0.04123	Uncharacterized ORF; Ortholog(s) have role in DNA-dependent DNA replication maintenance of fidelity and Ctf18 RFC-like complex, nuclear chromatin localization
CAGL0D04642g	CLB5	0.08	0.02227	Uncharacterized ORF; Ortholog(s) have cyclin-dependent protein serine/threonine kinase regulator activity
CAGL0F02035g	CTF19	0.20	0.03199	Uncharacterized ORF; Protein of unknown function
CAGL0F04939g	MCM5	0.17	0.04353	Uncharacterized ORF; Ortholog(s) have role in negative regulation of helicase activity and MCM complex, nucleus localization
CAGL0H02123g	NAM8	0.22	0.00069	Uncharacterized ORF; Ortholog(s) have mRNA binding activity, role in mRNA splice site selection, positive regulation of mRNA splicing, via spliceosome and U1 snRNP, U2-type prespliceosome, commitment complex, cytoplasm localization
CAGL0H05027g	CTF3	0.23	0.02952	Uncharacterized ORF; Ortholog(s) have role in DNA replication initiation, establishment of mitotic sister chromatid cohesion, mitotic spindle assembly checkpoint and condensed nuclear chromosome kinetochore localization
CAGL0H01661g	SPS2	0.16	0.00347	Uncharacterized ORF; Ecm33-family protein with a predicted role in cell wall biogenesis and organization; predicted GPI-anchor
CAGL0H09438g	BIM1	0.11	0.03064	Uncharacterized ORF; Ortholog(s) have ATPase activator activity, cytoskeletal adaptor activity, microtubule plus-end binding, protein homodimerization activity, structural constituent of cytoskeleton activity
CAGL0I05544g	RAD51	0.20	0.02557	Uncharacterized ORF; Ortholog(s) have ATP binding, DNA-dependent ATPase activity, Swi5-Sfr1 complex binding, double-stranded DNA binding, recombinase activity, single-stranded DNA binding activity
CAGL0J11638g	CDC5	0.19	0.00558	Uncharacterized ORF; Ortholog(s) have centromeric DNA binding, enzyme activator activity, phosphoprotein binding, protein serine/threonine kinase activity, protein-containing complex binding activity
CAGL0J01177g	ABF1	0.24	0.00027	Uncharacterized ORF; Has domain(s) with predicted DNA binding activity, role in chromatin remodeling and nucleus localization
CAGL0J08888g	TUB4	0.12	0.04367	Uncharacterized ORF; Ortholog(s) have role in microtubule nucleation, mitotic cytokinesis, site selection, mitotic spindle midzone assembly
CAGL0J06424g	MCM6	0.18	0.04856	Uncharacterized ORF; Ortholog(s) have 3'-5' DNA/RNA helicase activity, single-stranded DNA binding, single-stranded DNA-dependent ATP-dependent 3'-5' DNA helicase activity, single-stranded RNA binding activity
CAGL0K04543g	SPT4	0.25	0.01261	Uncharacterized ORF; Ortholog(s) have RNA polymerase II core binding, rDNA binding, single-stranded RNA binding activity

CAGL0K06655g	NGR1	0.16	0.00076	Uncharacterized ORF; Ortholog(s) have mRNA binding activity, role in 3'-UTR-mediated mRNA destabilization, mitochondrion organization and P-body, cytoplasmic stress granule, perinuclear region of cytoplasm localization
CAGL0K06633g	AME1	0.22	0.04038	Uncharacterized ORF; Ortholog(s) have role in attachment of spindle microtubules to kinetochore, protein localization to kinetochore and COMA complex localization
CAGL0L10252g	ASE1	0.23	0.0279	Uncharacterized ORF; Ortholog(s) have microtubule binding activity and role in cell separation after cytokinesis, microtubule bundle formation, mitotic spindle elongation, mitotic spindle pole body separation, spindle midzone assembly
CAGL0L03289g	UTH1	0.25	0.0007	Uncharacterized ORF; Ortholog(s) have role in autophagy of mitochondrion, fungal-type cell wall biogenesis, fungal-type cell wall organization
CAGL0L00495g	HSC82	0.20	5.1E-05	Verified ORF; Putative heat shock protein
CAGL0M04323g	ACE2	0.24	0.00578	Verified ORF; Putative transcription factor; null mutation results in hypervirulence in immunocompromised mice

CONSIDERAÇÕES FINAIS

CONSIDERAÇÕES FINAIS

Com o Capítulo 1, nós concluímos que:

- É possível obtermos um novo biomaterial contendo em sua composição nanopartículas de prata (NPsAg) (obtidas por uma síntese '*green*' utilizando diferentes partes de uma romã) e fosfato de cálcio (β-glicerofosfato de cálcio - GPCa) conferindo a este material propriedades antimicrobianas e remineralizadoras;
- Estes compostos apresentaram atividade antimicrobiana contra *S. mutans* e *C. albicans*, importantes patógenos orais relacionados com a cárie dentária e a candidíase bucal;
- Além disso, os nanocompósitos (NPsAg e NPsAg-GPCa) obtidos com o extrato da casca da romã apresentaram atividade antibiofilme semelhante e até mesmo melhor do que a clorexidina contra *S. mutans*.

Os Capítulos 2, 3, 4, 5 e 6 foram desenvolvidos com soluções antimicrobianas obtidas com o extrato da casca da romã. Com o Capítulo 2, concluí-se que:

- Estes nanocompósitos (NPsAg e NPsAg-GPCa) não foram citotóxicos às células L929 (fibroblastos) e estimularam a liberação de fator de crescimento celular o que pode favorecer o reparo tecidual em um processo inflamatório.

Os Capítulos 3 e 4 concluíram que:

- O uso combinado destas soluções antimicrobianas (NPsAg e NPsAg-GPCa) com o Tirosol pode ser uma alternativa viável contra patógenos orais.

No Capítulo 5, apenas as NPsAg foram avaliadas. É possível observar que:

- As NPsAg foram efetivas contra isolados clínicos orais de espécies de *Candida* (*C. albicans* e *C. glabrata*) incluindo isolados resistentes ao fluconazol. As células de *C. glabrata* foram mais susceptíveis às NPsAg. Além disso, houve uma redução no número de células de *C. albicans* que se mostraram com filamentação quando biofilmes foram formados na presença das NPsAg. Houve, também, uma redução na formação do biofilme das espécies de *Candida* na presença desta solução antimicrobiana;

- A combinação das NPsAg com diferentes agentes antifúngicos (fluconazol, nistatina e anfotericina B) foi eficaz contra os isolados clínicos orais resistentes ao fluconazol mostrando um efeito sinérgico.

E, por fim, no Capítulo 6, uma análise transcriptômica foi realizada a fim de avaliar quais genes estão mais ou menos expressos como resposta à exposição às NPsAg. A resposta transcriptômica das células de *C. glabrata* CBS138 frente às NPsAg foi determinada em duas situações: nos estados planctônico e formando biofilmes. A resposta transcriptômica das células expostas às NPsAg formando biofilmes foi comparada com a do íon Ag^{+}. Com este estudo, pode-se concluir que:

- No estado planctônico, os genes relacionados com a biossíntese de metionina e de lisina estão mais expressos, enquanto que os genes relacionados com o transporte transmembrana estão menos expressos;
- As células expostas às NPsAg responderam de forma distinta em relação ao Íon Ag^{+}, na formação do biofilme de *C. glabrata*;
- As NPsAg exercem o seu efeito na membrana citoplasmática da célula fúngica. Além disso, nós observamos efeitos distintos entre o Íon Ag^{+} e as NPsAg na formação do biofilme.